UNIVERSIDADE FEDERAL DE ITAJUBÁ - UNIFEI
GRADUATION PROGRAM IN
PHYSICS

Fluctuations of a Massive Scalar Field: Temperature and Boundary.

Alexsandre Leite Ferreira Junior

Itajubá, October 1, 2020

UNIVERSIDADE FEDERAL DE ITAJUBÁ - UNIFEI
GRADUATION PROGRAM IN
PHYSICS

Alexsandre Leite Ferreira Junior

Fluctuations of a Massive Scalar Field: Temperature and Boundary.

Dissertation submitted to the Physics Graduation Program as a requirement for the Master's of Science in Physics Degree.

Major: Quantum Field Theory, Cosmology and Gravitation

Supervisor: Prof. PhD Vitorio Alberto De Lorenci

October 1, 2020

Itajubá

Acknowledgements

I am thankful to my family, for being the roots attaching me to the ground. My friends and my companion, with whom I divided house and food, twigs and flowers. I am also thankful to the professors I encountered, the bole of my formation. Specially my adviser Prof. Vitorio De Lorenci. In the course of the present work I realized how much I have learned with him in the past years. This work was financially supported by CAPES.

"Estas coisas aconteceram em qualquer tempo e em qualquer parte. O certo é que aconteceram. E, como sempre se dá, ninguém apreendeu nada de seu misterioso sentido."

Ruth Guimarães, Água Funda

Abstract

It is well established that a change in the physical state of a quantum field induces dispersions on the velocity of a interacting non-relativistic test particle. Here such a interacting model is addressed with a finite transition time between states of the field. Underlining that such induced stochastic motion is different from an usual Brownian motion, as, at late times, the dispersions are bounded and do not depend on the interaction time, without the need for a dissipative force. Further, we study the case for a massive scalar field at finite temperatures, thus generalizing previous investigation in [1]. The results presented here show subvacuum effects even at finite temperature. Nonetheless, novel effects are also unveiled, as a detailed description of the thermal contribution highlights their discrepancy to the usual Brownian motion and stresses the opposing character of mass and temperature. The presence of the field mass weakens thermal contributions and temperature hides the characteristic oscillatory pattern of massive fields. Such interplay is even more relevant in the presence of a boundary, when investigating the distance behavior of the dispersions and the vacuum versus thermal dominance near the wall. As for higher masses the vacuum term dominates for larger distances, being able also to create and interchange in such dominance as the wall is approached.

Key-words: Boundary quantum field theory. Stochastic motion. Massive scalar field.

List of Figures

Table of Contents

Introduction

The Greek philosopher *Democritus* was one of the first to question about the vacuum. He proposed that matter was made up of tiny indivisible particles and in between them there was nothing, otherwise their motion was impossible–for a particle to move it must leave the space it is now to occupy an adjacent one, which could not be possible if all spaces were occupied. On the other hand *Aristoteles*, in his book *Physica*, argued that the motion in vacuum was impossible, as there exists no up or down, right or left no body would be able to move, and so there was no vacuum. Aristotle's theories dominated until the end of Medieval times when the question of the existence of the vacuum regain relevance.

Its existence was then established with the experiment done by Torricelli, in which he would pour mercury on a glass tube and then turn it upside down in a reservoir also filled with mercury. The height of the column of mercury was independent of the height of the glass tube above it, leading him to the conclusion that the space left in the tube was a vacuum. After that, many experiments were carried out with the vacuum, and many technologies developed from it [2].

Henceforth, with Rutherford it was established that not only the space between atoms was empty but the atoms themselves consist mainly of empty space. Further, the Michelson-Morley experiment, besides setting the ground for the development of special relativity, showed that there was no such a thing as an *aether* and the vacuum was the filling not only of the atoms that composes matter but of the vast Universe in which we live.

At first quantum mechanics did not added very much to the discussion, as it describes the dynamics of particles. That changed with the quantum description of relativistic systems through fields, a mathematical object that exists in every point in space and in quantum field theory it is the most fundamental object, particles being propagating perturbations in it. In such formalism we can describe the dynamics of a system with no particles, i.e., a field in its vacuum state.

Thus, in contrast to the nothingness of the old understanding of vacuum, now the fields are all over and the vacuum is just the absence of any excitation mode. However, as a quantum system, the physical state of the field cannot be sharply defined and the vacuum fluctuates around its mean value. The quantum vacuum fluctuations are a remarkable outcome of quantizing a field, as in the electromagnetic case, while many results can be obtained through the interaction of quantized matter with a classical field, the vacuum fluctuations are characteristic of quantum fields explaining and giving rise

to many relevant phenomena, such as spontaneous emission, Lamb shift and the Casimir effect.

Besides the astonishing outcome of a nothingness populated with fluctuations some relevant questions arose concerning interactions of the vacuum with spacetime [3, 4, 5]: The existence of a natural cut-off function for the propagating modes; The definition of an unique vacuum in curved spacetimes; The gravitational effects of quantum fluctuations and possible quantum fluctuations of the gravitational field.

Moreover, in absence of all fields we are confronted with another idea of empty space: The Minkowski vacuum. However the existence of a pure Minkowski vacuum implies the ontological existence of spacetime, even in the absence of all things, which invokes some problems as the hole argument [6]. Thus, some argue that spacetime could only exist as a relational ground between interacting entities, being meaningless on its own, i.e., there is no true vacuum. This question is a leading one concerning the development of a quantum gravity theory, as the non existence of a pure Minkowski vacuum implies that the theory must be background independent. There is no easy answer on what is the vacuum, or even if a total absence of everything really exists. Notwithstanding, we can see that our interest in the nothingness has always laid in the frontiers of knowledge.

Foremost, in the present work we investigate the stochastic motion induced by quantum vacuum fluctuations. In Ref. [7] is argued that this motion can be induced by the pure Minkowski vacuum. However, it was shown in [8, 9] that this effect does not occur due to the free vacuum fluctuations anti-correlations. Hence, we study the motion induced by a change in the vacuum state, as for example the introduction of a boundary. Such a model was originally presented in Ref. [10] as an electrically charged particle near an infinite reflective wall. There it was shown that some divergences appear near the boundary and when the interaction time equals a round trip of the photon. Which were linked back to some idealizations: a sudden transition between the system states, the perfectly reflective character of the boundary, and the particle non-quantum nature. This effect was also studied in a Robertson-Walker spacetime, where the change in the vacuum state occurs due to expansion of the spacetime [11], in analog models of light propagation in nonlinear materials [12], and in others gravitational scenarios where it was shown that active and passive fluctuations, i.e., fluctuations of the gravitational field or in the energy-momentum tensor that curves the spacetime, respectively, lead to fluctuations of the light-cone [13].

To describe a more realistic model of the boundary induced dispersion a switching function was introduced in Refs. [14, 15], modelling a smooth transition between states of the quantum field, and it was shown to regularize all divergences. Further, in Ref. [16] the quantum character of the particle was addressed, and the late-time regime was regularized. Also in Ref. [17] a toy model of a (1+1) dimensional scalar field was regularized by

substituting the point-like particle by a Gaussian wave packet.

Nonetheless, despite curing divergences, the sample function chosen in Ref. [15] suppressed the residual dispersion of the particle velocities. Thence, in Ref. [18], the effects of different choices of the sample function were investigated, for a massless scalar field at (3+1) dimensions, and it was demonstrated that the residual dispersion is related to the transition time between states.

Furthermore, the velocities dispersions caused by a boundary at finite temperature were treated for a sudden transition in [19] and with a smooth switching in Ref. [20]. In the latter was also investigated the late-time regime and the distance behavior, showing that, when regularized, the vacuum fluctuations can be dominated by thermal fluctuations near the boundary. Some interesting effects were also revealed in Ref. [1], where we have fluctuations of a massive scalar field at arbitrary spatial dimensions. There it was remarked that when the mass is present an oscillatory pattern is revealed, a consequence of the non-Huygesian character of the field.

In the present work previous result are generalized to the finite temperature case by the study of a thermal bath near a boundary. Besides, we also investigate the effects on the particle of a thermal bath of scalar bosons–showing that the resulting dispersions are different from the usual Brownian motion–, and of the boundary case at finite temperature, as the introduction of a thermal bath can be detached from it. It was noted that the presence of field mass opposes thermal effects, weakening the thermal contributions to the fluctuations. Also, subvacuum effects can be present even for finite temperature. Furthermore, interesting effects concerning the distance behavior of the dispersions are shown as vacuum versus thermal dominance near the wall is dependant on the mass. So, for some cases we can have an interchange between vacuum and thermal dominance as the boundary is approached.

The interest in studying a massive scalar field goes beyond its simpler treatment, as its existence is known in nature, the Higgs boson, it is of great interest in high energy physics, also a candidate to the inflation field [21], and for dark matter models [22]. So that the local thermal behavior of the massive scalar field was studied in detail near a wall in Ref. [23]. There important quantities as the fields fluctuations and its energy-momentum tensor were analysed, quantities which are closely related to the fluctuations here studied.

In the present text we begin, in the next Chapter, with a brief review of the formalism used, introducing quantum systems and quantum statistical mechanics followed by the quantization of a massive scalar field. In Chapter 2 we study some important quantities in quantum field theories: The vacuum expectation values of the field, i.e., the Green functions. Investigate their physical meaning and relations to each other through an analytic continuation in the complex plane. We also calculated, using the image method [24], the expectation values in the presence of a reflective boundary. Further, we also

investigate the Green functions in a statistical ensemble, where it was shown, also through analytic continuation, that it is analogue to a change in the topology of the complex-space in which the Green function is defined.

The main results are in Chapter 3. There we present the dispersions of the velocities of a test particle due to a change in the state of a massive scalar field. First for a thermal bath, then with the boundary at finite temperature and finally the pure boundary dispersions at finite temperature. For that we discuss the construction of the model, the mechanism thorough the sample functions regularize the divergences and their physical meaning. It is also addressed the differences in the choice of the sample function and how they affect the dispersions. We were able to show that the dispersions due to the thermal bath are substantially different from the usual Brownian motion, as there is no need of a dissipative force for the dispersions to be bounded at late times. Moreover, even at finite temperatures we saw that the vacuum effects play a major role, and the dispersions can be negative. Finally, it was noted that the field mass weakens its thermal effects, and the vacuum contribution gains relevance, creating an interesting dominance behavior as the boundary is approached.

We work in a (D+1) Minkowski spacetime with metric corresponding to the metric signature $(+\ -\ -\ -)$ in four dimensional spacetime. Unless stated otherwise natural units are used, $\hbar = c = 1$, and the Boltzmann constant $k_{_B}$ is also set to unity, so that $1\mathrm{K} \simeq 4.37 \times 10^2\,\mathrm{m}^{-1}$.

1 Field Quantization

Quantum mechanics arose from the necessity to explain experimental facts as black body radiation, the atomic structure, and absorption and emission phenomena. In this context, Heinsenberg and Schrödinger developed the matrix and wave theories, respectively, as mathematical frameworks describing quantum dynamics. Latter on, the main structure of both formulations was conveniently concatenated in an abstract Hilbert Space $\mathcal{H}$, possessing the structure of a linear vector space [25]. It is interesting to note that, besides the experimental success of the theory, its foundations remain object of intense debate.

In the beginning the dynamical evolution of quantum systems, that is, the Schrödinger equation, could only describe non-relativistic systems–in the sense that they do not obey special relativity, only galilean relativity. This can be seen by the different roles that time and position have in the theory. While the position is an operator, time can only be a parameter.

Furthemore, historically, the introduction of a relativistic equation for the dynamics of the systems has revealed itself to be cumbersome, as the relativistic formulation of Schrödinger equation, proposed primarily by himself, the Klein-Gordon equation, showed to be inconsistent with the probabilistic interpretation, as there negative probabilities appeared.

Was in order to solve this problem that Dirac developed the well known relativistic equation for the electron, the Dirac equation, in which he was able to find a dynamical equation consistent with special relativity and the probabilistic interpretation, besides leading to the correct prediction of the electron magnetic moment.

Dirac's theory of the relativistic electron proved his validity with the discovery of the positron, electron's antiparticle, which was theoretically predicted by him. The need for a "positive charged electron" came because Dirac's equation had infinite negative energy solution for the free relativistic electron, which would make impossible for the particle to be stable, as it would always decay to a less energetic state. The solution found by him was to propose that these negative energy state were not occupied by electrons, but by an opposite charged particle, later found out to be the positron, as the negative energy states were already occupied, the Pauli exclusion principle would assure that electrons would not decay.

Dirac's relativistic theory, however, do not accounted for a complete relativistic quantum mechanics, as it was not suited to describe bosons, which do not obey Pauli's exclusion principle.

The birth of Quantum Field Theory came simultaneously with these events, with the quantization of the electromagnetic field, followed by Dirac's field. The systematic quantization, as it will be presented here, came first with Heisenberg and Pauli in 1929 [26].

Thence, as in this theory both probability densities $\psi^\dagger\psi$ and $\phi^\dagger\phi$ from Dirac's and Klein-Gordon's equations could be negative–as these quantities, when renormalized, became negative–these were no longer interpreted as probability densities but just operators, spanning a basis on the Hilbert space, on which each eingenvector represented a state with a definite number of particles. Since then, QFT has proved to be the most successful theory in describing the fundamental processes in particles dynamics. For a complete historical setting of Quantum Field Theory see the first chapter the Ref. [26].

Notwithstanding, QFT was born with many flaws, the rudest being the infinities, as the vacuum infinite energy and number of particles, many of them could be circumvented through renormalization and the theory is today practically realizable and experimentally consistent.

In this chapter we give an outline of the quantum dynamics, introducing also its thermodynamics through statistical quantum mechanics, giving an example that will be very useful for what follows: the quantum harmonic oscillator. Forthwith, we quantize a charged scalar field, following the canonical approach of dividing it into normal modes. As said, this is an outline of the theory, and, as we try to be the most consistent as possible, many conceptual jumps are given, in which references are addressed where the reader can fully be aware of the actual development of the subject.

1.1 Quantum dynamics

In classical theories a physical system with n degrees of freedom is a vector in a $2n$-manifold (the phase space), in which the observable, a function taking a point from the manifold to the real line, acts. In contrast, a quantum system is described by a vector $|\psi\rangle \in \mathcal{H}$, and an observable is now a Hermitian linear operator acting on the Hilbert space. Through its eigenvectors we construct a basis, $\{|\alpha_i\rangle\}$, and its eigenvalues, $\{\alpha_i\}$, are the possible outcomes of a measurement.

Henceforth, operationally, the construction of our Hilbert space comes from the specification of a complete set of operators through its commutator algebra. To find this algebra we postulate a correspondence map between the quantum and classical operators, such that $\{f, g\} = i[\hat{f}, \hat{g}]$. From which we find the canonical commutation relations between generalized coordinate and momenta, $\hat{q}_i$ and $\hat{p}_i$

$$[\hat{q}_i, \hat{q}_j] = [\hat{p}_i, \hat{p}_j] = 0, \quad [\hat{q}_i, \hat{p}_j] = i\delta_{ij}. \tag{1.1}$$

Furthermore, these relations fix the representations of such operators, up to unitary equivalence, and, as every other classical corresponding quantity can be specified through these operators, we are able to define our system [25].

However, some ambiguities may arise when the dynamical system depends on a cross product between $\hat{q}_i$ and $\hat{p}_i$ (which must come first?), when describing observables with no classical counterpart, and also in the case of systems with infinite degrees of freedom. In such cases there exists others non-unitary equivalent representations of the same observables.

The evolution is given by a one-parameter unitary family of operators generated by the Hamiltonian operator . In the Schrödinger picture

$$i\frac{\partial}{\partial t}\left|\psi\right\rangle(t) = \hat{H}\left|\psi\right\rangle(t), \tag{1.2}$$

while the operators, $\hat{O}$, remain time independent.

In the Heisenberg picture (denoted here by a subscript H)

$$\frac{d}{dt}\hat{O}_H = i[H, O_H], \tag{1.3}$$

while the state vectors, $\left|\psi\right\rangle_H$, remain time independent.

Both are related by the unitary transformations $\hat{U}(t) = \exp(-i\hat{H}t)$, so that:

$$\hat{O}_H(t) = \hat{U}^\dagger(t)\hat{O}\hat{U}(t), \tag{1.4}$$

$$\left|\psi\right\rangle(t) = \hat{U}(t)\left|\psi\right\rangle_H. \tag{1.5}$$

Finally, despite some (many) conceptual and mathematical problems in the construction, the dynamics of quantum systems gave plenty of experimentally consistent results and made its way through a plethora of technological devices, asserting to it some reliability. In this chapter we will describe a simple quantum mechanical system, the quantum harmonic oscillator, which will be of great help in what follows: the quantization of the scalar field. Which will be done in the most simple way, by decomposing it into its normal modes, each of them consisting of a quantum mechanical oscillator.

1.2 Quantum statistical mechanics

A real physical system can never be truly isolated from the external world and, in order to describe realistic settings, one must introduce thermodynamics in the description. For that we use the statistical formulation of quantum mechanics, for a detailed construction see Ref. [27].

Therefore, instead of pure state $|\psi_n\rangle$ (an eingenvector of the Hamiltonian with energy E_n) we must now deal with statistical ensembles, that is, an incoherent superposition of pure states. This is done through the definition of the density matrix operator $\hat{\rho}$, with components

$$\rho_{mn} = \langle\psi_n|\,\hat{\rho}\,|\psi_m\rangle = \delta_{mn}|b_n|^2, \tag{1.6}$$

and normalization

$$\sum_n \delta_{mn}\rho_{mn} = 1. \tag{1.7}$$

The quantity $|b_n|$ gives the normalized number of states in our ensemble that have the energy E_n.

In what follows, as usual, we characterize the system using the Grand Canonical Ensemble, which is in thermal equilibrium with a reservoir, from which it can exchange energy and particles. For that we define the density matrix operator

$$\hat{\rho} = \frac{\mathrm{e}^{-\beta(\hat{H}-\mu\hat{N})}}{Z}, \tag{1.8}$$

where $\beta = T^{-1}$, μ being the chemical potential–which accounts for the change in the free energy due to exchange of particles with the reservoir–, $\hat{N}$ the operator that gives the number of particles of the system, and the partition function

$$Z = \sum_n \mathrm{e}^{-\beta(E_n-\mu N_n)}. \tag{1.9}$$

The expectations values in a statistical ensemble are given by

$$\langle\hat{O}\rangle_\beta = \sum_n \langle\psi_n|\,\hat{\rho}\hat{O}\,|\psi_n\rangle = Tr[\hat{\rho}\hat{O}]. \tag{1.10}$$

Thus, we are now able to describe a quantum system in thermal equilibrium with the external world.

1.3 Quantum harmonic oscillator

The Hamiltonian of a classical harmonic oscillator is

$$H = \frac{p^2}{2m} + \frac{m\omega^2}{2}q^2, \tag{1.11}$$

which is a fairly simple system, in the sense that no ambiguities appears and the quantum system is fully determined by identifying the generalized coordinates with operators and imposing the canonical commutation relations (1.1). It is convenient to introduce the operator

$$\hat{a} = \sqrt{\frac{\omega m}{2}}\hat{q} + i\sqrt{\frac{1}{2\omega m}}\hat{p}. \tag{1.12}$$

Thus,

$$[\hat{a}, \hat{a}^\dagger] = \hat{I}, \tag{1.13}$$

$$\hat{H} = \omega \left(\hat{a}\hat{a}^\dagger + \frac{1}{2}\hat{I} \right), \tag{1.14}$$

and

$$[\hat{H}, \hat{a}] = -\omega \hat{a}, \tag{1.15}$$

where $\hat{I}$ is the identity operator.
The time evolution

$$\frac{d}{dt}\hat{a}_H(t) = i[H, \hat{a}] = -i\omega \hat{a}_H(t), \tag{1.16}$$

hence

$$\hat{a}_H(t) = \hat{a}\, \mathrm{e}^{-i\omega t}. \tag{1.17}$$

The eigenvectors of the number operator $\hat{n} = \hat{a}^\dagger \hat{a}$, which are also eingenvectors of $\hat{H}$, provides a useful basis for the space. It can be seen that the eigenvalues of the number operator, $\{n\}$, are non-degenerate, non-negative, and integers (See Ref. [28, 29]). The energy of each state $|n\rangle$ is

$$\hat{H}\,|n\rangle = E_n\,|n\rangle = \left(n + \frac{1}{2}\right)\omega\,|n\rangle\,. \tag{1.18}$$

Acting with $\hat{a}$ and $\hat{a}^\dagger$ we see that

$$\hat{a}\,|n\rangle = \sqrt{n}\,|n-1\rangle\,, \quad \hat{a}^\dagger\,|n\rangle = \sqrt{n+1}\,|n+1\rangle\,. \tag{1.19}$$

From the expression for the energy and its dependence on the eigenvalues of the number operator these are interpreted as the number of energy *quanta* of the oscillator. It follows that the operators $\hat{a}$ and $\hat{a}^\dagger$ annihilate and create a quanta in the system, respectively. Furthermore, as the eigenvalues must be non-negative and integers, exists a state such that

$$\hat{a}\,|0\rangle = 0, \tag{1.20}$$

which is the state with lower energy, denominated vacuum state. From the vacuum we can construct any other state by successively acting with the creation operator

$$|n\rangle = \frac{(\hat{a}^\dagger)^n}{\sqrt{n!}}\,|0\rangle\,. \tag{1.21}$$

The generalization to the case of N coupled harmonic oscillators is straightforward. The complete Hilbert space is the tensor product of N simple harmonic oscillators

$$\mathcal{H}_T = \mathcal{H}_1 \otimes \mathcal{H}_2 ... \otimes \mathcal{H}_N, \tag{1.22}$$

and the operators now satisfy the commutation relations

$$[\hat{a}_i, \hat{a}_j^\dagger] = \delta_{ij}, \quad [\hat{a}_i, \hat{a}_j] = [\hat{a}_i^\dagger, \hat{a}_j^\dagger] = 0, \tag{1.23}$$

where the subscript indicates in which space the operators acts.

1.4 Quantum scalar field

The core of the present work is to investigate the quantum vacuum effects of a massive real scalar field in a general Minskoswki spacetime with (D+1) dimensions. Such a field is a Lorentz invariant which satisfy the Klein-Gordon equation

$$(\Box + m^2)\phi(t, \vec{x}) = 0, \tag{1.24}$$

where $\Box$ is the D'Alembertian: $\eta^{\mu\nu}\partial_\mu\partial_\nu$. The above dynamical equation is obtained through the action of the free field

$$S_F[\phi, \partial_\mu\phi] = \int dt d^{^D}x\mathcal{L} = \int dt d^D x \left(\partial_\mu\phi\partial^\mu\phi - m^2\phi^2\right). \tag{1.25}$$

Thus, the canonical momenta are

$$\pi = \frac{\partial\mathcal{L}}{\partial(\partial_t\phi)} = \partial_t\phi. \tag{1.26}$$

Finally, the Hamiltonian, obtained through a Legendre transformation, is

$$H = \frac{1}{2}\int d^{^D}x \left(\pi^{^2} + \nabla\phi^{^2} + m^2\phi^2\right). \tag{1.27}$$

Now, in order to describe our system through quantum mechanics, we identify the fields as operators by imposing the canonical equal time commutation relations

$$[\hat{\phi}(t, \vec{x}), \hat{\pi}(t, \vec{x'})] = i\delta^{(D)}(\vec{x} - \vec{x}'), \tag{1.28}$$

all other commutators between the fields vanish. Although some axiomatic construction of field theories states that the above commutations relations are not well defined, see Ref. [30], it is well suited for our purposes and this choice does not restrict the results, as the expectation values are not affected. Furthermore, to construct the basis of our Hilbert space we decompose the field

$$\hat{\phi}(t, \vec{x}) = \int_{-\infty}^{\infty} d^{^D}\vec{k}\ \hat{\phi}_{\vec{k}}(t) f_{\vec{k}}(\vec{x}), \tag{1.29}$$

from the dynamical equation we find that

$$\frac{1}{\hat{\phi}_{\vec{k}}(t)}\partial_t^2\hat{\phi}_{\vec{k}}(t) - \frac{1}{f_{\vec{k}}(\vec{x})}\nabla^2 f_{\vec{k}}(\vec{x}) + m^2 = 0, \tag{1.30}$$

thus

$$\partial_t^2\hat{\phi}_{\vec{k}}(t) = -\omega^2\hat{\phi}_{\vec{k}}(t), \tag{1.31}$$

and

$$\nabla^2 f_{\vec{k}}(\vec{x}) = -(\omega^2 - m^2) f_{\vec{k}}(\vec{x}) = -k^2 f_{\vec{k}}(\vec{x}), \tag{1.32}$$

with $\omega = \sqrt{k^2 + m^2}$.

The general solution for equation (1.31) is

$$\hat{\phi}_{\vec{k}}(t) = \hat{a}_{\vec{k}} \mathrm{e}^{-i\omega t} + \hat{a}^{\dagger}_{\vec{k}} \mathrm{e}^{i\omega t}, \tag{1.33}$$

where the operators must be Hermitian conjugates of each other, as the field is reals. Also, $\hat{a}_{\vec{k}}$ and $\hat{a}^{\dagger}_{\vec{k}}$ must be such that the canonical commutation relations, Eq. (1.28), holds, from which

$$[\hat{a}_{\vec{k}}, \hat{a}^{\dagger}_{\vec{k}'}] = \delta^{(D)}(\vec{k} - \vec{k}'), \tag{1.34}$$

and all the others commutators vanish.

The notation gave to them was convenient because they satisfy the commutation algebra corresponding to the creation and annihilation operators described above for the harmonic oscillator. Hence, for each label $\vec{k}$ we have a vacuum state $\hat{a}_{\vec{k}} |0\rangle = 0$, through which we construct a Fock space.

Generally, the expansion of the field and its canonically conjugated momenta becomes

$$\hat{\phi}(t, \vec{x}) = \int d^D \vec{k} \left[\hat{a}_{\vec{k}} f_{\vec{k}}(\vec{x}) \mathrm{e}^{-i\omega t} + \hat{a}^{\dagger}_{\vec{k}} f^{*}_{\vec{k}}(\vec{x}) \mathrm{e}^{i\omega t} \right] \tag{1.35}$$

$$\hat{\pi}(t, \vec{x}) = \int d^D \vec{k} (i\omega) \left[\hat{a}^{\dagger}_{\vec{k}} f^{*}_{\vec{k}}(\vec{x}) \mathrm{e}^{i\omega t} - \hat{a}_{\vec{k}} f_{\vec{k}}(\vec{x}) \mathrm{e}^{-i\omega t} \right]. \tag{1.36}$$

The functions $f_{\vec{k}}(\vec{x})$ and its complex conjugated forms an orthonormal basis in the space of solutions of Eq. (1.32). In cartesian coordinates, this solution is the plane wave

$$f_{\vec{k}}(\vec{x}) = N_{\vec{k}} \mathrm{e}^{\vec{k} \cdot \vec{x}}. \tag{1.37}$$

To find the value of the normalization constant $N_{\vec{k}}$ we calculate the commutator

$$\begin{aligned} [\hat{\phi}(t, \vec{x}), \hat{\pi}(t, \vec{x'})] = \int d^D \vec{k} \int d^D \vec{k'} i\omega_k N_{\vec{k}} N_{\vec{k'}} \Big\{ & [\hat{a}_{\vec{k}}, \hat{a}^{\dagger}_{\vec{k'}}] \mathrm{e}^{-i(\omega t - \vec{k} \cdot \vec{x})} \mathrm{e}^{i(\omega' t' - \vec{k'} \cdot \vec{x'})} \\ & - [\hat{a}^{\dagger}_{\vec{k}}, \hat{a}_{\vec{k'}}] \mathrm{e}^{i(\omega t - \vec{k} \cdot \vec{x})} \mathrm{e}^{-i(\omega' t' - \vec{k'} \cdot \vec{x'})} \Big\} \\ [\hat{\phi}(t, \vec{x}), \hat{\pi}(t, \vec{x'})] = \int d^D \vec{k} 2i\omega_k N^2_{\vec{k}} \mathrm{e}^{-i(\omega \Delta t - \vec{k} \cdot \Delta \vec{x})}, \end{aligned} \tag{1.38}$$

the normalization constant must be $N_{\vec{k}} = 1/[(2\pi)^{D/2} \sqrt{2\omega}]$. Then, using the orthogonal relations for exponential functions, we recover the canonical commutation relations.

Finally, the complete expression for our quantized field

$$\hat{\phi}(t, \vec{x}) = \int \frac{d^D \vec{k}}{(2\pi)^{\frac{D}{2}} \sqrt{2\omega}} \left[\hat{a}_{\vec{k}} \mathrm{e}^{-i(\omega t - k \cdot \vec{x})} + \hat{a}^{\dagger}_{\vec{k}} \mathrm{e}^{i(\omega t - k \cdot \vec{x})} \right]. \tag{1.39}$$

Substituting the expansion of the field in terms of the creation and annihilation operators in the Hamiltonian, given by Eq. (1.27), and using the orthogonal relations of the

exponential functions we find that

$$\begin{aligned}\hat{H} &= \int \frac{d^D k}{4\omega_k^2} \Big\{ \omega_k \left[\hat{a}_{\vec{k}} \hat{a}^\dagger_{\vec{k}} - \hat{a}_{\vec{k}} \hat{a}_{-\vec{k}} \mathrm{e}^{-i2t\omega_k} - \hat{a}^\dagger_{\vec{k}} \hat{a}^\dagger_{-\vec{k}} \mathrm{e}^{i2t\omega_k} + \hat{a}_{\vec{k}} \hat{a}^\dagger_{\vec{k}} \right] \\ &+ k^2 \left[\hat{a}^\dagger_{\vec{k}} \hat{a}_{\vec{k}} + \hat{a}_{\vec{k}} \hat{a}_{-\vec{k}} \mathrm{e}^{-i2t\omega_k} + \hat{a}^\dagger_{\vec{k}} \hat{a}^\dagger_{-\vec{k}} \mathrm{e}^{i2t\omega_k} + \hat{a}^\dagger_{\vec{k}} \hat{a}_{\vec{k}} \right] \\ &+ M^2 \left[\hat{a}^\dagger_{\vec{k}} \hat{a}_{\vec{k}} + \hat{a}_{\vec{k}} \hat{a}_{-\vec{k}} \mathrm{e}^{-i2t\omega_k} + \hat{a}^\dagger_{\vec{k}} \hat{a}^\dagger_{-\vec{k}} \mathrm{e}^{i2t\omega_k} + \hat{a}^\dagger_{\vec{k}} \hat{a}_{\vec{k}} \right] \Big\} \\ &= \int d^D k \frac{\omega_k}{4} \left[\hat{a}_{\vec{k}} \hat{a}^\dagger_{\vec{k}} + \hat{a}^\dagger_{\vec{k}} \hat{a}_{\vec{k}} + \hat{a}_{\vec{k}} \hat{a}^\dagger_{\vec{k}} + \hat{a}^\dagger_{\vec{k}} \hat{a}_{\vec{k}} \right] \\ &= \int d^D k \omega_k \left[\hat{n}_{\vec{k}} + \frac{1}{2} \hat{I} \right]\end{aligned} \tag{1.40}$$

Therefore, the Hilbert space which contains the system is a tensor product of the Hilbert spaces for each quantum number k, on which we construct a Fock space representation. Hence, one can see that, in a flat spacetime, a quantum field (whose dynamics is governed by a linear equation) is just infinite coupled harmonic oscillators with a classical spacetime dependence given by the solutions of the dynamical equation.

As said before, here is just an outline of the theory, where we followed a didactic approach, encountered in introductory books. However, the canonical commutations relations do not suffices for the quantization of the field, because, as we are dealing with infinite modes of propagation and, with that, a tensor product of infinite Hilbert spaces, the Von-Neumann theorem does not apply. Notwithstanding, when dealing with a flat space-time, Lorentz symmetry defines irreducible representations for the field, and the problem is solved. For an accurate statement of the problem and how one can construct a more fundamental quantization so that these problems, and its solutions, become evident see the first chapters of Wald's book [5] and the formally constructions of field theories by Haag [31] and Streater & Wightman [30].

2 Green Functions

A great deal of problems in physics, after a proper description of the system, is to solve its dynamical equation. Hence, the problem is reduced to differential equations of the type

$$\mathcal{L}f(u) = g(u), \tag{2.1}$$

where $\mathcal{L}$ is a differential operator, and $g(u)$ is the source of our equation [32]. Thus, for $\mathcal{L}$ linear, as will be our case, we find the integral kernel of $\mathcal{L}$, that is, its Green function, given by

$$\mathcal{L}G(u,\xi) = \delta(u-\xi). \tag{2.2}$$

Which is the solution of the dynamical equation for a localized source, giving the influence on u of a point source at ξ. Note also that, as on the right hand side we have a distribution, the Green function is not properly a function, but a distribution. Then, as an extend source is just the volume integral of point-like sources, we have

$$f(u) = \int G(u,\xi)g(\xi)d\xi, \tag{2.3}$$

so that, acting with the operator gives

$$\mathcal{L}f(u) = \int \mathcal{L}G(u,\xi)g(\xi)d\xi = \int \delta(u-\xi)g(\xi)d\xi = g(u). \tag{2.4}$$

Henceforth, to calculate the Green Functions is an important step to solve the problem. Furthemore, for our case, the Green function is also associated with important quantities of the theory, besides enlightening causality and other relevant physical information of the fields.

Thus, in this chapter, we will define the expectation values that are related to the Green function of our dynamical equation, see how they are related to each other by an analytic continuation and how they define important properties of the fields, calculating also the Green functions in the presence of a boundary. Moreover, we will define it for systems at finite temperature, and show that the temperature can bee seen as a translation in imaginary time.

2.1 Green functions at zero temperature

As we have seen, the number states that constitutes the bases of our Fock space can all be constructed through the successive application of the creation operator in the vacuum state. Henceforth, the study of the aspects of the quantum vacuum has a central role in the construction of other quantities in quantum field theories. Accordingly, following Ref. [4] we now study the vacuum expectation values of some important quantities

that appears in the theory and, as we will see, are associated with the Green functions of the Klein-Gordon equation. First, the positive frequency Wightman function:

$$\begin{aligned} G^{+}(t,\vec{x};t',\vec{x}') &= \langle 0|\,\hat{\phi}(t,\vec{x})\hat{\phi}(t',\vec{x}')\,|0\rangle \\ &= \int \frac{d^{D}\vec{k}d^{D}\vec{k}'}{2(2\pi)^{D}}\frac{\mathrm{e}^{i\vec{k}\cdot\vec{x}}\mathrm{e}^{-i\vec{k}'\cdot\vec{x}'}}{\sqrt{\omega_k\omega'_k}}\,\langle 0|\,\hat{a}_{\vec{k}}\hat{a}^{\dagger}_{\vec{k}'}\,|0\rangle\,\mathrm{e}^{-i\omega_k t}\mathrm{e}^{i\omega'_k t'}, \end{aligned}$$

were we have used that $\hat{a}_{\vec{k}}\,|0\rangle = 0$. Using the commutation rules for the creation and annihilation operators, Eq. (1.34), we find

$$G^{+}(t,\vec{x};t',\vec{x}') = \int \frac{d^{D}\vec{k}}{2(2\pi)^{D}}\frac{\mathrm{e}^{i\vec{k}\cdot\Delta\vec{x}}\mathrm{e}^{-i\omega\Delta t}}{\omega}. \tag{2.5}$$

Analogously the negative frequency Wightman function is

$$\begin{aligned} G^{-}(t,\vec{x};t',\vec{x}') &= \langle 0|\,\hat{\phi}(t',\vec{x}')\hat{\phi}(t,\vec{x})\,|0\rangle \\ &= \int \frac{d^{D}\vec{k}}{2(2\pi)^{D}}\frac{\mathrm{e}^{i\vec{k}\cdot\Delta\vec{x}}\mathrm{e}^{i\omega\Delta t}}{\omega}, \end{aligned} \tag{2.6}$$

where we changed $\vec{k}\to-\vec{k}$ to stress that the only difference in the Wightman functions is in the sign of the frequency, we also used the notation $\Delta a = a - a'$. The positive/negative frequency Wightman function is just a transition amplitude between the creation of a particle at the point $(t,\vec{x})/(t',\vec{x}')$ and its detection at $(t',\vec{x}')/(t,\vec{x})$.

In addition, one sees that in the limit of point coincidence we have the usual divergence associated with the Minkowski vacuum. Which occurs when $k\to\infty$, being a ultraviolet divergence, i.e., due to high-energy modes.

Another important quantities are the expectation values of the fields commutator and anti-commutator, given by

$$\begin{aligned} iG(t,\vec{x};t',\vec{x}') &= \langle 0|\left[\hat{\phi}(t,\vec{x}),\hat{\phi}(t',\vec{x}')\right]|0\rangle \\ &= G^{+}(t,\vec{x};t',\vec{x}') - G^{-}(t,\vec{x};t',\vec{x}'), \end{aligned} \tag{2.7}$$

$$\begin{aligned} G^{(1)}(t,\vec{x};t',\vec{x}') &= \langle 0|\left\{\hat{\phi}(t,\vec{x}),\hat{\phi}(t',\vec{x}')\right\}|0\rangle \\ &= G^{+}(t,\vec{x};t',\vec{x}') + G^{-}(t,\vec{x};t',\vec{x}'), \end{aligned} \tag{2.8}$$

denoted by the Pauli-Jordan and Hadamard functions, respectively. Also the Feynman propagator, given by the time ordered product of the fields:

$$\begin{aligned} iG_{F}(t,\vec{x};t',\vec{x}') &= \langle 0|\,T\left(\hat{\phi}(t,\vec{x})\hat{\phi}(t',\vec{x}')\right)|0\rangle \\ &= \Theta(t-t')G^{+}(t,\vec{x};t',\vec{x}') + \Theta(t'-t)G^{-}(t,\vec{x};t',\vec{x}'). \end{aligned} \tag{2.9}$$

Finally, the retarded and advanced Green Functions are

$$G_{R}(t,\vec{x};t',\vec{x}') = -\Theta(t-t')G(t,\vec{x};t',\vec{x}'), \tag{2.10}$$

$$G_{_A}(t,\vec{x};t',\vec{x}') = \Theta(t'-t)G(t,\vec{x};t',\vec{x}'). \tag{2.11}$$

Another interesting remark is that the Feynman propagator is also given by [4]

$$G_{_F}(t,\vec{x};t',\vec{x}') = -\bar{G}(t,\vec{x};t',\vec{x}') - \frac{i}{2}G^{(1)}(t,\vec{x};t',\vec{x}'), \tag{2.12}$$

where:

$$\bar{G}(t,\vec{x};t',\vec{x}') = \frac{1}{2}\left[G_{_A}(t,\vec{x};t',\vec{x}') + G_{_R}(t,\vec{x};t',\vec{x}')\right]. \tag{2.13}$$

Note that when $\vec{x}\to\vec{x}'$ and $t\to t'$ we have $G_{_R} = -G_{_A}$, so $\bar{G}=0$ and $G_{_F} = -iG^{(1)}/2$. Further, the functions $G^{\pm}$ satisfy the homogeneous equation, as one can see by

$$(\Box_{(t,\vec{x})}+m^2)G^{+}(t,\vec{x};t',\vec{x}') = \langle 0|\,(\Box_{(t,\vec{x})}+m^2)\hat{\phi}(t,\vec{x})\hat{\phi}(t',\vec{x}')\,|0\rangle = 0, \tag{2.14}$$

as the field is a solution of the homogeneous equations. The above results straightforwardly extend to G^{-}, $G^{(1)}$ and iG, as the operator is linear.

For the advanced and retarded propagators, as they are multiplied by the Heaviside distribution, we have

$$\begin{aligned}(\Box_{(t,\vec{x})}+m^2)G_{_R}(t,\vec{x};t',\vec{x}') &= -(\Box_{(t,\vec{x})}+m^2)\Big[\Theta(t-t')G(t,\vec{x};t',\vec{x}')\Big].\\ &= -[\partial_t\delta(t-t')]G(t,\vec{x};t',\vec{x}') - 2\delta(t-t')\partial_t G(t,\vec{x};t',\vec{x}')\\ &\quad - \Theta(t-t')(\Box_{(t,\vec{x})}+m^2)G(t,\vec{x};t',\vec{x}')\\ &= -[\partial_t\delta(t-t')]G(t,\vec{x};t',\vec{x}') - 2\delta(t-t')\partial_t G(t,\vec{x};t',\vec{x}'),\end{aligned} \tag{2.15}$$

note that

$$\begin{aligned}\delta(t-t')\partial_t G(t,\vec{x};t',\vec{x}') &= -i\delta(t-t')\,\langle 0|\left[\partial_t\hat{\phi}(t,\vec{x}),\hat{\phi}(t',\vec{x}')\right]|0\rangle\\ &= -i\delta(t-t')\left[\hat{\pi}(t,\vec{x}),\hat{\phi}(t,\vec{x}')\right] = -\delta(t-t')\delta^D(\vec{x}-\vec{x}').\end{aligned} \tag{2.16}$$

Also, as we are dealing with a distribution, we must understand that the above expression only makes sense when integrated together with a suitable function f which has a compact support–see [30] for a proper description of distributions. Thence, note that

$$\begin{aligned}\int dt[\partial_t\delta(t-t')]G(t,\vec{x};t',\vec{x}')f(t) &= -\int dt\delta(t-t')[\partial_t G(t,\vec{x};t',\vec{x}')]f(t)\\ &\quad -\int dt\delta(t-t')G(t,\vec{x};t',\vec{x}')\partial_t f(t)\\ &= -\int dt\delta(t-t')[\partial_t G(t,\vec{x};t',\vec{x}')]f(t),\end{aligned} \tag{2.17}$$

where the Pauli-Jordan function is zero for $t=t'$ as one can see from the equal time commutation relations (1.28). Finally, we find

$$(\Box_{(t,\vec{x})}+m^2)G_{_R}(t,\vec{x};t',\vec{x}') = -\delta(t-t')\partial_t G(t,\vec{x};t',\vec{x}') = \delta(t-t')\delta^D(\vec{x}-\vec{x}'). \tag{2.18}$$

Thus, analogously for the advanced and Feynman propagator we have

$$(\Box + m^2)G_{_A}(t, \vec{x}; t', \vec{x}') = \delta(t - t')\delta^D(\vec{x} - \vec{x}'), \tag{2.19}$$

$$(\Box + m^2)G_{_F}(t, \vec{x}; t', \vec{x}') = -\delta(t - t')\delta^D(\vec{x} - \vec{x}') \tag{2.20}$$

Moreover, as we have defined the Green functions, we now examine some properties of the Wightman functions from which we infer important properties of the fields. Thence, for space-like intervals, i.e., $|\Delta\vec{x}| > |\Delta t|$, one can always make $|\Delta t| = 0$ by a suitable Lorentz transformation. Therefore, as for equal times the Pauli-Jordan function vanishes, so does the retarded and advanced propagators intervals, ensuring the micro-causality condition, i.e., there is no signal propagation between events separated by space-like intervals. Additionally, for time-like intervals, $|\Delta\vec{x}| < |\Delta t|$, we can make, as before, $|\Delta\vec{x}| = 0$, so that

$$\begin{aligned} G^{\pm}(t, \vec{x}; t'\vec{x}') = \int \frac{d^D k}{2(2\pi)^D} \frac{\mathrm{e}^{\mp i\omega\Delta t}}{\omega} &\propto \int_0^\infty dk\, k^{D-1} \frac{\mathrm{e}^{\mp i\sqrt{k^2+m^2}\Delta t}}{\sqrt{k^2+m^2}} \\ &= \int_m^\infty dE\, (E^2 - m^2)^{D/2-1} \mathrm{e}^{\mp iE\Delta t}, \end{aligned} \tag{2.21}$$

where we substituted $E = \sqrt{k^2 + m^2}$. Moreover, when $m \to 0$

$$G^{\pm}(t, \vec{x}; t'\vec{x}') \propto \lim_{\varepsilon\to 0^+} \int_0^\infty dE\, E^{D-2} \mathrm{e}^{-(\varepsilon \mp i\Delta t)E} = \frac{\Gamma(D-1)}{(\mp\Delta t)^{D-1}}. \tag{2.22}$$

The integration is valid for $D > 1$, where for $D = 1$ we have an infrared divergence, which will be discussed later. Thence, in the massless regime when D is odd the Wightman functions G^+ and G^- are equal and their commutator vanishes in the time-like region. Hence, the retarded and advanced propagator also vanish for time-like intervals, that is, satisfy the Huygens principle (note that for massive field and when D is even that is not true). Which states that two events can only be causally related when separated by light-like intervals.

The non-Huygesian character of the massive scalar fields–or massless fields with D even–will be extensively exploited in this work. For those fields, in addition to the light-like signal, the retarded propagator is different from zero for every time-like interval. Which means that a standing observer will receive a never ending oscillatory signal, in contrast to an unique light-like signal of the Huygesian fields. As stated in Ref. [1], in the case of massive fields one can understand this behavior by analyzing the propagation modes for the scalar field in Equation (1.39), which has the group velocity $v_g = k/\sqrt{k^2 + m^2}$. The modes then propagates in all possible velocities–below that of the light in vacuum–, which causes an interference pattern, i.e., oscillations in the propagating signals.

Further, the above defined Green functions are actually distributions in the real axis, however, through an analytic continuation to the complex plane, we can define

them as functions of complex numbers, revealing some interesting properties. For that we introduce a complex variable $z = t + is$, with $t, s \in \mathbb{R}$. Hence, in the complex plane spawned by Δz, it is clear from the expressions (2.5) and (2.6) that the functions are only well defined in the lower and upper half-plane, respectively [33]–as otherwise they diverge exponentially as $\Delta s \to \infty$.

Moreover, both functions are equal when $|\Delta\vec{x}| > |\Delta t|$. Then, by the edge-of-the-wedge theorem–see [30] for a statement and proof of the theorem–both functions are analytic continuations of each other. Thereby, we can define, for fixed unequal $\vec{x}$ and $\vec{x'}$, a holomorphic function such that

$$\mathcal{G}(z, \vec{x}; z', \vec{x}') = \begin{cases} G^{+}(z, \vec{x}; z', \vec{x}') & \text{if } \mathrm{Im}\Delta z < 0, \\ G^{-}(z, \vec{x}; z', \vec{x}') & \text{if } \mathrm{Im}\Delta z > 0. \end{cases} \tag{2.23}$$

Note that both equalities holds if $\mathrm{Im}\Delta z = 0$ and $\mathrm{Re}|\Delta z| < |\Delta\vec{x}|$. With poles at $\mathrm{Re}|\Delta z| = |\Delta\vec{x}|$ and, if they don't obey the Huygens principle, branch cuts for $\mathrm{Re}|\Delta z| > |\Delta\vec{x}|$. We can write this function as

$$\mathcal{G}(z, \vec{x}; z', \vec{x}') = \frac{i}{(2\pi)^{D+1}} \int d^{D}\vec{k} \int dk_0 \frac{\exp(i\vec{k}\cdot\Delta\vec{x} - ik_0\Delta z)}{k_0^2 - k^2 - m^2}. \tag{2.24}$$

Which is the integral representation of the defined Green functions. Each one given by a suitable choice of the contour taken to avoid the poles $k_0 = \pm\sqrt{k^2 + m^2}$ in the real line.

For pure imaginary values of $\Delta z = i\Delta s$, changing the variable $k_0 = i\kappa$ we find that

$$\begin{aligned} \mathcal{G}(is, \vec{x}; is', \vec{x}') = G_{E}(s, \vec{x}; s', \vec{x}') &= \frac{1}{(2\pi)^{D+1}} \int d^{D}\vec{k} \int d\kappa \frac{\exp(i\vec{k}\cdot\Delta\vec{x} + i\kappa\Delta s)}{\kappa^2 + k^2 + m^2} \\ &= \int \frac{d^{D}\vec{k}}{2(2\pi)^{D}} \frac{\mathrm{e}^{i\vec{k}\cdot\Delta\vec{x}}\mathrm{e}^{-i\omega|\Delta s|}}{\omega}, \end{aligned} \tag{2.25}$$

which is the Euclidean Green function, because it satisfies the dynamical Equation (1.24) on an Euclidean space, that is

$$(\Box_{E} - m^2)G_{E}(s, \vec{x}; s', \vec{x}') = \delta(s - s')\delta^{(D)}(\vec{x} - \vec{x}'), \tag{2.26}$$

with the elliptic operator

$$\Box_{E} = \frac{\partial^2}{\partial s^2} + \frac{\partial^2}{\partial x_1^2} + ... + \frac{\partial^2}{\partial x_{D}^2}, \tag{2.27}$$

that is the D'Alambertian in a D+1-dimensional Euclidean space.

The elliptic operator has an advantage because it has an unique inverse, which states that the function $G_{E}(s, \vec{x}; s', \vec{x}')$ is the unique solution to Eq. (2.26) which decays as $|\Delta s| \to \infty$, avoiding the ambiguity in choosing between contours in Eq. (2.24).

The Euclidean Green function can be turned into the Feynman propagator through a rigid rotation from the Δs axis to the Δt axis:

$$G_{_E}(-it,\vec{x};-it',\vec{x}') = G_{_F}(t,\vec{x};t',\vec{x}'). \tag{2.28}$$

Thence, when ambiguities arise, an usual strategy to choose between Green functions is to change coordinates to an Euclidean space, which, when changed back to the usual Minkowski spacetime gives the Feynman propagator.

Finally, in order to evaluate the integrals presented in the positive and negative frequency Wightman functions, Eq. (2.5) and Eq. (2.6), we rewrite it using generalized spherical coordinates in D-dimensions, where we have that [34]

$$\begin{aligned}
k_1 &= k\cos\theta_{_1},\\
k_2 &= k\cos\theta_{_2}\sin\theta_{_1},\\
&\cdot\\
&\cdot\\
&\cdot\\
k_{D-1} &= k\cos\theta_{_{D-1}}\prod_{i=1}^{D-2}\sin\theta_{_i},\\
k_D &= k\prod_{i=1}^{D-1}\sin\theta_{_i},
\end{aligned} \tag{2.29}$$

and the Jacobian is

$$J = k^{^{D-1}}\sin^{^{D-2}}\theta_{_1}\sin^{^{D-3}}\theta_{_2}...\sin\theta_{_{D-2}}. \tag{2.30}$$

Furthermore, without loss of generality, we let $|\Delta\vec{x}|$ be in the k_1-direction, and the Wightman functions becomes

$$\begin{aligned}
G^{\pm}(t,\vec{x};t',\vec{x}') &= \frac{2\pi}{2(2\pi)^{^D}}\prod_{i=2}^{D-2}\left(\int_0^{\pi} d\,\theta_{_i}\sin^{^{D-1-i}}\theta_{_i}\right)\int_0^{\infty} dk k^{^{D-1}}\frac{\mathrm{e}^{\pm i\omega\Delta t}}{\omega}\int_0^{\pi} d\,\theta_{_1}\sin^{^{D-2}}\theta_{_1}\mathrm{e}^{ik|\Delta\vec{x}|\cos\theta_{_1}}\\
&= \frac{1}{2^{^D}\pi^{^{\frac{D+1}{2}}}\Gamma(\frac{D-1}{2})}\int_0^{\infty} dk k^{^{D-1}}\frac{\mathrm{e}^{\pm i\omega\Delta t}}{\omega}\int_0^{\pi} d\,\theta_{_1}\sin^{^{D-2}}\theta_{_1}\mathrm{e}^{ik|\Delta\vec{x}|\cos\theta_{_1}},
\end{aligned} \tag{2.31}$$

using that [32]

$$\int_0^{\pi} d\,\theta_{_1}\sin^{^{D-2}}\theta_{_1}\mathrm{e}^{ik|\Delta\vec{x}|\cos\theta_{_1}} = \pi^{^{\frac{1}{2}}}\Gamma\left(\frac{D-1}{2}\right)\left(\frac{2}{k|\Delta\vec{x}|}\right)^{^{\frac{D}{2}-1}} J_{_{\frac{D}{2}-1}}(k|\Delta\vec{x}|), \tag{2.32}$$

we find that,

$$G^{\pm}(t,\vec{x};t',\vec{x}') = \frac{1}{2(2\pi)^{^{\frac{D}{2}}}|\Delta\vec{x}|^{^{\frac{D}{2}-1}}}\lim_{\epsilon\to 0^+}\int_0^{\infty} dk k^{^{\frac{D}{2}}}\frac{\mathrm{e}^{\mp i\omega(\Delta t\mp i\epsilon)}}{\omega}J_{_{\frac{D}{2}-1}}(k|\Delta\vec{x}|), \tag{2.33}$$

where a small number ϵ is added to ensure convergence, underlining the distributional character of the above Green functions.

To solve the above integral, we make the change of coordinates $u = \sqrt{(k/m)^2 + 1}$, thence

$$\begin{aligned}\int_0^\infty dk k^{\frac{D}{2}} \frac{\mathrm{e}^{\mp im(\Delta t \mp i\epsilon)\sqrt{(k/m)^2+1}}}{m\sqrt{(k/m)^2+1}} J_{\frac{D}{2}-1}(k|\Delta\vec{x}|) \\ = m^{\frac{D}{2}} \int_1^\infty du\Big(\sqrt{x^2-1}\Big)^{\frac{D}{2}-1} \mathrm{e}^{\mp im(\Delta t \mp i\epsilon)x} J_{\frac{D}{2}-1}\Big(m|\Delta\vec{x}|\sqrt{x^2-1}\Big) \\ = m^{\frac{D-1}{2}} \sqrt{\frac{2}{\pi}} \frac{|\Delta\vec{x}|^{\frac{D}{2}-1}}{\Big[\sqrt{(\Delta\vec{x})^2 - (\Delta t \mp i\epsilon)^2}\Big]^{\frac{D-1}{2}}} K_{\frac{D-1}{2}}\Big[m\sqrt{(\Delta\vec{x})^2 - (\Delta t \mp i\epsilon)^2}\Big], \quad (2.34)\end{aligned}$$

where we used the result found in Ref. [35] (eq. 6.645.2).

The Wightman functions becomes

$$G^{\pm}(t,\vec{x};t',\vec{x}') = \lim_{\epsilon\to 0^+} \frac{1}{2\pi}\left(\frac{m}{2\pi i\sigma}\right)^{\frac{D-1}{2}} K_{\frac{D-1}{2}}(im\sigma), \quad (2.35)$$

with $\sigma = \sqrt{(\Delta t \mp i\epsilon)^2 - (\Delta\vec{x})^2}$. Note that, despite the above expression seems the same for G^+ and G^-, they differ in the sign for ϵ. Moreover, in the rest of the work, the above distribution will only be used smeared over differentiable functions defined on compact domains, which will ensure convergence without the need to take the limit $\epsilon \to 0^+$. Thence, from now on, we will omit ϵ from the expressions for the Green Function, unless stated otherwise.

As the Wightman functions are just the complex conjugate of one another, the Hadamard function $G^{(1)}$, which is the sum of both becomes

$$G^{(1)}(t,\vec{x};t',\vec{x}') = 2Re\left[G^{\pm}(t,\vec{x};t',\vec{x}')\right] = \frac{1}{\pi} Re\left\{\left(\frac{m}{2\pi i\sigma}\right)^{\frac{D-1}{2}} K_{\frac{D-1}{2}}(im\sigma)\right\}. \quad (2.36)$$

In addition, note that, for $D = 1$, we have

$$G^{\pm}(t,\vec{x};t',\vec{x}') = \frac{1}{2\pi} K_0(im\sigma). \quad (2.37)$$

Which diverges as $m \to 0$, a well known infrared divergence, which is a major problem for quantum field theories at two dimensions as a definition for the Wightman functions is crucial for the construction of the theory [33].

The ultraviolet divergence appearing on the light-cone display the well known divergence at the vacuum energy, it is fairly understood that these divergences would not occur in a more realistic setup, as the high energy modes would activate gravitational effects. However, Quantum Gravity remains a reverie and, as the observable are constructed upon the vacuum expectation values, these must be renormalized. That is, for every expectation value, the Minkowski vacuum contribution must be subtracted.

At last, in the present work we will be interested in the modified vacuum, caused by the presence of a reflective boundary at $x_1 = 0$, in which we impose Dirichlet boundary conditions $\phi(t, x_1 = 0) = 0$. In order to do this one must solve again the dynamical equation submitted to such conditions. However, we follow here the image charge procedure, proposed by Brown and McClay [24], in which the field of an image charge with coordinates $\tilde{x}_1 = -x_1$ is subtracted from the usual field, so that the boundary conditions are satisfied.

With that the Wightman functions in the presence of a reflective boundary are

$$\begin{aligned}\tilde{G}^{\pm}(t,\vec{x};t',\vec{x}') &= G^{\pm}(t,\vec{x};t',\vec{x}') - G^{\pm}(t,\vec{x};t',\vec{\tilde{x}}') \\ &= \int \frac{d^D\vec{k}}{2(2\pi)^D}\frac{e^{i\vec{k}\cdot\Delta\vec{x}}e^{\mp i\omega\Delta t}}{\omega} - \int \frac{d^D\vec{k}}{2(2\pi)^D}\frac{e^{i\vec{k}\cdot\hat{\Delta}\vec{x}}e^{\mp i\omega\Delta t}}{\omega} \\ &= \frac{1}{2\pi}\left(\frac{m}{2\pi i\sigma}\right)^{\frac{D-1}{2}} K_{\frac{D-1}{2}}(im\sigma) - \frac{1}{2\pi}\left(\frac{m}{2\pi i\hat{\sigma}}\right)^{\frac{D-1}{2}} K_{\frac{D-1}{2}}(im\hat{\sigma}),\end{aligned} \tag{2.38}$$

where $\Delta\vec{x} \to \hat{\Delta}\vec{x}$ as $x_1' \to -x_1'$ and $\sigma \to \hat{\sigma}$ when $\Delta\vec{x} \to \hat{\Delta}\vec{x}$. It is clear that this functions satisfies the boundary condition $\tilde{G}^{\pm}(t,\vec{x};t',\vec{x}') = 0$ when $x_1 = 0$ or $x_1' = 0$.

Further, the boundary condition changes the topology of the space in which $G^{\mp}$ acts and, as the renormalization procedure imposes that the contribution from the pure vacuum must be subtracted, only the image charge will contribute to measurable quantities.

In the present work we are interested in the effects of the renormalized Hadamard function

$$\tilde{G}^{(1)}_{Ren}(t,\vec{x};t',\vec{x}') = 2\mathrm{Re}\tilde{G}^{+}_{Ren}(t,\vec{x};t',\vec{x}') = -\frac{1}{\pi}\mathrm{Re}\left\{\left(\frac{m}{2\pi i\hat{\sigma}}\right)^{\frac{D-1}{2}} K_{\frac{D-1}{2}}(im\hat{\sigma})\right\}. \tag{2.39}$$

Physically, when the boundary condition is introduced, the propagation modes of the field that don't satisfy it are no more allowed solutions of the dynamical equation. Then, as the vacuum is subtracted, the modes that were present in the vacuum, but not in the presence of a plate remain; and they produce measurable effects, as in the Casimir effect [4]. Also, as the function is constructed to vanish at the plate, it becomes clear that, when the Minkowski contribution–an infinite quantity–is subtracted from it, what remains is an infinite quantity at the boundary.

2.2 Green functions at finite temperature

Up to now, we have dealt only with physical systems defined in pure states, meaning that they are isolated. So that, in order to bring more reality to the model, we suppose the system is in a thermal state in equilibrium with the external world.

The system, at temperature $T = \beta^{-1}$, will now be described by a statistical ensemble through the density operator defined by Eq. (1.8). Also, as we are dealing with a relativistic field, particles can be created and destroyed at any time within our system, hence we assume that there is no exchange of particles with the external reservoir, so the chemical potential μ is zero.

It follows that the Wightman function for a scalar field at finite temperature is simply the expectation value on the statistical ensemble

$$G^{+}_{\beta}(t,\vec{x};t',\vec{x}') = \langle\hat{\phi}(t,\vec{x})\hat{\phi}(t',\vec{x}')\rangle_{\beta}, \tag{2.40}$$

$$G^{-}_{\beta}(t,\vec{x};t',\vec{x}') = \langle\hat{\phi}(t',\vec{x}')\hat{\phi}(t,\vec{x})\rangle_{\beta}. \tag{2.41}$$

An important property of quantum fields at finite temperature is the KMS relations [4]:

$$G^{+}_{\beta}(t,\vec{x};t',\vec{x}') = G^{-}_{\beta}(t+i\beta,\vec{x};t',\vec{x}'). \tag{2.42}$$

To assert the above expression, first remember that the time evolution of an operator is

$$\hat{\phi}(t,\vec{x}) = \mathrm{e}^{i\hat{H}t}\hat{\phi}(0,\vec{x})\mathrm{e}^{-i\hat{H}t}. \tag{2.43}$$

Hence, we have that

$$\begin{aligned} G^{+}_{\beta}(t,\vec{x};t',\vec{x}') = \langle\hat{\phi}(t,\vec{x})\hat{\phi}(t',\vec{x}')\rangle_{\beta} &= \frac{tr[\mathrm{e}^{-\beta\hat{H}}\hat{\phi}(t,\vec{x})\hat{\phi}(t',\vec{x}')]}{tr[\mathrm{e}^{-\beta\hat{H}}]} \\ &= \frac{tr[\mathrm{e}^{-\beta\hat{H}}\hat{\phi}(t,\vec{x})\mathrm{e}^{\beta\hat{H}}\mathrm{e}^{-\beta\hat{H}}\hat{\phi}(t',\vec{x}')]}{tr[\mathrm{e}^{-\beta\hat{H}}]} \\ &= \frac{tr[\mathrm{e}^{-\beta\hat{H}}\hat{\phi}(t',\vec{x}')\hat{\phi}(t+i\beta,\vec{x})]}{tr[\mathrm{e}^{-\beta\hat{H}}]} \\ &= G^{-}_{\beta}(t+i\beta,\vec{x};t',\vec{x}'). \end{aligned} \tag{2.44}$$

Following the steps on Ref. [4], note that for G, as the commutator is a c-number, the expectation value is the same as the one in the vacuum

$$\begin{aligned} iG_{\beta}(t,\vec{x};t',\vec{x}') &= \langle[\hat{\phi}(t,\vec{x})\hat{\phi}(t',\vec{x}')]\rangle_{\beta} \\ &= [\hat{\phi}(t,\vec{x})\hat{\phi}(t',\vec{x}')]\sum_{n}\delta_{mn}\rho_{mn} = [\hat{\phi}(t,\vec{x})\hat{\phi}(t',\vec{x}')], \end{aligned}$$

so that $iG_{\beta}(t,\vec{x};t',\vec{x}') = iG(t,\vec{x};t',\vec{x}')$. Nonetheless, it is convenient to use the Pauli-Jordan function to calculate others Green functions. Note that

$$\begin{aligned} iG(t,\vec{x};t',\vec{x}') &= \int\frac{d^{D}\vec{k}}{(2\pi)^{D}}\frac{\mathrm{e}^{i\vec{k}\cdot\Delta\vec{x}}}{2\omega}\left(\mathrm{e}^{-i\omega\Delta t}-\mathrm{e}^{i\omega\Delta t}\right) \\ &= \int\frac{d^{D}\vec{k}}{(2\pi)^{D}}\frac{\mathrm{e}^{i\vec{k}\cdot\Delta\vec{x}}}{2\omega}\int dk_0\left[\delta(k_0-\omega)\mathrm{e}^{-ik_0\Delta t}-\delta(k_0+\omega)\mathrm{e}^{-ik_0\Delta t}\right]. \end{aligned} \tag{2.45}$$

Where we rewrote it as a Fourier transform

$$iG(t,\vec{x};t',\vec{x}') = \frac{1}{2\pi}\int dk_0 c(k_0,\vec{x},\vec{x}')\mathrm{e}^{-ik_0\Delta t}, \tag{2.46}$$

with

$$c(k_0,\vec{x},\vec{x}') = \int \frac{d^D\vec{k}}{(2\pi)^{D-1}}\mathrm{e}^{i\vec{k}\cdot\Delta\vec{x}}\delta(k_0^2-\omega^2)\left[\Theta(k_0)-\Theta(-k_0)\right]. \tag{2.47}$$

Forthwith, the Wightman functions can also be rewrote as Fourier transforms

$$G^{\pm}_{\beta} = \frac{1}{2\pi}\int dk_0 g^{\pm}(k_0,\vec{x},\vec{x}')\mathrm{e}^{-ik_0\Delta t}, \tag{2.48}$$

from which, by using the KMS condition

$$g^{+}(k_0,\vec{x},\vec{x}') = g^{-}(k_0,\vec{x},\vec{x}')\mathrm{e}^{k_0\beta}. \tag{2.49}$$

Thence, from the definition of the Pauli-Jordan function,

$$c(k_0,\vec{x},\vec{x}') = g^{+}(k_0,\vec{x},\vec{x}') - g^{-}(k_0,\vec{x},\vec{x}') = -g^{-}(k_0,\vec{x},\vec{x}')(1-\mathrm{e}^{k_0\beta}), \tag{2.50}$$

and we have:

$$g^{\pm}(k_0,\vec{x},\vec{x}') = \pm\frac{c(k_0,\vec{x},\vec{x}')}{1-\mathrm{e}^{\mp k_0\beta}}. \tag{2.51}$$

From which we find that

$$\begin{aligned} G^{\pm}_{\beta}(t,\vec{x};t',\vec{x}') &= \pm\frac{1}{2\pi}\int dk_0 \frac{c(k_0)}{1-\mathrm{e}^{\mp k_0\beta}}\mathrm{e}^{-ik_0\Delta t} \\ &= \pm\int \frac{d^D\vec{k}}{(2\pi)^D}\frac{\mathrm{e}^{i\vec{k}\cdot\Delta\vec{x}}}{2\omega}\left(\frac{\mathrm{e}^{-i\omega\Delta t}}{1-\mathrm{e}^{\mp\omega\beta}} - \frac{\mathrm{e}^{i\omega\Delta t}}{1-\mathrm{e}^{\pm\omega\beta}}\right). \end{aligned} \tag{2.52}$$

First, for the positive part

$$\begin{aligned} G^{+}_{\beta}(t,\vec{x};t',\vec{x}') &= \int \frac{d^D\vec{k}}{(2\pi)^D}\frac{\mathrm{e}^{i\vec{k}\cdot\Delta\vec{x}}}{2\omega}\left(\frac{\mathrm{e}^{-i\omega\Delta t}+\mathrm{e}^{-\omega\beta}\mathrm{e}^{i\omega\Delta t}}{1-\mathrm{e}^{-\omega\beta}}\right) \\ &= \int \frac{d^D\vec{k}}{(2\pi)^D}\frac{\mathrm{e}^{i\vec{k}\cdot\Delta\vec{x}}}{2\omega}\sum_{l=0}^{\infty}\mathrm{e}^{-\omega l\beta}\left(\mathrm{e}^{-i\omega\Delta t}+\mathrm{e}^{-\omega\beta}\mathrm{e}^{i\omega\Delta t}\right) \\ &= \int \frac{d^D\vec{k}}{(2\pi)^D}\frac{\mathrm{e}^{i\vec{k}\cdot\Delta\vec{x}}}{2\omega}\left[\mathrm{e}^{-i\omega\Delta t}+\sum_{l=1}^{\infty}\left(\mathrm{e}^{-i\omega(\Delta t-il\beta)}+\mathrm{e}^{i\omega(\Delta t+il\beta)}\right)\right]. \end{aligned} \tag{2.53}$$

Analogously, for the negative part

$$G^{-}_{\beta}(t,\vec{x};t',\vec{x}') = \int \frac{d^D\vec{k}}{(2\pi)^D}\frac{\mathrm{e}^{i\vec{k}\cdot\Delta\vec{x}}}{2\omega}\left[\mathrm{e}^{i\omega\Delta t}+\sum_{l=1}^{\infty}\left(\mathrm{e}^{-i\omega(\Delta t-il\beta)}+\mathrm{e}^{i\omega(\Delta t+il\beta)}\right)\right]. \tag{2.54}$$

Finally, the Hadamard function

$$G^{(1)}_{\beta}(t,\vec{x};t',\vec{x}') = G^{(1)}(t,\vec{x};t'\vec{x}') + 2\sum_{l=1}^{\infty}\int \frac{d^D\vec{k}}{(2\pi)^D}\frac{\mathrm{e}^{i\vec{k}\cdot\Delta\vec{x}}}{2\omega}\left[\mathrm{e}^{-i\omega(\Delta t-il\beta)}+\mathrm{e}^{i\omega(\Delta t+il\beta)}\right]. \tag{2.55}$$

Using the same procedure used to find Eq. (2.33), we can rewrite $G^{(1)}$ as

$$\begin{aligned} G^{(1)}_{\beta}(t,\vec{x};t',\vec{x}') &= G^{(1)}(t,\vec{x};t'\vec{x}') + 2\sum_{l=1}^{\infty}\frac{1}{2(2\pi)^{\frac{D}{2}}|\Delta\vec{x}|^{\frac{D}{2}-1}} \\ &\times\int_0^{\infty}dk\frac{k^{\frac{D}{2}}}{\omega}J_{\frac{D}{2}-1}(k|\Delta\vec{x}|)\left[\mathrm{e}^{-i\omega(\Delta t-il\beta)}+\mathrm{e}^{i\omega(\Delta t+il\beta)}\right] \\ &= G^{(1)}(t,\vec{x};t'\vec{x}') + \frac{1}{(2\pi)^{\frac{D}{2}}|\Delta\vec{x}|^{\frac{D}{2}-1}}\left[\sum_{l=-\infty}^{-1}\int_0^{\infty}dk\frac{k^{\frac{D}{2}}}{\omega}\mathrm{e}^{-i\omega(\Delta t+il\beta)}J_{\frac{D}{2}-1}(k|\Delta\vec{x}|)\right. \\ &\left.+\sum_{l=1}^{\infty}\int_0^{\infty}dk\frac{k^{\frac{D}{2}}}{\omega}\mathrm{e}^{i\omega(\Delta t+il\beta)}J_{\frac{D}{2}-1}(k|\Delta\vec{x}|)\right], \end{aligned} \tag{2.56}$$

integrating, as was done in Equation (2.33), we find

$$\begin{aligned} G^{(1)}_{\beta}(t,\vec{x};t',\vec{x}') &= \frac{1}{\pi}\mathrm{Re}\left\{\left(\frac{m}{2\pi i\sigma}\right)^{\frac{D-1}{2}}K_{\frac{D-1}{2}}(im\sigma)\right\}+\sum_{l\neq 0}\frac{1}{\pi}\left(\frac{m}{2\pi i\sigma_l}\right)^{\frac{D-1}{2}}K_{\frac{D-1}{2}}(im\sigma_l) \\ &= \sum_{l=-\infty}^{\infty}G^{(1)}(t+il\beta,\vec{x};t'\vec{x}'), \end{aligned} \tag{2.57}$$

with $\sigma_l = \sqrt{(\Delta t+il\beta)^2-(\Delta\vec{x})^2}$, which is the well known imaginary time summation formula.

The above formula clearly suggests a periodicity of the function in imaginary time. In order to state that in a correct manner, we investigate, as before, the behavior of the function in the complex plane given by Δz. So, as before, with $z = t+is$, we have

$$G^{+}_{\beta}(z,\vec{x};z',\vec{x}') = \int\frac{d^D\vec{k}}{(2\pi)^D}\frac{\mathrm{e}^{i\vec{k}\cdot\Delta\vec{x}}}{2\omega}\left\{\mathrm{e}^{-i\omega\Delta t}\mathrm{e}^{\omega\Delta s}+\sum_{l=1}^{\infty}\left[\mathrm{e}^{-\omega(l\beta-\Delta s)}\mathrm{e}^{-i\omega\Delta t}+\mathrm{e}^{-\omega(l\beta+\Delta s)}\mathrm{e}^{i\omega\Delta t}\right]\right\}, \tag{2.58}$$

$$G^{-}_{\beta}(z,\vec{x};z',\vec{x}') = \int\frac{d^D\vec{k}}{(2\pi)^D}\frac{\mathrm{e}^{i\vec{k}\cdot\Delta\vec{x}}}{2\omega}\left\{\mathrm{e}^{i\omega\Delta t}\mathrm{e}^{-\omega\Delta s}+\sum_{l=1}^{\infty}\left[\mathrm{e}^{-\omega(l\beta+\Delta s)}\mathrm{e}^{-i\omega\Delta t}+\mathrm{e}^{-\omega(l\beta-\Delta s)}\mathrm{e}^{i\omega\Delta t}\right]\right\}. \tag{2.59}$$

Hence, one sees that the functions G^{+}_{β} and G^{-}_{β} are holomorphic in the strips where $0 > \Delta s > -\beta$ and $\beta > \Delta s > 0$. Moreover, from the KMS condition, the Wightman functions are defined in the complex plane by intercalating strips in which G^{+} and G^{-} are defined. Note also that the complex-plane is now turned into a cylinder, with the imaginary axis being a circumference of length equal 2β.

Remember that the Pauli-Jordan function, as a complex number, is the same as the one for the vacuum, so that results obtained remain valid, i.e, the Huygesian or non-Huygesian character of the propagators and that the commutator vanishes in space-like intervals, where both Wightman functions coincide. Then, again by the edge-of-the-wedge

theorem, the functions are analytic continuations of each other, and we can define the holomorphic function

$$\mathcal{G}_{\beta}(z,\vec{x};z',\vec{x}') = \begin{cases} G^{+}_{\beta}(z,\vec{x};z',\vec{x}') & \text{if } 0 > \mathrm{Im}\Delta z > -\beta, \\ G^{-}_{\beta}(z,\vec{x};z',\vec{x}') & \text{if } \beta > \mathrm{Im}\Delta z > 0. \end{cases} \tag{2.60}$$

Which is periodic in the imaginary axis with period 2β. Thus, this function acting on the space $\mathbb{R}\times\mathbb{R}^{D+1}$ is just the zero temperature function acting on $\mathbb{S}^1\times\mathbb{R}^{D+1}$, in which the imaginary time axis is turned into a circumference.

In addition, the Euclidean function is defined as before, and all its relations with the others remains the same as for the zero temperature case. However, when the field is massless, an infrared divergence do not appear only for $D=1$, as the periodicity in imaginary times creates an infrared divergence also for $D=2$ [33], as $K_{\frac{1}{2}}(z)=\sqrt{\pi/(2z)}\,\mathrm{e}^{-z}$ for $D=2$ we have that

$$G^{(1)}_{\beta}(t,\vec{x};t'\vec{x}') = \mathrm{Re}\left[\frac{1}{2\pi i\sigma}\mathrm{e}^{-im\sigma} + \sum_{l=1}^{\infty}\frac{1}{\pi i\sigma_l}\mathrm{e}^{-im\sigma_l}\right], \tag{2.61}$$

which diverges as $m\to 0$. Hence, as for $D=1$, quantum field theory is not well defined for $D=2$ at finite temperature [33]. Which amounts to saying that massless fields at 2 spatial dimensions cannot attain thermal equilibrium.

Finally, in the presence of the boundary at $x_1=0$, just as the case for zero temperature, we have that

$$\tilde{G}^{\pm}_{\beta}(t,\vec{x};t'\vec{x}') = \int\frac{d^D\vec{k}}{(2\pi)^D}\frac{\left(\mathrm{e}^{i\vec{k}\cdot\Delta\vec{x}}-\mathrm{e}^{i\vec{k}\cdot\hat{\Delta}\vec{x}}\right)}{2\omega}\left\{\mathrm{e}^{\mp i\omega\Delta t}+\sum_{l=1}^{\infty}\left[\mathrm{e}^{-i\omega(\Delta t-il\beta)}+\mathrm{e}^{i\omega(\Delta t+il\beta)}\right]\right\}. \tag{2.62}$$

And, the renormalized Hadamard function, that will be used to calculate the dispersion

$$\tilde{G}^{(1)}_{\beta,Ren}(t,\vec{x};t'\vec{x}') = \tilde{G}^{(1)}_{Ren}(t,\vec{x};t'\vec{x}') + \sum_{l\neq 0}\left[\frac{1}{\pi}\left(\frac{m}{2\pi i\sigma_l}\right)^{\frac{D-1}{2}}K_{\frac{D-1}{2}}(im\sigma_l)\right.$$
$$\left.-\frac{1}{\pi}\left(\frac{m}{2\pi i\hat{\sigma}_l}\right)^{\frac{D-1}{2}}K_{\frac{D-1}{2}}(im\hat{\sigma}_l)\right]. \tag{2.63}$$

Where we have excluded the vacuum term, when $l=0$, in the summations. Note that a convenient division appears between the terms in the right hand side of the above equation. First, the modified vacuum contribution, given by Eq. (2.39). Then the pure thermal part, that is just the renormalized free Hadamard function for a thermal state, which gives the black-body radiation energy of the gas. And the last is the mixed part, i.e., the thermal contribution coming from the gas in the presence of a reflective boundary. Also, from the relation (2.13), in the limit of point coincidence we obtain the Feynman propagator from the above equation and recover the results presented in Ref. [23], where the local thermal behavior of a massive scalar field is studied near a reflective wall.

3 Stochastic Motion due to the Fluctuations of a Massive Scalar Field

We studied the general aspects of a quantum massive scalar field both at zero and finite temperature, and now present its effects in an interaction with a test particle. As said, we investigate the stochastic motion induced by a change in the vacuum state of the field. The effects of this interaction for the case of a massive scalar field were studied in [1]. Here we generalize previous results to the finite temperature case, investigating first the motion due to a change from the Minkowski vacuum to a thermal bath of scalar bosons, followed by the introduction of a reflective boundary, and, at last, the effect due to the boundary term at finite temperature.

Moreover, we use switching functions to model the transition between the physical states of the field, bringing more reality to the model and regularizing divergences. Which were seen to occur in the original model [10] near the plate and when the interaction time τ equals two times the distance to the plate x, that is, a round trip of the photon. Such divergences link back to the problems found for the renormalized Green functions in the presence of a boundary and are connected to the sudden transition implemented between the states of the field, the perfectly reflective character of the boundary, and the non-quantum character of the test particle. Finally, we also analyze the behavior of the velocities dispersions with the distance of the particle to the plate, and show the interplay between vacuum and thermal contribution to the dispersions as the wall is approached.

3.1 Model of a test particle interacting with a scalar field

The interaction of a particle with a massive scalar field in a Minkowski spacetime with D spatial dimensions is obtained through the action [36]

$$S[\phi, \partial_\mu\phi; \tau, \vec{x}] = S_F - M\int ds - e\int ds\left[\int dt d^D z\, \phi(t, \vec{z})\delta(t-\tau)\delta(\vec{z}-\vec{x})\right], \tag{3.1}$$

where S_F is the action for the free scalar field (1.25), the point $(\tau, \vec{x})$ being the location of the test particle, M its mass, e the coupling charge through which it interacts with the scalar field, and $ds^2 = \eta_{\mu\nu}dx^\mu dx^\nu$ the infinitesimal interval between two events in the particle worldline.

Notwithstanding, we are interested in a classical non-relativistic test particle. Thence, to reduce the above action to the Newtonian regime we will, just for now, explicitly write the constant c, and assume the particles velocity $\vec{v} = d\vec{x}/d\tau$ is such that

$|\vec{v}| \ll c$. We have

$$\begin{aligned} S[\phi, \partial_\mu\phi; \tau, \vec{x}] &= S_F - \int d\tau \left[Mc^2\sqrt{1-\frac{v^2}{c^2}} + e\,\phi(\tau,\vec{x})\sqrt{1-\frac{v^2}{c^2}} \right] \\ &\simeq S_F + \int d\tau \left[\frac{M}{2}v^2 - e\,\phi(\tau,\vec{x}) \right] + \mathcal{O}(v^2/c^2). \end{aligned} \tag{3.2}$$

Thence, through the principle of least action, we find the dynamical equation for the test particle

$$\frac{dv_i}{d\tau} = -g\frac{\partial\phi(\tau,\vec{x})}{\partial x_i}, \tag{3.3}$$

where we denoted $g = e/M$. We assume that the particle position do not change significantly and that there is no dissipation, as in the original model [10]. Then, quantizing the field as was described in the previous chapter, the quantum mechanical operator for the velocity of the particle in the i-direction becomes

$$v_i(\tau) = -g\int_0^\tau dt \frac{\partial\hat{\phi}(t,\vec{x})}{\partial x_i}. \tag{3.4}$$

As the test particle will be immersed in the vacuum and in a field at thermal equilibrium, the mean value of the velocities will be zero, $\langle v_i\rangle$=0. However, quantum fluctuations of the field cause dispersions in the particle velocities, given by

$$\langle(\Delta v_i)^2\rangle_D = \langle v_i^2\rangle_\beta = g^2 \lim_{x\to x'}\left[\frac{\partial}{\partial x_i}\frac{\partial}{\partial x_i'}\int_0^\tau dt\int_0^\tau dt' \left\langle \hat{\phi}(t,\vec{x})\hat{\phi}(t',\vec{x}')\right\rangle_\beta \right]. \tag{3.5}$$

Note also that, in the presence of a classical force, it would not contribute to the dispersion, and the above formula would describe the dipersions of the velocities around the particle classical trajectory [10, 15]. Moreover, as the above equation has a product of non-commuting operators, the product must be symmetrized to avoid ambiguities, giving

$$\begin{aligned} \langle(\Delta v_i)^2\rangle_D &= \frac{g^2}{2}\lim_{x\to x'}\left[\frac{\partial}{\partial x_i}\frac{\partial}{\partial x_i'}\int_0^\tau dt\int_0^\tau dt' \left\langle \hat{\phi}(t,\vec{x})\hat{\phi}(t',\vec{x}') + \hat{\phi}(t',\vec{x}')\hat{\phi}(t,\vec{x})\right\rangle_\beta \right] \\ &= \frac{g^2}{2}\lim_{x\to x'}\left[\frac{\partial}{\partial x_i}\frac{\partial}{\partial x_i'}\int_0^\tau dt\int_0^\tau dt' G^{(1)}_{\beta,Ren}(t,\vec{x};t',\vec{x}') \right]. \end{aligned} \tag{3.6}$$

The above expression was renormalized, i.e., the Minkowski vacuum contribution was subtracted. Nonetheless, the dispersions given by Eq. (3.6), when the field is in the presence of a reflective boundary, was extensively studied for the massless case [15, 17, 18], and for the massive case at zero temperature [1]. Hence, as said, it was found that for a sudden transition the dispersion diverge at $x = 0$ and for $\tau = 2x$.

Henceforth, in order to describe a more realistic system, we introduce a switching function $F(t)$ that models a smooth transition between states of the system. Through this sample function we are able to regularize the appearing divergences. The interaction time τ must remain the same, so that

$$\int_{-\infty}^{\infty} dt F(t) = \tau. \tag{3.7}$$

The expression for the dispersion now becomes

$$\langle(\Delta v_i)^2\rangle_D = \frac{g^2}{2}\lim_{x\to x'}\left[\frac{\partial}{\partial x_i}\frac{\partial}{\partial x_i'}\int_{-\infty}^{\infty}dtF(t)\int_{\infty}^{\infty}dt'F(t')G^{(1)}_{\beta,\mathrm{Ren}}(t,\vec{x};t',\vec{x}')\right]. \tag{3.8}$$

In the next section we explore some properties of the function $F(t)$, how it regularizes the expression by dumping the high energy modes and will give some expressions for it.

3.2 Smooth switching function

As said, the divergences appearing in QFT are a problem of the theory, and many ways were encountered to circumvent them. Namely, it is understood that the high energy modes could not be described by quantum field theory in a flat space-time, as they would significantly curve it. Thence, a natural cut-off function could appear from these interactions [3]. However, as a Quantum Gravity theory is not yet present, the arose of such cuf-off is not clear. Furthermore, in the axiomatic construction of the theory proposed by Streater & Wightman, see Ref. [30], the quantum fields can only be defined smeared over test functions that are elements of the Schwartz space $\mathcal{P}$–the space of differentiable function that decay rapidly–stating the necessity of smearing the fields in order to obtain a consistent theory. Thence, in accordance with this axiomatic construction, here the fields will be defined over switching functions that models a smooth interaction between the field and the particle, bringing more reality to the system.

These functions, as we will see, suppresses the high-energy modes regularizing ultraviolet divergences–the infrared divergences, as we will see, are not regularized. Physically, what happens is that, as the switching is done smoothly, the transition for the high-energy modes is done adiabatically–compared to the frequency of the modes–and with that they do not contribute to the dispersions.

Forthwith, in the case of a boundary, applying Dirichlet's condition for all propagating modes implies an infinite potential barrier (or a perfectly reflective mirror in the electromagnetic case), which does not exists in nature. As it is changed to a physical potential, a smooth one, another cut-off function would be introduced. Nonetheless, if the value of this cut-off is higher then the one introduced by the switching function, the modes to be discarded by it are already suppressed by the smooth transition. So, the results presented here would remain completely valid.

Note also that these physical constrains on the propagation modes have no connection to gravitational interactions, and are not defined by a more fundamental theory. However, the physical constraints presented here discard modes of energy way lower than the ones that would be affected by gravitational interactions, so that these are irrelevant for our purpose.

A suitable choice of switching function is the generalized Lorentzian [37, 38, 15]

$$F_n^{(1)}(t) = \frac{c_n}{\left[1 + \left(\frac{2t}{\tau}\right)^{2n}\right]}, \tag{3.9}$$

with $c_n = (2n/\pi)\sin(\pi/2n)$, in order to satisfy the condition of Eq.(3.7). The behavior of the function for different values of n is depicted in Fig. 1. Note that, the index n indicates how smooth is the transition and as $n \to \infty$ we recover the sudden transition.

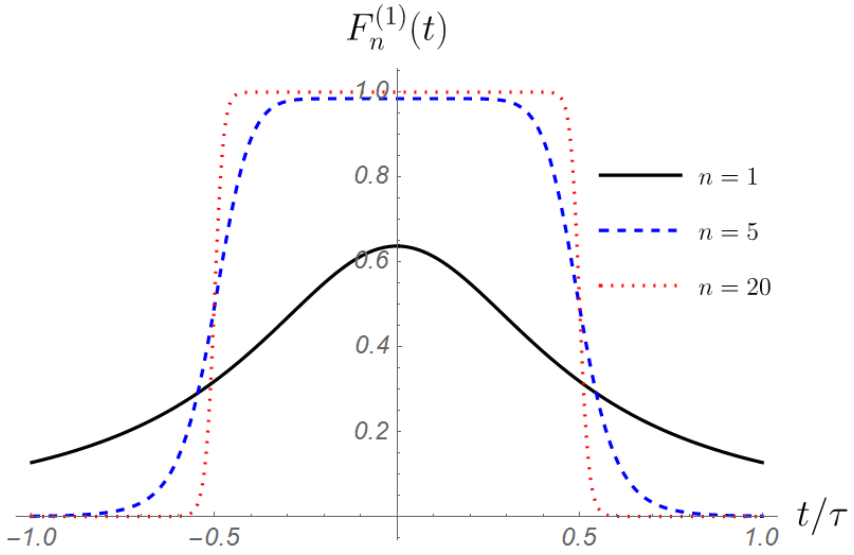

Fig. 1 – Behavior of the switching function $F_n^{(1)}(t)$. As n grows the transition becomes abrupter and, when $n \to \infty$, we recover the sudden transition.

The transition time τ_s is given by the difference between the nearest points of maximum curvature of the function, which are the zeros of its third derivative [15]. We find that

$$\begin{aligned}\tau_s = \frac{\tau}{2}\left(\frac{2n-1}{n+1}\right)^{\frac{1}{2n}} \Bigg[&\left(1 + \sqrt{1 - \frac{(n+1)(n-1)}{(2n+1)(2n-1)}}\right)^{\frac{1}{2n}} \\ &- \left(1 - \sqrt{1 - \frac{(n+1)(n-1)}{(2n+1)(2n-1)}}\right)^{\frac{1}{2n}} \Bigg].\end{aligned} \tag{3.10}$$

Note that τ_s grows with τ, and tends to infinity as $\tau \to \infty$, in such case there is no transition. Hence, this choice of switching function is not suitable to investigate the late-time regime.

Now, as it will reveal some interesting properties and will be useful later, we investigate the Fourier transform of $F_n^{(1)}(t)$,

$$\hat{F}_n^{(1)}(\omega) = \int_{-\infty}^{\infty} dt\, \mathrm{e}^{-i\omega t} F_n^{(1)}(t) = \frac{i\tau\pi c_n}{2n} \sum_{q=n}^{2n-1} \psi_{n,q} \mathrm{e}^{-i\omega\tau\psi_{n,q}/2}, \tag{3.11}$$

with $\psi_{n,p} = \exp[i(\pi/2n)(1+2p)]$. The full derivation is done in Ref. [15].

Furthermore, as the divergences appearing in Eq. (3.6) occurs because of the ultraviolet modes, i.e., modes with large values of ω, Fig. 2 clarify how $F_n^{(1)}(t)$ regularizes the problem: $|\hat{F}_n^{(1)}(\omega)|$ decreases exponentially with ω–remember that we define it as a positive quantity–suppressing the high-energy modes contribution to the dispersion.

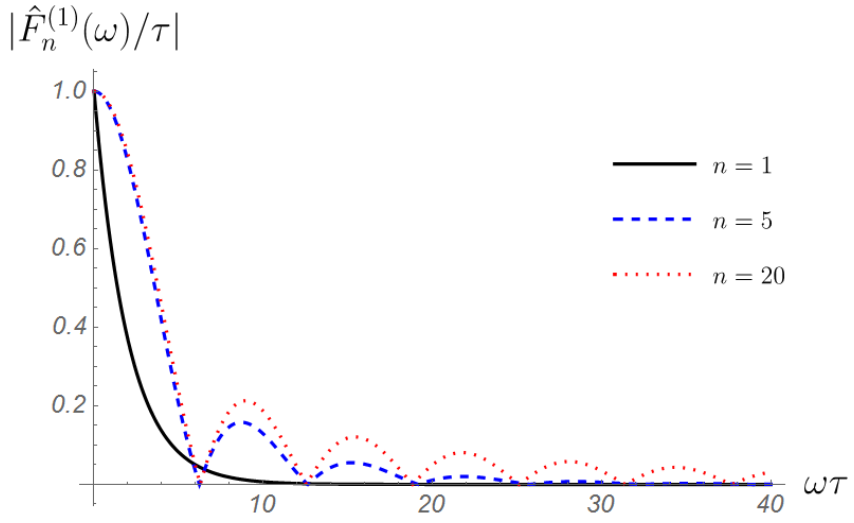

Fig. 2 – Plot of the Fourier transform of the function $F_n^{(1)}(t)$. The function decreases as $\omega\tau$ increases.

Accordingly, any function whose Fourier transform exponentially suppresses the high-energy modes is suitable to regularize the divergences. Thus, we can construct a switching function, with controllable switching time τ_s, following what was done in Ref. [1].

Starting from the transform of the sudden transition, $F^{(0)}(t) = \Theta(t)\Theta(\tau - t)$, $\hat{F}^{(0)}(\omega) = (1/i\omega)(1 - \mathrm{e}^{-i\omega\tau})$. We introduce a factor $\mathcal{D}(\omega)$, so that

$$\hat{F}(\omega) = \frac{1}{i\omega}(1 - \mathrm{e}^{-i\omega\tau})\mathcal{D}(\omega). \tag{3.12}$$

Which must be bounded as $\omega \to \infty$ and, to satisfy the normalization (3.7), $\mathcal{D}(0) = 1$. Additionally, as stated in [1], $\mathcal{D}(\omega)$ must be continuous, for $F(t)$ to be non-negative, and we should have that $F(t) = \Theta(t)\Theta(\tau - t)$ as $\tau_s \to 0$.

The most obvious choice is $\mathcal{D}(\omega) = e^{-\tau_s|\omega|}$, from which we have the test function

$$F_{\tau_s}^{(2)}(t) = \frac{1}{\pi}\left[\arctan\left(\frac{t}{\tau_s}\right) + \arctan\left(\frac{\tau - t}{\tau_s}\right)\right], \tag{3.13}$$

which derivative can be written in terms of Lorentzian functions. This switching was implemented in [18, 20] and is more accurate to describe the physical situation, as the interaction and the switching time can be independently set, which makes it also appropriate to investigate the late-time regime of the dispersion.

3.3 Velocity dispersions in a thermal bath

Forthwith, provided with the necessary tools, we calculate the velocity fluctuations caused by a quantum scalar field. First, we calculate it for a field in thermal equilibrium at temperature T, i.e., a gas of massive scalar bosons. The setup is as follows, the particle is immersed in a field at zero temperature, then the temperature is raised until the desired value. The switching function models the interaction between the field and the particle as they are smoothly taken into and out of equilibrium.

Substituting Expression (2.56) into Eq. (3.8) we have

$$\begin{aligned}\langle(\Delta v_i)^2\rangle_{D,\text{thermal}} &= g^2 \lim_{x\to x'}\left[\frac{\partial}{\partial x_i}\frac{\partial}{\partial x'_i}\sum_{l=1}^{\infty}\frac{1}{2(2\pi)^{\frac{D}{2}}|\Delta\vec{x}|^{\frac{D}{2}-1}}\int_0^\infty dk\frac{k^{\frac{D}{2}}}{\omega}J_{\frac{D}{2}-1}(k|\Delta\vec{x}|)\mathrm{e}^{-\omega l\beta}\right.\\ &\left.\times\left(\int_{-\infty}^{\infty}dtF(t)\int_{-\infty}^{\infty}dt'F(t')\mathrm{e}^{-i\omega\Delta t}+\int_{-\infty}^{\infty}dtF(t)\int_{-\infty}^{\infty}dt'F(t')\mathrm{e}^{i\omega\Delta t}\right)\right]\\ &= g^2\lim_{x\to x'}\left[\frac{\partial}{\partial x_i}\frac{\partial}{\partial x'_i}\frac{1}{2(2\pi)^{\frac{D}{2}}|\Delta\vec{x}|^{\frac{D}{2}-1}}\sum_{l=1}^{\infty}\int_0^\infty dk\frac{k^{\frac{D}{2}}}{\omega}2|\hat{F}(\omega)|^2e^{-l\beta\omega}J_{\frac{D}{2}-1}(k|\Delta\vec{x}|)\right].\end{aligned} \tag{3.14}$$

First, choosing the switching function $F_n^{(1)}(t)$, given by Eq. (3.10), which enables us to obtain a closed formula, and using Eq. (3.11) we have

$$\begin{aligned}\langle(\Delta v_i)^2\rangle^{(1)}_{D,\text{thermal}} = \left(\frac{g\tau\pi c_n}{2n}\right)^2\lim_{x\to x'}\left[\frac{\partial}{\partial x_i}\frac{\partial}{\partial x'_i}\frac{1}{(2\pi)^{\frac{D}{2}}|\Delta\vec{x}|^{\frac{D}{2}-1}}\sum_{p,q=n}^{2n-1}\sum_{l=1}^{\infty}\psi_{n,p}\psi^*_{n,q}\right.\\ \left.\times\int_0^\infty dk\frac{k^{\frac{D}{2}}}{\omega}e^{-i\omega\beta a_l}J_{\frac{D}{2}-1}(k|\Delta\vec{x}|)\right],\end{aligned} \tag{3.15}$$

with $a_l = (\tau/2\beta)(\psi_{n,p}-\psi^*_{n,q}) - il$.

By the same procedure used to solve the integral in Eq. (2.33), we solve the above integral, obtaining the same result with $\Delta t \to \beta a_l$. Then, note that

$$\begin{aligned}\lim_{x\to x'}\left\{\frac{\partial}{\partial x_i}\frac{\partial}{\partial x'_i}\left[\left(\frac{m}{\sqrt{|\Delta\vec{x}|^2-(\beta a_l)^2}}\right)^{(\frac{D-1}{2})}K_{\frac{D-1}{2}}\left(m\sqrt{|\Delta\vec{x}|^2-(\beta a_l)^2}\right)\right]\right\}\\ = \frac{1}{\beta^{D+1}}\left(\frac{m\beta}{\sqrt{-a_l^2}}\right)^{\frac{D+1}{2}}K_{\frac{D+1}{2}}\left(m\beta\sqrt{-a_l^2}\right).\end{aligned} \tag{3.16}$$

Thus, the closed expression for the dispersion caused by a thermal bath is

$$\langle(\Delta v_i)^2\rangle^{(1)}_{D,\text{thermal}} = \frac{2g^2}{\beta^{D-1}}\left[\frac{(\tau/\beta)\pi c_n}{2n}\right]^2\sum_{p,q=n}^{2n-1}\sum_{l=1}^{\infty}\psi_{n,p}\psi^*_{n,q}\left(\frac{m\beta}{2\pi\sqrt{-a_l^2}}\right)^{\frac{D+1}{2}}K_{\frac{D+1}{2}}\left(m\beta\sqrt{-a_l^2}\right). \tag{3.17}$$

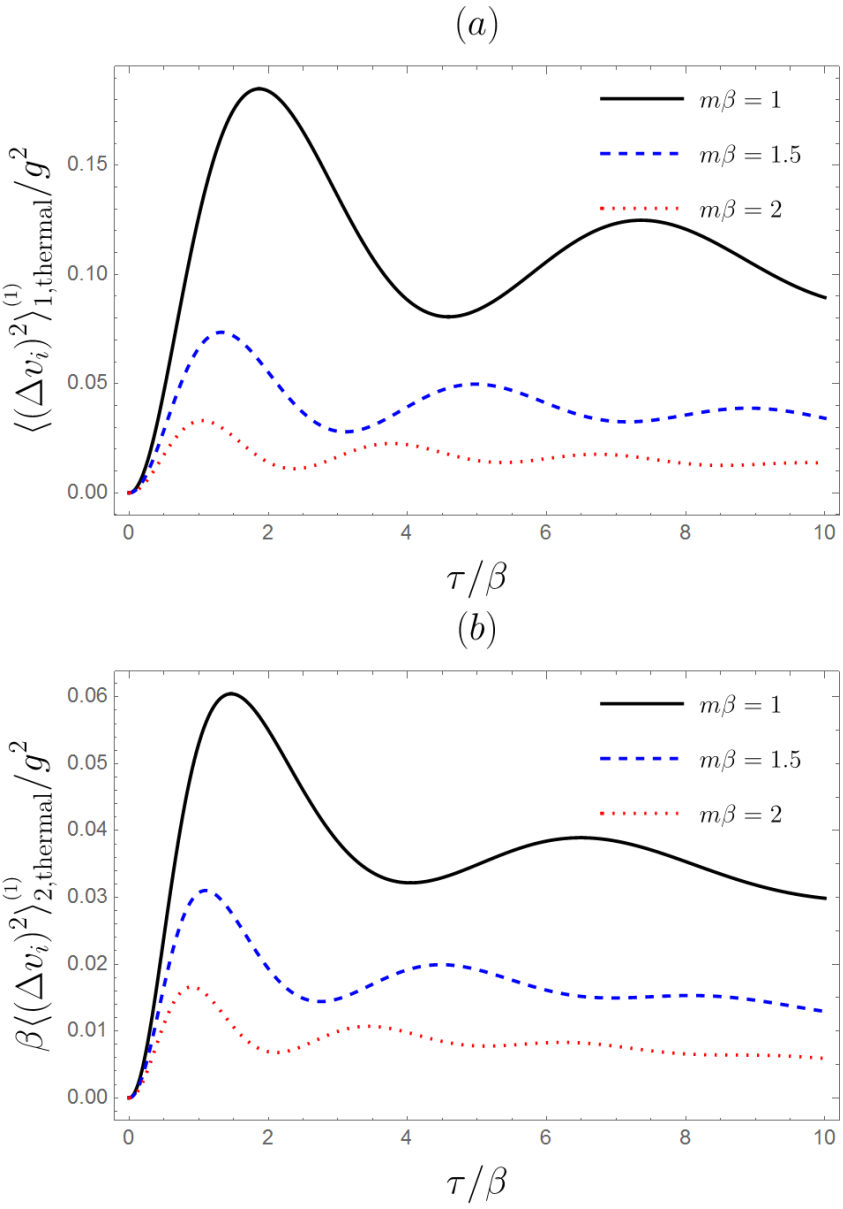

Fig. 3 – Velocity dispersions at two and one spatial dimensions, Figures (a) and (b), respectively, caused by a thermal bath by different values of the mass with $n = 20$. The behavior for both is similar, increasing the mass weakens the dispersiona and raises the oscillation frequency. However, for $D = 1$ the magnitudes of the dispersions are higher.

Note that at zero temperature, when $\beta \to \infty$, and for $m \to \infty$ the above dispersions are exponentially suppressed by the modified Bessel function.

These dispersions for $D = 1$ and $D = 2$ are depicted in Figure 3–for $m = 0$ infrared divergences appears, such situation will be considered next. The representative curves are similar, the fluctuations grows, until they reach a peak, then start to oscillate, as a characteristic of the non-Huygesian behavior of the fields, i. e., the interference pattern due to the existence of signals at arbitrary low group velocities. It appears that

the dispersion then lowers with τ. However, as discussed, this choice of sample function is such that, as τ increases the switching time τ_s increases as well, lowering the dispersions.

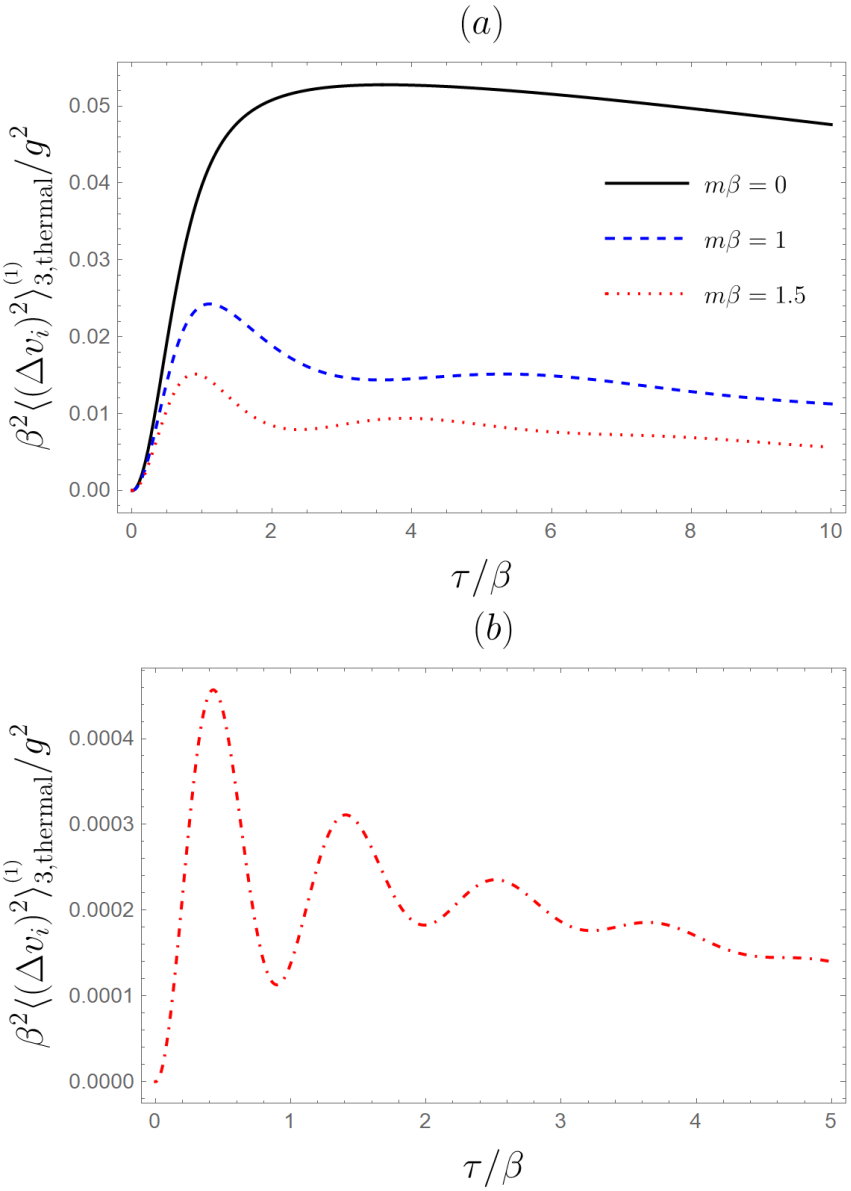

Fig. 4 – Velocity dispersions at three spatial dimensions caused by a thermal bath for different values of the mass, here $n = 20$. (a) Dispersions for different values of the mass. (b) Dispersions for a high value of the mass, $m\beta = 5$, the frequency of the oscillations increases. The behavior is analogous as for $D = 2$ and $D = 1$. However, for $D = 3$ the massless limit is well behaved, and we can see that for Huygesian fields there are no oscillations.

Nonetheless, the dispersion are dependent on $m\beta = m/T$, thence, there is an opposition between field mass and temperature. As the mass grows the field acquires more inertia, and therefore reacts less to thermal energy. One can also understand this as a dissipation of the energy into propagating modes. As, when the field acquires mass, they travel with slower group velocities, and the fields reacts less to temperature effects.

For $D = 3$ the behavior is similar, as one can see in Fig. 4. As then the massless field do not present divergences, we can see the difference in the dispersion when $m = 0$, a Huygesian field, and for the massive non-Huygesian case. In the former the dispersions do not present oscillations, in contrast to the latter case. In Fig. 4 (b) one can see how the increase of the mass raises the frequency of oscillation.

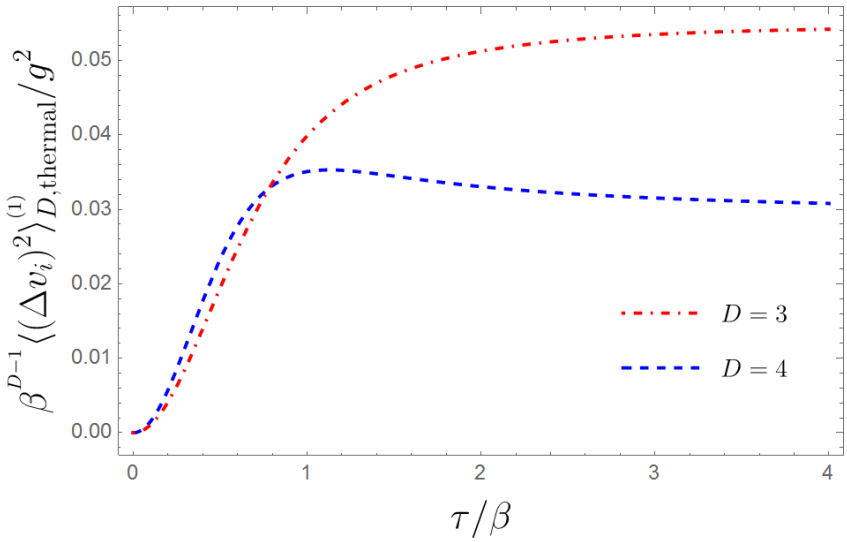

Fig. 5 – Comparison between the thermal dispersions caused by a massless field at $D = 3$, a Huygesian field, and a massless field at $D = 4$, a non-Huygesian field.

Moreover, as stated before, when D is even the fields present a non-Huygesian behavior even when their mass is zero. In Figure 5 we note that while for the massless field in $D = 3$ the fluctuations increases until its maximum value and then slowly decreases. In $D = 4$ we note a slight oscillation of the dispersions, which is suppresed by temperature.

Notwithstanding, the introduction of a switching function modeling the interaction between field and test particle creates a more realistic setup. However, opposing the boundary case, where divergences appears, the sudden transition case for a thermal bath is well behaved, as one can see in Fig. 6. While for the sudden transition case the dispersion grows and then oscillates around its late-time value, the smooth transition attenuates the dispersion and, for the switching function $F_n^{(1)}(t)$, it decays as τ grows.

Further, to investigate the infrared divergences that appears note that for $D = 1$ the modified Bessel function appearing in (3.17) is of integer order, so we can use that $K_n(z) \simeq 1/2(n-1)!(2/z)^n$ when $z \to 0$ [32], and we find

$$\langle(\Delta v_i)^2\rangle^{(1)}_{1,\text{thermal}} \overset{m\to 0}{=} \pi\left(\frac{g\tau c_n}{2\beta n}\right)^2 \sum_{p,q=n}^{2n-1} \psi_{n,p}\psi^*_{n,q}\psi^{(1)}(1 + ia_0), \tag{3.18}$$

remember that $a_0 = (\tau/2\beta)(\psi_{n,p} - \psi^*_{n,q})$ and the polygamma function $\psi^{(m)}(x)$ is given by

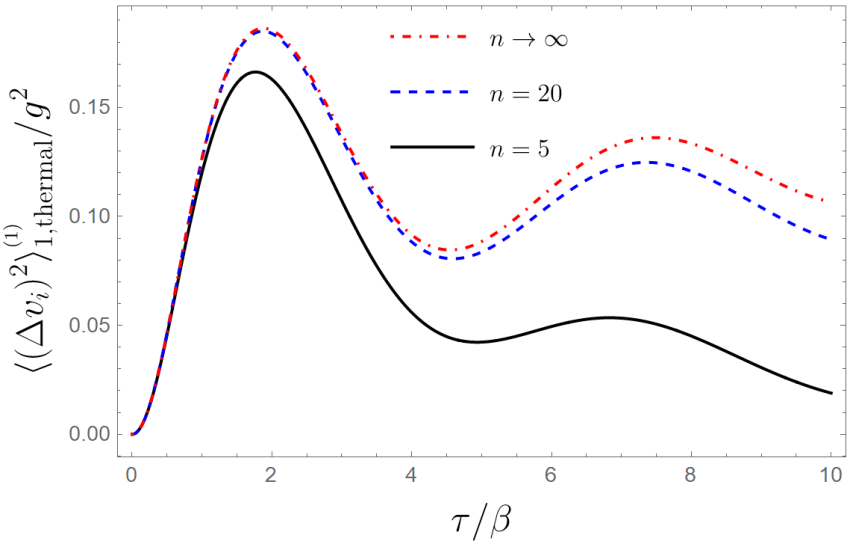

Fig. 6 – Velocity dispersions at one spatial dimension caused by a thermal bath for different values of n in $F^{(1)}_n(t)$.

[32]

$$\psi^{(m)}(x) = (-1)^{m+1}\, m! \sum_{k=0}^{\infty} \frac{1}{(k+x)^{m+1}}. \tag{3.19}$$

Then, for $D = 2$ we have a modified Bessel function of order $\nu = 3/2$, which is $K_{\frac{3}{2}}(z) = (1 + 1/z)\sqrt{\pi/(2z)}\, \mathrm{e}^{-z}$ [35], and we find

$$\langle(\Delta v)^2\rangle^{(1)}_{2,\text{thermal}} \overset{m\to 0}{=} -\frac{\pi}{\beta}\left[\frac{g(\tau/\beta)c_n}{4n}\right]^2 \sum_{p,q=n}^{2n-1} \psi_{n,p}\psi^*_{n,q}\psi^{(2)}(1 + ia_0). \tag{3.20}$$

The above sums converge, however, when $D = 1$ the dispersion grows almost linearly with τ, diverging as τ goes to infinity.

$$\lim_{\tau\to\infty}\langle(\Delta v_i)^2\rangle^{(1)}_{1,\text{thermal}} \overset{m\to 0}{\propto} \sum_{l=1}^{\infty} \lim_{\tau\to\infty} \frac{\tau^2}{[(2\tau/\beta)(\psi_{n,p} - \psi^*_{n,q}) - il]^2} \to \infty. \tag{3.21}$$

For $D = 2$ the divergence is apparently stabilized

$$\lim_{\tau\to\infty}\langle(\Delta v_i)^2\rangle^{(1)}_{2,\text{thermal}} \overset{m\to 0}{\propto} \sum_{l=1}^{\infty} \lim_{\tau\to\infty} \frac{\tau^2}{[(2\tau/\beta)(\psi_{n,p} - \psi^*_{n,q}) - il]^3} \to 0. \tag{3.22}$$

As we have seen, the chosen switching function $F^{(1)}_n(t)$ is such that the switching time grows with the interaction time. Thence, in the late-time behavior the switching time goes to infinity as well and the dispersions are suppressed, causing the apparent regularization. However, in a physical setup, the switching time must be detached from the interaction time. So, the above chosen switching function is not suited to investigate the late-time regime and the infrared divergences.

3.3.1 Late-time behavior of the thermal dispersions

Hence, in order to investigate the late-time regime, the dispersions are recalculated using the switching function $F^{(2)}_{\tau_s}(t)$ given by Eq. (3.13). Substituting in Eq. (3.14)

$$\langle(\Delta v_i)^2\rangle^{(2)}_{D,\text{thermal}} = g^2 \lim_{x\to x'}\left[\frac{\partial}{\partial x_i}\frac{\partial}{\partial x'_i}\frac{2}{(2\pi)^{\frac{D}{2}}|\Delta\vec{x}|^{\frac{D}{2}-1}}\right.$$
$$\left.\times\sum_{l=1}^{\infty}\int_0^\infty dk\frac{k^{\frac{D}{2}}}{\omega^3}(1-\cos(\omega\tau))\mathrm{e}^{-\omega(2\tau_s+l\beta)}J_{\frac{D}{2}-1}(k|\Delta\vec{x}|)\right]. \quad (3.23)$$

Taking the limit $\tau\to\infty$ the integration over the term multiplied by $\cos(\omega\tau)$ goes to 0, as it is shown in Ref. [1]. Thus, to solve the integral in the above expression, note that

$$\frac{2}{(2\pi)^{\frac{D}{2}}|\Delta\vec{x}|^{\frac{D}{2}-1}}\int_0^\infty dk\frac{k^{\frac{D}{2}}}{\omega^3}\mathrm{e}^{-\omega(2\tau_s+l\beta)}J_{\frac{D}{2}-1}(k|\Delta\vec{x}|)$$
$$=-\frac{1}{m}\frac{\partial}{\partial m}\left[\frac{2}{(2\pi)^{\frac{D}{2}}|\Delta\vec{x}|^{\frac{D}{2}-1}}\int_0^\infty dk\frac{k^{\frac{D}{2}}}{\omega}\mathrm{e}^{-\omega(2\tau_s+l\beta)}J_{\frac{D}{2}-1}(k|\Delta\vec{x}|)\right]$$
$$-\frac{2(2\tau_s+l\beta)}{(2\pi)^{\frac{D}{2}}|\Delta\vec{x}|^{\frac{D}{2}-1}}\int_0^\infty dk\frac{k^{\frac{D}{2}}}{\omega^2}\mathrm{e}^{-\omega(2\tau_s+l\beta)}J_{\frac{D}{2}-1}(k|\Delta\vec{x}|) \quad (3.24)$$

The first integral is straightforward, as was done in Eq. (2.33), we have

$$-\frac{1}{m}\frac{\partial}{\partial m}\left[\frac{2}{(2\pi)^{\frac{D}{2}}|\Delta\vec{x}|^{\frac{D}{2}-1}}\int_0^\infty dk\frac{k^{\frac{D}{2}}}{\omega}\mathrm{e}^{-\omega(2\tau_s+l\beta)}J_{\frac{D}{2}-1}(k|\Delta\vec{x}|)\right]$$
$$=-\frac{4}{m(2\pi)^{\frac{D+1}{2}}}\frac{\partial}{\partial m}\left[\left(\frac{m}{\sqrt{(2\tau_s+l\beta)^2+|\Delta\vec{x}|^2}}\right)^{\frac{D-1}{2}}K_{\frac{D-1}{2}}\left(m\sqrt{(2\tau_s+l\beta)^2+|\Delta\vec{x}|^2}\right)\right]$$
$$=\frac{4}{(2\pi)^{\frac{D+1}{2}}}\left(\frac{m}{\sqrt{(2\tau_s+l\beta)^2+|\Delta\vec{x}|^2}}\right)^{\frac{D-3}{2}}K_{\frac{D-3}{2}}\left(m\sqrt{(2\tau_s+l\beta)^2+|\Delta\vec{x}|^2}\right), \quad (3.25)$$

Further, derivating we find

$$\lim_{\vec{x}\to\vec{x}'}\left[\frac{\partial}{\partial x_i}\frac{\partial}{\partial x'_i}\left(\frac{m}{\sqrt{(2\tau_s+l\beta)^2+|\Delta\vec{x}|^2}}\right)^{\frac{D-3}{2}}K_{\frac{D-3}{2}}\left(m\sqrt{(2\tau_s+l\beta)^2+|\Delta\vec{x}|^2}\right)\right]$$
$$=\left(\frac{m}{2\tau_s+l\beta}\right)^{\frac{D-1}{2}}K_{\frac{D-1}{2}}\left(m(2\tau_s+l\beta)\right). \quad (3.26)$$

Now, for the integral in the second term on the right hand side of Eq. (3.24) note that

$$\lim_{\vec{x}\to\vec{x}'}\left[\frac{\partial}{\partial x_i}\frac{\partial}{\partial x'_i}\frac{k^{\frac{D}{2}-1}}{|\Delta\vec{x}|^{\frac{D}{2}-1}}J_{\frac{D}{2}-1}(k|\Delta\vec{x}|)\right]$$
$$=\lim_{\vec{x}\to\vec{x}'}\left[\frac{k^{\frac{D}{2}}}{|\Delta\vec{x}|^{\frac{D}{2}}}J_{\frac{D}{2}}(k|\Delta\vec{x}|)\right]=\frac{k^D}{2^{\frac{D}{2}}\Gamma(\frac{D}{2}+1)}. \quad (3.27)$$

So, substituting $u = \sqrt{k^2/m^2 + 1}$, gives

$$\lim_{\vec{x}\to\vec{x}'} \frac{\partial}{\partial x_i}\frac{\partial}{\partial x_i'}\left[-\frac{2(2\tau_s + l\beta)}{(2\pi)^{\frac{D}{2}}|\Delta\vec{x}|^{\frac{D}{2}-1}}\int_0^\infty dk \frac{k^{\frac{D}{2}}}{\omega^2}\mathrm{e}^{-\omega(2\tau_s+l\beta)}J_{\frac{D}{2}-1}(k|\Delta\vec{x}|)\right]$$
$$= -\frac{(2\tau_s + l\beta)m^D}{2^{D-1}\pi^{\frac{D}{2}}\Gamma(\frac{D}{2}+1)}\int_1^\infty du \frac{(u^2-1)^{\frac{D}{2}}}{u}\mathrm{e}^{-m(2\tau_s+l\beta)u}$$
$$= -\frac{(2\tau_s + l\beta)m^D}{2^{D-1}\pi^{\frac{D}{2}}\Gamma(\frac{D}{2}+1)} I(D, m(2\tau_s + l\beta)), \quad (3.28)$$

where we define

$$I(D,\alpha) = \int_1^\infty du \frac{(u^2-1)^{\frac{D}{2}}}{u}\mathrm{e}^{-\alpha u} = -\frac{\pi}{2}\mathrm{cosec}\left(\frac{\pi}{2}D\right)$$
$$- \frac{\alpha}{2\sqrt{\pi}}\Gamma\left(-\frac{D}{2}-1\right)\Gamma\left(\frac{D}{2}+1\right){}_1F_2\left[1/2; 3/2, (D+3)/2; \alpha^2/4\right]$$
$$+ \frac{1}{\alpha^D}\Gamma(D){}_1F_2\left[-D/2; (1-D)/2, 1-D/2; \alpha^2/4\right]. \quad (3.29)$$

The generalized Hypergeometric functions are given by [35]

$${}_pF_q[a_1, ..., a_p; b_1, ..., b_q; z] = \sum_{n=0}^{\infty}\frac{(a_1)_n...(a_p)_n}{(b_1)_n...(b_q)_n}\frac{z^n}{n!}, \quad (3.30)$$

with the Pochhammer symbol [35]

$$(a)_0 = 1,$$
$$(a)_n = a(a+1)(a+2)...(a+n-1), \;\; n \geq 1. \quad (3.31)$$

Finally, the late-time behavior of the dispersion due to a thermal bath of scalar bosons is

$$\lim_{\tau\to\infty}\langle(\Delta v_i)^2\rangle^{(2)}_{\text{thermal}} = \frac{2g^2}{\pi\beta^{D-1}}\sum_{l=1}^{\infty}\left\{\left[\frac{m\beta}{2\pi(2\tau_s/\beta + l)}\right]^{\frac{D-1}{2}} K_{\frac{D-1}{2}}\left(m\beta(2\tau_s/\beta + l)\right)\right.$$
$$\left. - \frac{(2\tau_s/\beta + l)(m\beta)^D}{2^D\pi^{\frac{D}{2}-1}\Gamma(\frac{D}{2}+1)} I(D, m\beta(2\tau_s/\beta + l))\right\}. \quad (3.32)$$

To investigate the massless regime, first note that transforming the integral back to $k = m\sqrt{u^2-1}$ in $I(D, m\beta(2\tau_s/\beta + l))$ we have that

$$m^D I(D, m\beta(2\tau_s/\beta + l)) = \int_0^\infty dk \frac{k^{D+1}}{k^2+m^2}\mathrm{e}^{-\sqrt{k^2+m^2}(2\tau_s+l\beta)}$$
$$\overset{m\to 0}{=} \int_0^\infty dk k^{D-1}\mathrm{e}^{-k(2\tau_s+l\beta)} = \frac{\Gamma(D)}{\beta^D(2\tau_s/\beta + l)^D}. \quad (3.33)$$

For $D = 3$ the modified Bessel function is of order one, and we can expand as before. We obtain that

$$\lim_{\tau\to\infty}\langle(\Delta v_i)^2\rangle^{(2)}_{3,\text{thermal}} \overset{m\to 0}{=} \frac{g^2}{3\pi^2\beta^2}\psi^{(1)}(1 + \frac{2\tau_s}{\beta}), \quad (3.34)$$

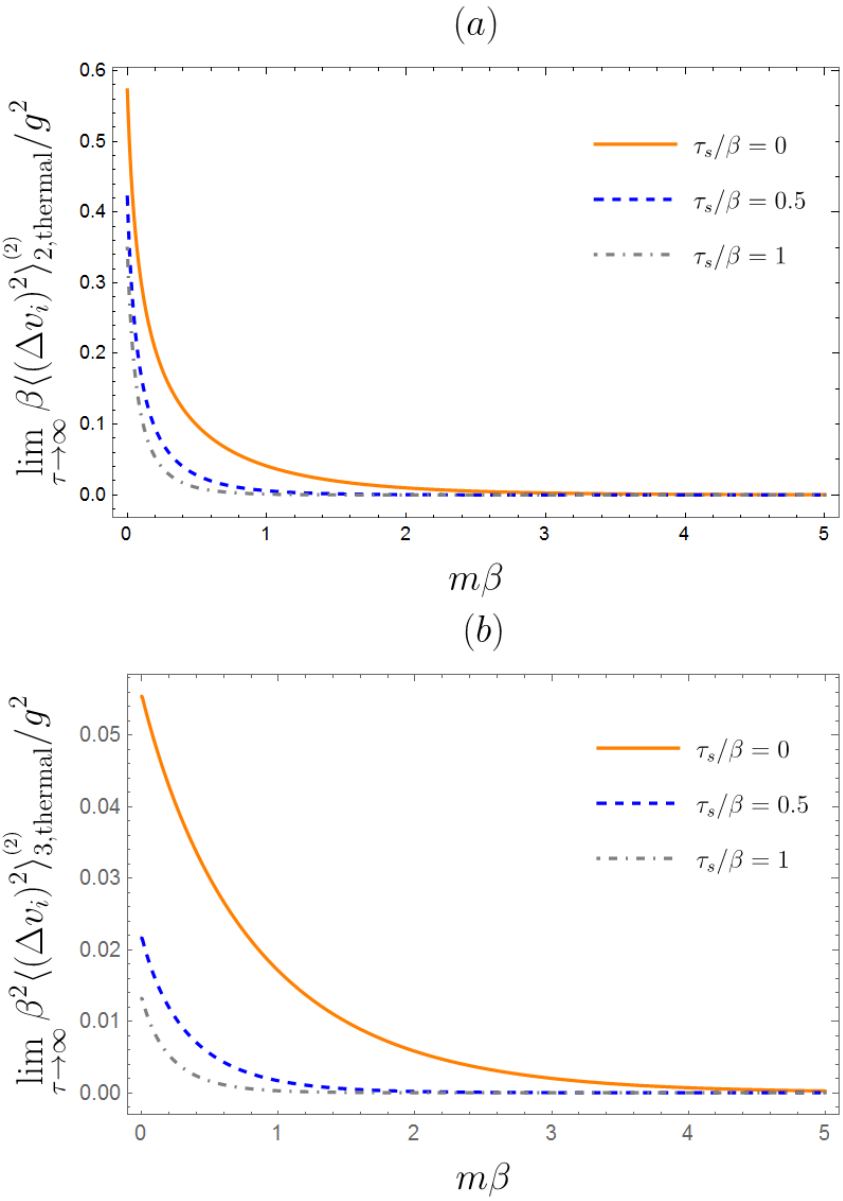

Fig. 7 – Late time behavior of the velocity dispersion with the mass, for $D = 2$ and for $D = 3$. The residual dispersion decays with the mass and with τ_s, rapidly becoming zero. (a) late-time regime of the dispersions for $D = 2$ where the divergence in the massless limits is present. (b) late-time regime for $D = 3$, we see that the function is regular for all masses.

which is half the electromagnetic case [20], as expected as the thermal contribution is isotropic.

For $D = 2$, we have the function $K_{\frac{1}{2}}(z) = \sqrt{\pi/(2z)}\,\mathrm{e}^{-z}$, and we find

$$\lim_{\tau\to\infty}\langle(\Delta v_i)^2\rangle^{(2)}_{2,\text{thermal}} \overset{m\to 0}{=} \frac{g^2}{2\pi\beta}\sum_{l=1}^{\infty}\frac{1}{(l+2(\tau_s/\beta))}, \tag{3.35}$$

and when $D = 1$

$$\lim_{\tau\to\infty}\langle(\Delta v_i)^2\rangle^{(2)}_{1,\text{thermal}} \overset{m\to 0}{=} \frac{2g^2}{\pi}\sum_{l=1}^{\infty}\left[\lim_{m\to 0}K_0(m(2\tau_s+l\beta))-\pi\right]. \tag{3.36}$$

Both expressions diverge for any finite value of τ_s–remember that $\lim_{z\to 0}K_0(z)\simeq\lim_{z\to 0}ln(2/z)$. Thus, we see that even the averaging through a suitable test function cannot regularize the appearing infrared divergences for field theories when $D = 1$ and $D = 2$ at finite temperature. In contrast to the apparent regularization done with the switching function $F_n^{(1)}(t)$, that, as we have seen, is not suited to calculate the late-time fluctuations.

In Fig. 7 we see the behavior of the late-time regime for $D = 2$ and for $D = 3$. In the sudden switching the residual dispersions are bigger, and it decays with mass and with switching time. For $D = 2$ we see the infrared divergence. When $D = 1$ the behavior is similar, but it diverges more rapidly when the mass approaches zero.

3.4 Velocity dispersions due to a thermal bath in the presence of a boundary

Now, we extend our investigation to the interaction of the particle with a thermal bath of scalar bosons near a boundary, where Dirichlet's conditions were imposed. Thus, for a better comprehension we separate each contribution to the dispersion as follows

$$\langle(\Delta v_i)^2\rangle_D = \langle(\Delta v_i)^2\rangle_{D,\text{thermal}} + \langle(\Delta v_i)^2\rangle_{D,\text{vacuum}} + \langle(\Delta v_i)^2\rangle_{D,\text{mixed}}. \tag{3.37}$$

The thermal part is given in Eq. (3.15), the vacuum term states for the contribution due to the modified vacuum caused by the presence of the boundary, and the mixed part is the contribution from the boundary with temperature.

The contribution from the modified vacuum is

$$\begin{aligned}\langle(\Delta v_i)^2\rangle_{D,\text{vacuum}} &= \frac{g^2}{2}\lim_{x\to x'}\left[\frac{\partial}{\partial x_i}\frac{\partial}{\partial x_i'}\int_{-\infty}^{\infty}dtF(t)\int_{\infty}^{\infty}dt'F(t')\tilde{G}^{(1)}_{Ren}(t,\vec{x};t',\vec{x}')\right]\\ &= -g^2\lim_{x\to x'}\text{Re}\left[\frac{\partial}{\partial x_i}\frac{\partial}{\partial x_i'}\frac{1}{2(2\pi)^{\frac{D}{2}}|\hat{\Delta}\vec{x}|^{\frac{D}{2}-1}}\int_0^{\infty}dk\frac{k^{\frac{D}{2}}}{\omega}|\hat{F}(\omega)|^2J_{\frac{D}{2}-1}(k|\hat{\Delta}\vec{x}|)\right],\end{aligned} \tag{3.38}$$

which were studied in Ref. [1]. Then, the contribution from the mixed part

$$\begin{aligned}\langle(\Delta v_i)^2\rangle_{D,\text{mixed}} &= \frac{g^2}{2}\lim_{x\to x'}\left[\frac{\partial}{\partial x_i}\frac{\partial}{\partial x_i'}\int_{-\infty}^{\infty}dtF(t)\int_{\infty}^{\infty}dt'F(t')\tilde{G}^{(1)}_{\beta,Ren}(t,\vec{x};t',\vec{x}')\right]\\ &= -g^2\lim_{x\to x'}\left[\frac{\partial}{\partial x_i}\frac{\partial}{\partial x_i'}\frac{1}{2(2\pi)^{\frac{D}{2}}|\hat{\Delta}\vec{x}|^{\frac{D}{2}-1}}\sum_{l=1}^{\infty}\int_0^{\infty}dk\frac{k^{\frac{D}{2}}}{\omega}2|\hat{F}(\omega)|^2e^{-l\beta\omega}J_{\frac{D}{2}-1}(k|\hat{\Delta}\vec{x}|)\right].\end{aligned} \tag{3.39}$$

Note that the vacuum term is just half the mixed part with $l = 0$. So that we will carry over all calculations for the mixed part and then obtain the vacuum contribution. That said, substituting the Fourier transform of the switching function $F_n^{(1)}(t)$, found in (3.10), in the above equation

$$\langle(\Delta v_i)^2\rangle^{(1)}_{D,\text{mixed}} = -\left(\frac{g\tau\pi c_n}{2n}\right)^2 \lim_{x\to x'}\left[\frac{\partial}{\partial x_i}\frac{\partial}{\partial x_i'}\frac{1}{(2\pi)^{\frac{D}{2}}|\hat{\Delta}\vec{x}|^{\frac{D}{2}-1}}\sum_{p,q=n}^{2n-1}\sum_{l=1}^{\infty}\psi_{n,p}\psi^*_{n,q}\right.$$
$$\left.\times\int_0^\infty dk\frac{k^{\frac{D}{2}}}{\omega}e^{-i\omega\beta a_l}J_{\frac{D}{2}-1}(k|\hat{\Delta}\vec{x}|)\right]. \quad (3.40)$$

Solving the integral is straightforward, as it is equal the one for the thermal part. So, as was done in Eq. (2.33), we find

$$\frac{1}{(2\pi)^{\frac{D}{2}}|\hat{\Delta}\vec{x}|^{\frac{D}{2}-1}}\int_0^\infty dk\frac{k^{\frac{D}{2}}}{\omega}e^{-i\omega\beta a_l}J_{\frac{D}{2}-1}(k|\hat{\Delta}\vec{x}|)$$
$$= \frac{1}{\pi}\left(\frac{m}{2\pi\sqrt{|\hat{\Delta}\vec{x}|^2-a_l^2}}\right)^{\frac{D-1}{2}}K_{\frac{D-1}{2}}\left(m\sqrt{|\hat{\Delta}\vec{x}|^2-a_l^2}\right). \quad (3.41)$$

In the derivation of the above expression note that, because of the anisotropic character of $\hat{\Delta}\vec{x}$, the expression will differ in the direction perpendicular to the boundary. Thence, for the parallel directions–where we now denote x as the distance to the plate–we find

$$\lim_{x\to x'}\left[\frac{\partial}{\partial x_\parallel}\frac{\partial}{\partial x_\parallel'}\left(\frac{m}{\sqrt{|\hat{\Delta}\vec{x}|^2-a_l^2}}\right)^{\frac{D-1}{2}}K_{\frac{D-1}{2}}\left(m\sqrt{|\hat{\Delta}\vec{x}|^2-a_l^2}\right)\right]$$
$$= \left(\frac{m}{\sqrt{4x^2-a_l^2}}\right)^{\frac{D+1}{2}}K_{\frac{D+1}{2}}\left(m\sqrt{4x^2-a_l^2}\right). \quad (3.42)$$

For the perpendicular direction

$$\lim_{x\to x'}\left[\frac{\partial}{\partial x_\perp}\frac{\partial}{\partial x_\perp'}\left(\frac{m}{\sqrt{|\hat{\Delta}\vec{x}|^2-a_l^2}}\right)^{\frac{D-1}{2}}K_{\frac{D-1}{2}}\left(m\sqrt{|\hat{\Delta}\vec{x}|^2-a_l^2}\right)\right]$$

$$= -\left(\frac{m}{\sqrt{4x^2-a_l^2}}\right)^{\frac{D+1}{2}}K_{\frac{D+1}{2}}\left(m\sqrt{4x^2-a_l^2}\right)+4x^2\left(\frac{m}{\sqrt{4x^2-a_l^2}}\right)^{\frac{D+3}{2}}K_{\frac{D+3}{2}}\left(m\sqrt{4x^2-a_l^2}\right). \quad (3.43)$$

Substituting these results in Equation (3.40) we find

$$\langle(\Delta v_\parallel)^2\rangle^{(1)}_{D,\text{mixed}} = -\frac{2g^2}{x^{D-1}}\left(\frac{(\tau/x)\pi c_n}{2n}\right)^2\sum_{p,q=n}^{2n-1}\sum_{l=1}^{\infty}\psi_{n,p}\psi^*_{n,q}\left(\frac{mx}{4\pi\sqrt{1-\gamma_l^2}}\right)^{\frac{D+1}{2}}K_{\frac{D+1}{2}}\left(2mx\sqrt{1-\gamma_l^2}\right),$$
$$\langle(\Delta v_\perp)^2\rangle^{(1)}_{D,\text{mixed}} = 8\pi x^2\langle(\Delta v_\parallel)^2\rangle^{(1)}_{D+2,\text{mixed}} - \langle(\Delta v_\parallel)^2\rangle^{(1)}_{D,\text{mixed}}. \quad (3.44)$$

where we have defined $\gamma_l = (\tau/4x)(\psi_{n,p} - \psi^*_{n,q}) - il(\beta/2x)$. Furthermore, as was said, the vacuum term is just half the above expression with $l = 0$. We then found

$$\langle(\Delta v_\parallel)^2\rangle^{(1)}_{D,\text{vacuum}} = -\frac{g^2}{x^{D-1}}\left(\frac{(\tau/x)\pi c_n}{2n}\right)^2 \sum_{p,q=n}^{2n-1} \psi_{n,p}\psi^*_{n,q}\left(\frac{mx}{4\pi\sqrt{1-\gamma_0^2}}\right)^{\frac{D+1}{2}} K_{\frac{D+1}{2}}\left(2mx\sqrt{1-\gamma_0^2}\right),$$
$$\langle(\Delta v_\perp)^2\rangle^{(1)}_{D,\text{vacuum}} = 8\pi x^2\langle(\Delta v_\parallel)^2\rangle^{(1)}_{D+2,\text{vacuum}} - \langle(\Delta v_\parallel)^2\rangle^{(1)}_{D,\text{vacuum}}. \tag{3.45}$$

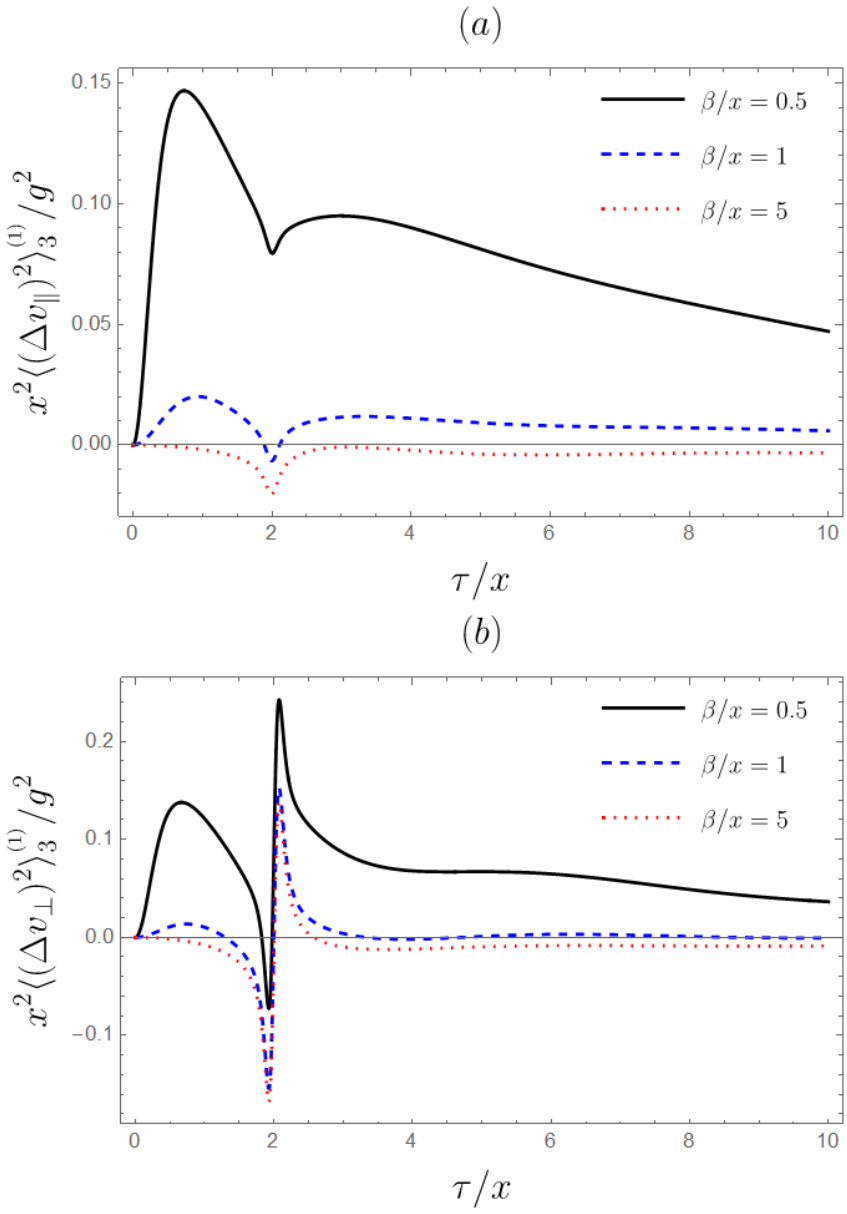

Fig. 8 – Fluctuations caused by a thermal bath near a reflective boundary for $D = 3$. Here we set $n = 20$ and $mx = 1$.(a) Velocity fluctuations in the parallel directions.(b) Velocity fluctuations in the perpendicular direction.

Also, in order to be able to plot the complete dispersion in terms of τ/x, β/x, and

mx we rewrite the homogeneous thermal contribution as

$$\langle(\Delta v_i)^2\rangle^{(1)}_{D,\text{thermal}} = \frac{2g^2}{x^{D-1}}\left(\frac{(\tau/x)\pi c_n}{2n}\right)^2 \sum_{p,q=n}^{2n-1}\sum_{l=1}^{\infty}\psi_{n,p}\psi^*_{n,q}\left(\frac{mx}{4\pi\sqrt{-\gamma_l^2}}\right)^{\frac{D+1}{2}} K_{\frac{D+1}{2}}\left(2mx\sqrt{-\gamma_l^2}\right). \tag{3.46}$$

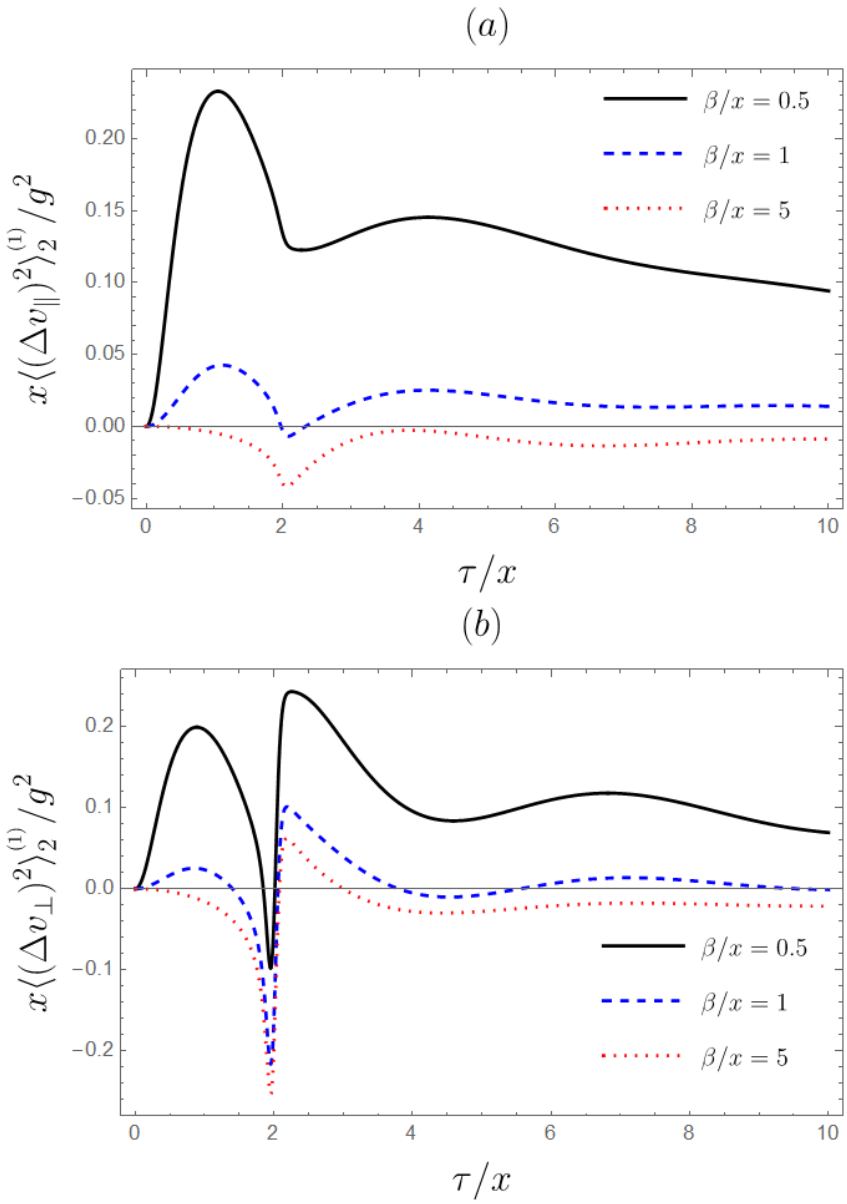

Fig. 9 – Fluctuations caused by a thermal bath near a reflective boundary, for $D = 2$. Here we set $n = 20$ and $mx = 1$.(a) Velocity fluctuations in the parallel directions.(b) Velocity fluctuations in the perpendicular direction.

Again, as $\beta \to \infty$, the mixed and thermal contributions are exponentially suppressed and the only remaining is the boundary term at zero temperature, recovering the results in [1]. Furthermore, when $m \to \infty$ all contributions to the dispersions vanish,

however, as the modified vacuum is the zeroth order term in the summation on powers of l, the temperature contributions are suppressed earlier. So, for high values of the mass, only the modified vacuum contribution remains.

From now on, as for the massive field the behavior of the fluctuations is very similar for different values of D, we present only the curves for $D = 2$ and $D = 3$, an even and an odd number of dimensions. Thus, the complete velocity dispersions are shown in Figures 8 and 9, for $D = 3$ and $D = 2$, respectively.

Initially, the thermal part dominates, but near $\tau = 2x$ we have the valley associated with the boundary interaction [1], which have a different sign from the thermal part. Hence, even in the finite temperature case we are able to encounter negative values for the dispersions.

Moreover, the spatial dimension does not change the overall behavior. But, for $D = 2$, as the thermal contribution is higher, the valleys are less inclined. Note also that for $\beta/x = 5$ the contribution from the temperature are suppressed and we have only the modified vacuum contribution found in Ref. [1]. Also as mx increases, the vacuum term dominates over the thermal contribution, as we will see more closely in another section.

Lastly, as the effect in the dispersions due to the boundary for different values of n is well understood (See Ref. [15]), here we have shown only the curves for $n = 20$. For this value the divergences are regularized but not greatly weakened, maintaining its principal features.

3.4.1 Dispersions due to a boundary at finite temperature

In a physical setup, the pure thermal contribution is detached from the boundary terms. That is, we can propose a situation were the gas is heated before the boundary is inserted, and both could be switched on with different switching times. Then the thermal contribution will be only the constant residual fluctuations, which can also be zero for values of τ_s high enough.

Hence, it is of our interest to investigate the boundary term of the dispersion alone, defined by

$$\langle(\Delta v_i)^2\rangle_{D,\text{boundary}} = \langle(\Delta v_i)^2\rangle_{D,\text{vacuum}} + \langle(\Delta v_i)^2\rangle_{D,\text{mixed}}. \tag{3.47}$$

The plots in Fig. 11 and Fig. 10 depict the behavior of the boundary contribution to the dispersions when the temperature is raised. It is shown that the temperature deepens and smooths the valleys, in the sense that the curve is less declined, while decreases the peaks in the perpendicular part, when $\beta \to \infty$ we recover the results in Ref. [1]. Also, in the perpendicular direction, the temperature effects are smaller, as the curves does not deviates much from the zero temperature case. Further, for $D = 2$ the temperature effects are more pronounced then that for $D = 3$.

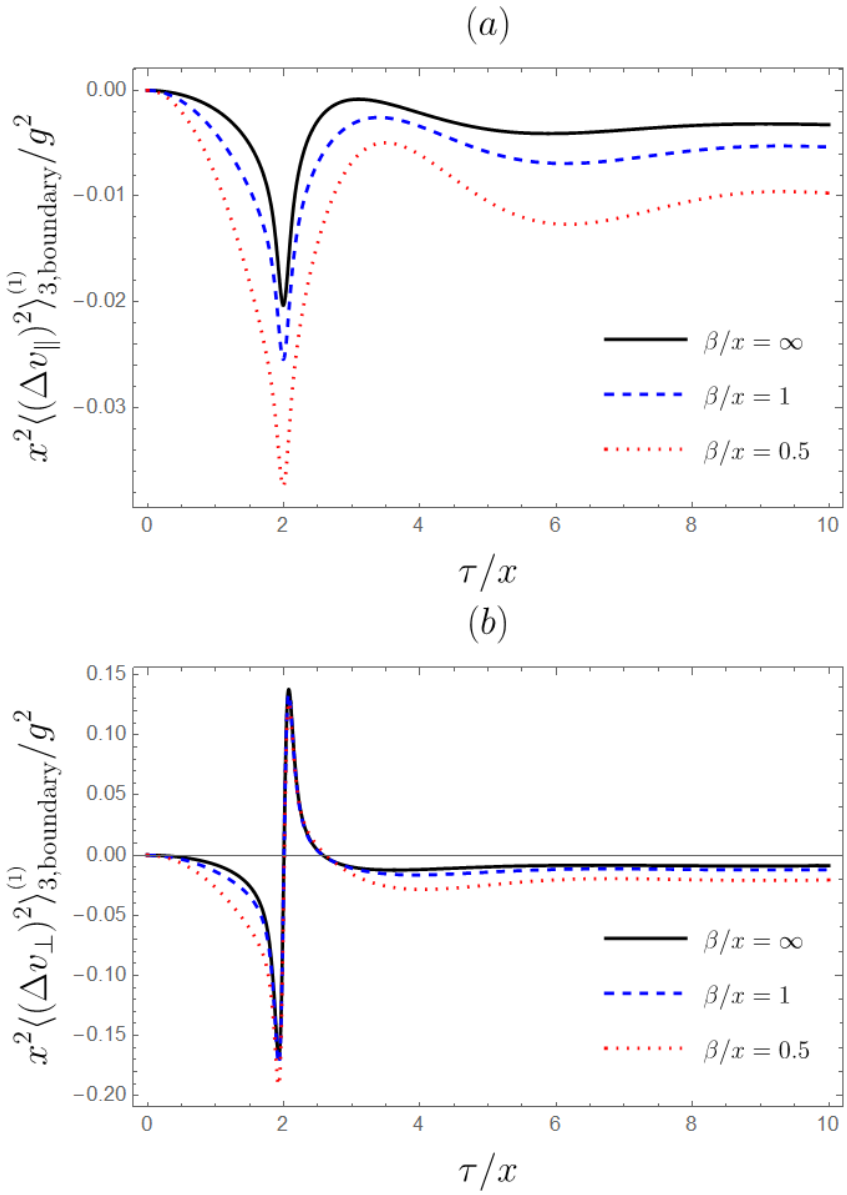

Fig. 10 – Dispersion caused by a reflective boundary at finite temperature for $D = 3$. We set $n = 20$ and $mx = 1$. (a) Velocity dispersions in the parallel directions. (b) Velocity dispersions in the perpendicular direction. As the temperature increases the dispersion grows and the peaks are less abrupt.

Nonetheless, as we have seen, mass opposes temperature effects, so that when field mass is raised the oscillations are pronounced and the magnitude of the dispersions lowers, Figures 12 and 13. Note that, for high values of mass, temperature effects are suppressed and we recover the figure presented in Ref. [1], with the vacuum dominating the mixed contribution. Again, for $D = 2$ the fluctuations are higher and the peaks smoother as for $D = 3$.

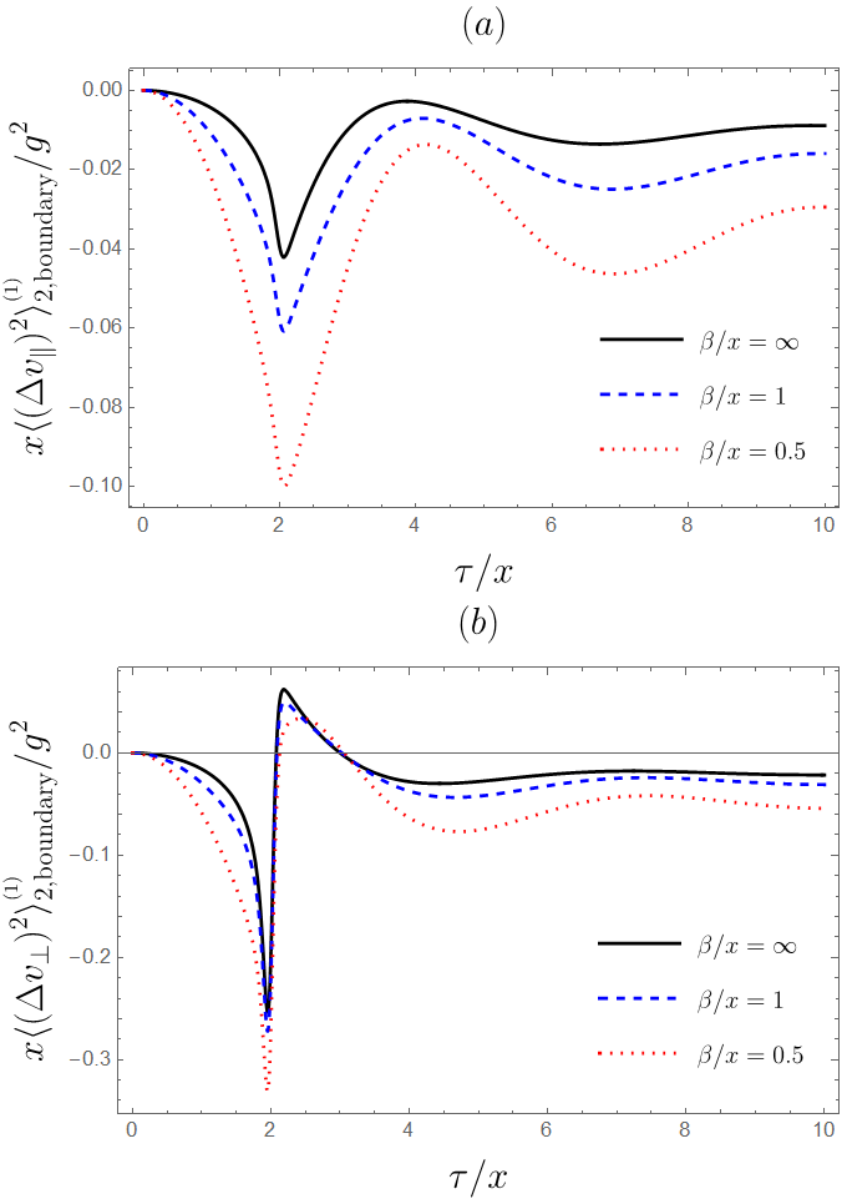

Fig. 11 – Dispersion caused by a reflective boundary at finite temperature for $D=2$. We set $n=20$ and $mx=1$. (a) Velocity dispersions in the parallel directions. (b) Velocity dispersions in the perpendicular direction.

3.4.2 Late-time behavior of the dispersions

At last, the late time behavior is again found through the sample function $F^{(2)}_{\tau_s}(t)$. Then, taking $\tau\to\infty$, the mixed contribution is

$$\lim_{\tau\to\infty}\langle(\Delta v_i)^2\rangle^{(2)}_{D,\text{mixed}} = -g^2\lim_{\vec{x}\to\vec{x}'}\left[\frac{\partial}{\partial x_i}\frac{\partial}{\partial x_i'}\frac{2}{(2\pi)^{\frac{D}{2}}|\hat{\Delta}\vec{x}|^{\frac{D}{2}-1}}\right.$$
$$\left.\times\sum_{l=1}^{\infty}\int_0^{\infty}dk\frac{k^{\frac{D}{2}}}{\omega^3}\mathrm{e}^{-\omega(2\tau_s+l\beta)}J_{\frac{D}{2}-1}(k|\hat{\Delta}\vec{x}|)\right]. \quad (3.48)$$

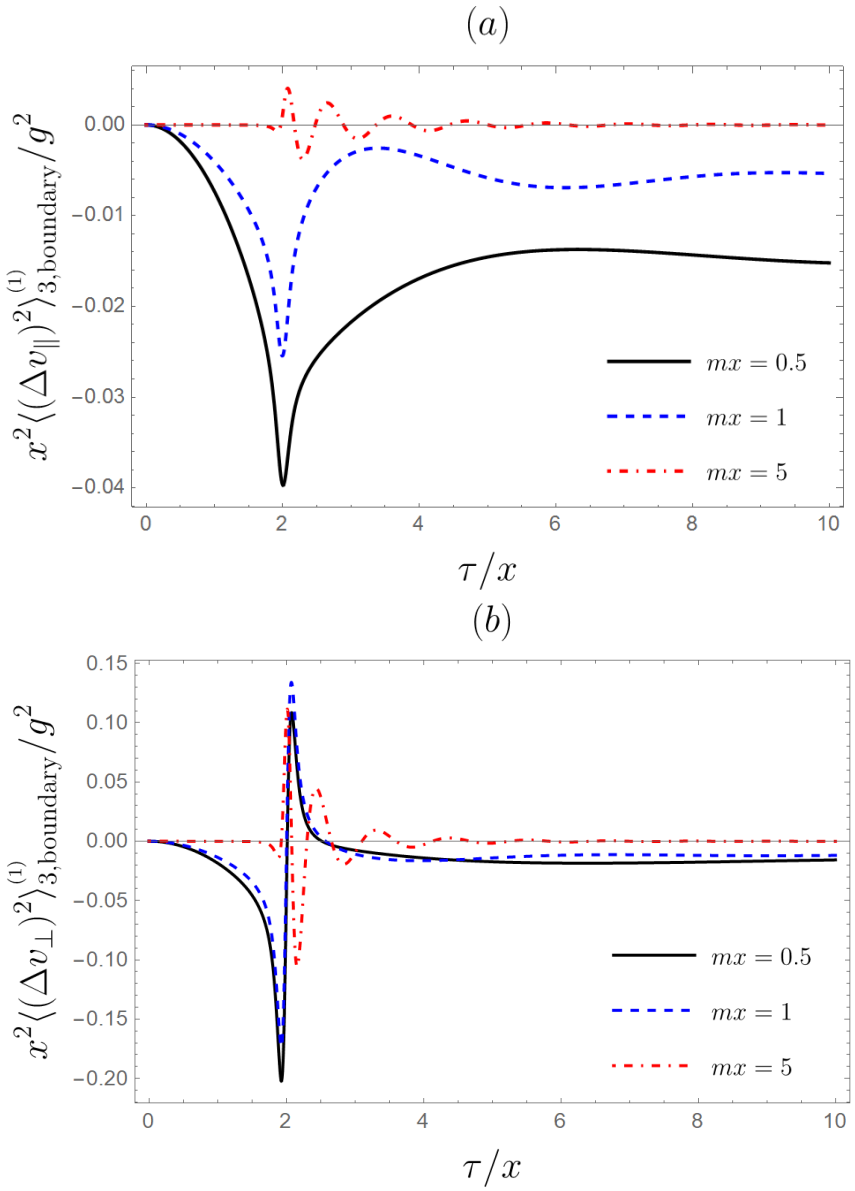

Fig. 12 – Dispersion caused by a reflective boundary at finite temperature for $D = 3$. We set $n = 20$ and $\beta/x = 1$. (a) Velocity dispersions in the parallel directions. (b) Velocity dispersions in the perpendicular direction. With the increase of the mass, the modified vacuum dominates the finite temperature contributions.

We rewrite the integral, as previously, as

$$\begin{aligned}
&\frac{2}{(2\pi)^{\frac{D}{2}}|\hat{\Delta}\vec{x}|^{\frac{D}{2}-1}}\int_0^\infty dk\frac{k^{\frac{D}{2}}}{\omega^3}\mathrm{e}^{-\omega(2\tau_s+l\beta)}J_{\frac{D}{2}-1}(k|\hat{\Delta}\vec{x}|)\\
&\qquad=-\frac{1}{m}\frac{\partial}{\partial m}\left[\frac{2}{(2\pi)^{\frac{D}{2}}|\hat{\Delta}\vec{x}|^{\frac{D}{2}-1}}\int_0^\infty dk\frac{k^{\frac{D}{2}}}{\omega}\mathrm{e}^{-\omega(2\tau_s+l\beta)}J_{\frac{D}{2}-1}(k|\hat{\Delta}\vec{x}|)\right]\\
&\qquad\qquad-\frac{2(2\tau_s+l\beta)}{(2\pi)^{\frac{D}{2}}|\hat{\Delta}\vec{x}|^{\frac{D}{2}-1}}\int_0^\infty dk\frac{k^{\frac{D}{2}}}{\omega^2}\mathrm{e}^{-\omega(2\tau_s+l\beta)}J_{\frac{D}{2}-1}(k|\hat{\Delta}\vec{x}|). \quad (3.49)
\end{aligned}$$

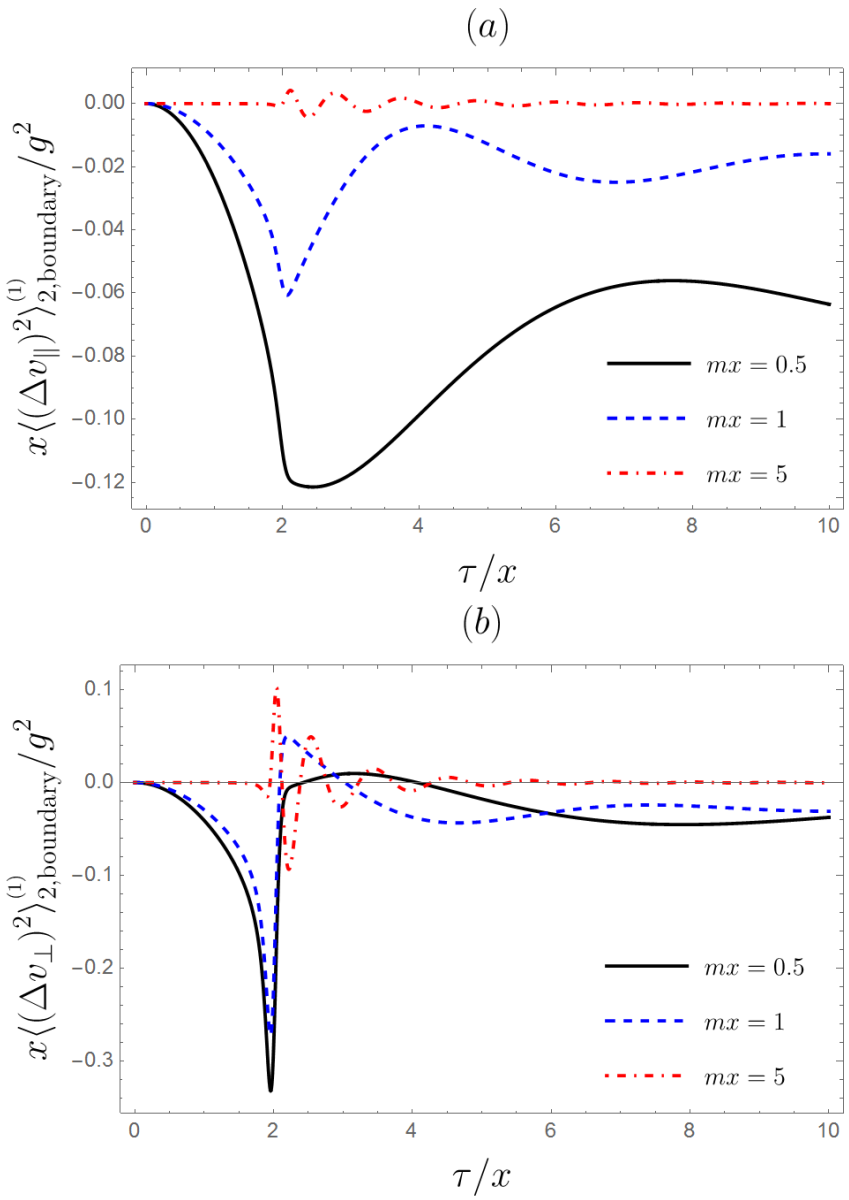

Fig. 13 – Dispersion caused by a reflective boundary at finite temperature for $D = 2$. We set $n = 20$ and $\beta/x = 1$. (a) Velocity dispersions in the parallel directions. (b) Velocity dispersions in the perpendicular direction.

Now, as in Eq. (3.25), we find for the first integral on the right hand side of the above equation

$$-\frac{1}{m}\frac{\partial}{\partial m}\left[\frac{2}{(2\pi)^{\frac{D}{2}}|\hat{\Delta}\vec{x}|^{\frac{D}{2}-1}}\int_0^\infty dk\frac{k^{\frac{D}{2}}}{\omega}\mathrm{e}^{-\omega(2\tau_s+l\beta)}J_{\frac{D}{2}-1}(k|\hat{\Delta}\vec{x}|)\right]$$
$$=\frac{4}{(2\pi)^{\frac{D+1}{2}}}\left(\frac{m}{\sqrt{(2\tau_s+l\beta)^2+|\hat{\Delta}\vec{x}|^2}}\right)^{\frac{D-3}{2}}K_{\frac{D-3}{2}}\left(m\sqrt{(2\tau_s+l\beta)^2+|\hat{\Delta}\vec{x}|^2}\right). \quad (3.50)$$

Evaluating the derivatives in the parallel and perpendicular directions we have

$$\lim_{\vec{x}\to\vec{x}'}\left[\frac{\partial}{\partial x_\parallel}\frac{\partial}{\partial x'_\parallel}\left(\frac{m}{\sqrt{(2\tau_s+l\beta)^2+|\hat{\Delta}\vec{x}|^2}}\right)^{\frac{D-3}{2}}K_{\frac{D-3}{2}}\left(m\sqrt{(2\tau_s+l\beta)^2+|\hat{\Delta}\vec{x}|^2}\right)\right]$$
$$=\left[\frac{m}{\sqrt{(2\tau_s+l\beta)^2+4x^2}}\right]^{\frac{D-1}{2}}K_{\frac{D-1}{2}}\left(m\sqrt{(2\tau_s+l\beta)^2+4x^2}\right),$$

and

$$\lim_{\vec{x}\to\vec{x}'}\left[\frac{\partial}{\partial x_\perp}\frac{\partial}{\partial x'_\perp}\left(\frac{m}{\sqrt{(2\tau_s+l\beta)^2+|\hat{\Delta}\vec{x}|^2}}\right)^{\frac{D-3}{2}}K_{\frac{D-3}{2}}\left(m\sqrt{(2\tau_s+l\beta)^2+|\hat{\Delta}\vec{x}|^2}\right)\right]$$
$$=-\left[\frac{m}{\sqrt{(2\tau_s+l\beta)^2+4x^2}}\right]^{\frac{D-1}{2}}K_{\frac{D-1}{2}}\left(m\sqrt{(2\tau_s+l\beta)^2+4x^2}\right)$$
$$+4x^2\left[\frac{m}{\sqrt{(2\tau_s+l\beta)^2+4x^2}}\right]^{\frac{D+1}{2}}K_{\frac{D+1}{2}}\left(m\sqrt{(2\tau_s+l\beta)^2+4x^2}\right).$$

For the second integral on the right hand side of Eq. (3.48) note that, for the parallel part

$$\lim_{\vec{x}\to\vec{x}'}\left[\frac{\partial}{\partial x_\parallel}\frac{\partial}{\partial x'_\parallel}\frac{k^{\frac{D}{2}-1}}{|\hat{\Delta}\vec{x}|^{\frac{D}{2}-1}}J_{\frac{D}{2}-1}(k|\hat{\Delta}\vec{x}|)\right]=\frac{k^{\frac{D}{2}}}{(2x)^{\frac{D}{2}}}J_{\frac{D}{2}}(2kx). \tag{3.51}$$

So that, again with $u=\sqrt{k^2/m^2+1}$, we find that

$$\lim_{\vec{x}\to\vec{x}'}\frac{\partial}{\partial x_\parallel}\frac{\partial}{\partial x'_\parallel}\left[\frac{2(2\tau_s+l\beta)}{(2\pi)^{\frac{D}{2}}|\hat{\Delta}\vec{x}|^{\frac{D}{2}-1}}\int_0^\infty dk\frac{k^{\frac{D}{2}}}{\omega^2}\mathrm{e}^{-\omega(2\tau_s+l\beta)}J_{\frac{D}{2}-1}(k|\hat{\Delta}\vec{x}|)\right]$$
$$=\frac{(2\tau_s+l\beta)m^{D/2}}{(2\pi)^{\frac{D}{2}}(2x)^{\frac{D}{2}}}\int_1^\infty du\frac{(\sqrt{u^2-1})^{\frac{D}{2}}}{u}\mathrm{e}^{-m(2\tau_s+l\beta)u}J_{\frac{D}{2}}(2mx\sqrt{u^2-1}). \tag{3.52}$$

For the perpendicular component

$$\lim_{\vec{x}\to\vec{x}'}\left[\frac{\partial}{\partial x_\perp}\frac{\partial}{\partial x'_\perp}\frac{k^{\frac{D}{2}-1}}{|\hat{\Delta}\vec{x}|^{\frac{D}{2}-1}}J_{\frac{D}{2}-1}(k|\hat{\Delta}\vec{x}|)\right]=4x^2\frac{k^{\frac{D}{2}+1}}{(2x)^{\frac{D}{2}+1}}J_{\frac{D}{2}+1}(2kx)-\frac{k^{\frac{D}{2}}}{(2x)^{\frac{D}{2}}}J_{\frac{D}{2}}(2kx). \tag{3.53}$$

Thence

$$\lim_{\vec{x}\to\vec{x}'}\frac{\partial}{\partial x_\perp}\frac{\partial}{\partial x'_\perp}\left[\frac{2(2\tau_s+l\beta)}{(2\pi)^{\frac{D}{2}}|\hat{\Delta}\vec{x}|^{\frac{D}{2}-1}}\int_0^\infty dk\frac{k^{\frac{D}{2}}}{\omega^2}\mathrm{e}^{-\omega(2\tau_s+l\beta)}J_{\frac{D}{2}-1}(k|\hat{\Delta}\vec{x}|)\right]$$
$$=\frac{(2\tau_s+l\beta)m^{D/2+1}}{(2\pi)^{\frac{D}{2}}(2x)^{\frac{D}{2}+1}}\int_1^\infty du\frac{(\sqrt{u^2-1})^{\frac{D}{2}+1}}{u}\mathrm{e}^{-m(2\tau_s+l\beta)u}J_{\frac{D}{2}+1}(2mx\sqrt{u^2-1})$$
$$-\frac{(2\tau_s+l\beta)m^{D/2}}{(2\pi)^{\frac{D}{2}}(2x)^{\frac{D}{2}}}\int_1^\infty du\frac{(\sqrt{u^2-1})^{\frac{D}{2}}}{u}\mathrm{e}^{-m(2\tau_s+l\beta)u}J_{\frac{D}{2}}(2mx\sqrt{u^2-1}). \tag{3.54}$$

Finally, substituting the above results in Eq. (3.48) we find that

$$\lim_{\tau\to\infty}\langle(\Delta v_{\parallel})^2\rangle^{(2)}_{D,\text{mixed}} = -\frac{2g^2}{\pi x^{D-1}}\sum_{l=1}^{\infty}\left\{\left[\frac{mx}{4\pi\sqrt{1+\alpha_l^2}}\right]^{\frac{D-1}{2}} K_{\frac{D-1}{2}}\left(2mx\sqrt{1+\alpha_l^2}\right)\right. \tag{3.55}$$
$$\left. - \frac{\alpha_l (mx)^{\frac{D}{2}}}{2^{D-1}\pi^{\frac{D}{2}-1}}\int_1^{\infty} du \frac{(\sqrt{u^2-1})^{\frac{D}{2}}}{u} \mathrm{e}^{-2mx\,\alpha_l} J_{\frac{D}{2}}(2mx\sqrt{u^2-1})\right\},$$

$$\lim_{\tau\to\infty}\langle(\Delta v_{\perp})^2\rangle^{(2)}_{D,\text{mixed}} = 8\pi x^2 \lim_{\tau\to\infty}\langle(\Delta v_{\parallel})^2\rangle^{(2)}_{D+2,\text{mixed}} - \lim_{\tau\to\infty}\langle(\Delta v_{\parallel})^2\rangle^{(2)}_{D,\text{mixed}}, \tag{3.56}$$

with $\alpha_l = \tau_s/x + l\beta/2x$. Again, the vacuum contribution is just half the mixed part with $l = 0$. Thus

$$\lim_{\tau\to\infty}\langle(\Delta v_{\parallel})^2\rangle^{(2)}_{D,\text{vacuum}} = -\frac{g^2}{\pi x^{D-1}}\left\{\left[\frac{mx}{4\pi\sqrt{1+(\tau_s/x)^2}}\right]^{\frac{D-1}{2}} K_{\frac{D-1}{2}}\left(2mx\sqrt{1+(\tau_s/x)^2}\right)\right. \tag{3.57}$$
$$\left. - \frac{(\tau_s/x)(mx)^{\frac{D}{2}}}{2^{D-1}\pi^{\frac{D}{2}-1}}\int_1^{\infty} du \frac{(\sqrt{u^2-1})^{\frac{D}{2}}}{u} \mathrm{e}^{-2mx(\tau_s/x)} J_{\frac{D}{2}}(2mx\sqrt{u^2-1})\right\},$$

$$\lim_{\tau\to\infty}\langle(\Delta v_{\perp})^2\rangle^{(2)}_{D,\text{vacuum}} = 8\pi x^2 \lim_{\tau\to\infty}\langle(\Delta v_{\parallel})^2\rangle^{(2)}_{D+2,\text{vacuum}} - \lim_{\tau\to\infty}\langle(\Delta v_{\parallel})^2\rangle^{(2)}_{D,\text{vacuum}}. \tag{3.58}$$

We also conveniently rewrite the homogeneous thermal late-time expression, Eq. (3.32), as

$$\lim_{\tau\to\infty}\langle(\Delta v_i)^2\rangle^{(2)}_{D,\text{thermal}} = \frac{2g^2}{\pi x^{D-1}}\sum_{l=1}^{\infty}\left[\left(\frac{mx}{4\pi\alpha_l}\right)^{\frac{D-1}{2}} K_{\frac{D-1}{2}}(2mx\alpha_l)\right.$$
$$\left. - \frac{\alpha_l (mx)^D}{2^{D-1}\pi^{\frac{D}{2}-1}\Gamma(\frac{D}{2}+1)} I(D, mx\alpha_l)\right]. \tag{3.59}$$

In Figure 14 we plotted the late-time regime of the boundary contribution, opposing the thermal part, and the total dispersions. Hence, as the boundary contribution is negative, it lowers the total dispersions, and for both directions we found negative values for the dispersions. Lowering the mass and raising the temperature raises the curves, and eventually the contributions of the thermal effect will dominate, eliminating the subvacuum signature.

Furthermore, as said, it is possible to detach in a physical setup the thermal from the boundary part, and. in such case, the late-time could be just the boundary curve in Fig. 14.

Now we investigate more closely the case of a massless field at three dimensions.

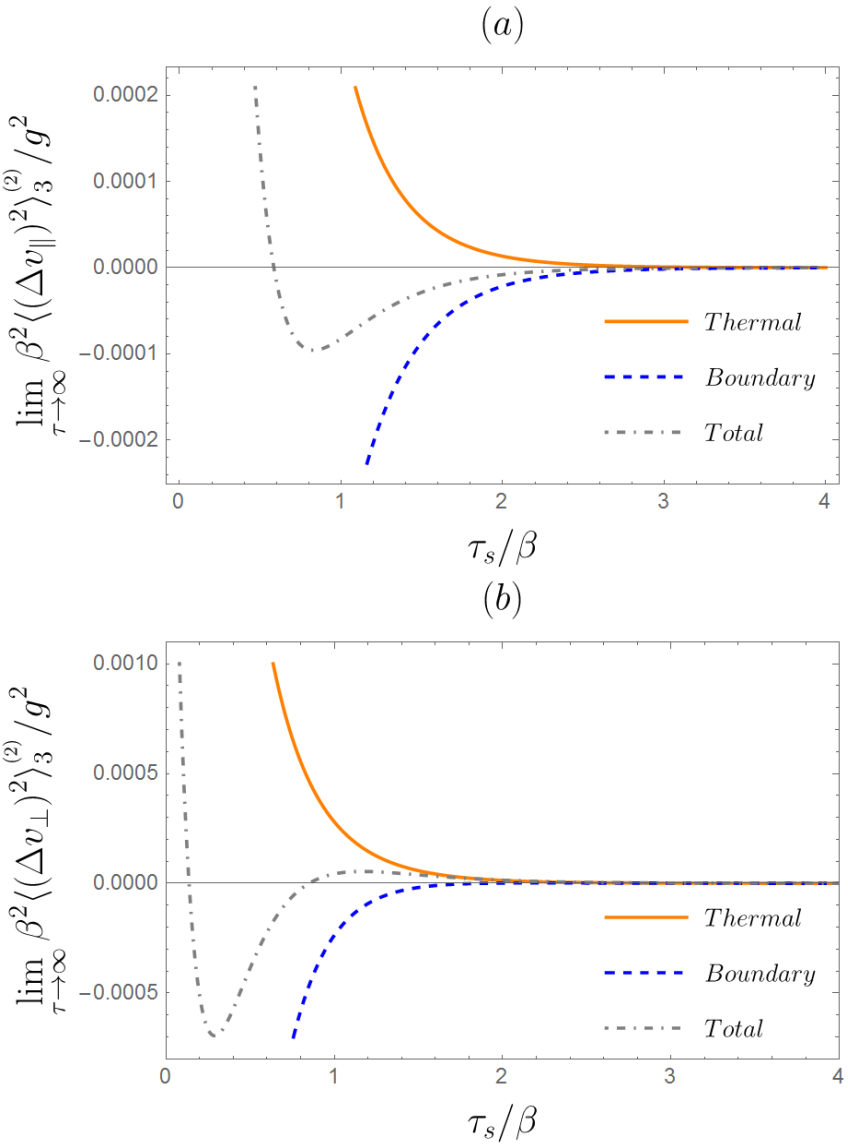

Fig. 14 – Late-time behavior of the velocity dispersions with τ_s, for $D = 3$, $mx = 1$, and $\beta/x = 1$. The boundary contribution is negative, opposing the thermal part. The dispersions become negative for some values of τ_s/β, a subvacuum effect.

For that, we have

$$\int_0^\infty dk\, k^{1/2} \mathrm{e}^{-k(2\tau/s+l\beta)} J_{3/2}(2kx) = \sqrt{\frac{2}{\pi}} \left\{ \frac{1}{(2x)^{\frac{3}{2}}} \arctan\left(\frac{2x}{2\tau_s + l\beta}\right) - \frac{2x(2\tau_s + l\beta)}{(2x)^{\frac{3}{2}}[4x^2 + (2\tau_s + l\beta)^2]} \right\}. \quad (3.60)$$

Using the above integral in the massless limit of equation (3.55) and the limit of the modified Bessel function used in (3.18) we have

$$\lim_{\tau\to\infty} \langle(\Delta v_\parallel)^2\rangle_{3,\mathrm{mixed}}^{(2)} \overset{m\to 0}{=} -\frac{g^2}{4\pi^2 x^2} \sum_{l=1}^{\infty} \left[1 - \alpha_l \arctan\left(\frac{1}{\alpha_l}\right)\right]. \quad (3.61)$$

For the perpendicular part, with

$$\int_0^\infty dk\, k^{3/2} \mathrm{e}^{-k(2\tau/s+l\beta)} J_{5/2}(2kx) = \sqrt{\frac{2}{\pi}} \left\{ \frac{3}{(2x)^{\frac{5}{2}}} \arctan\left(\frac{2x}{2\tau_s + l\beta}\right) - \frac{5(2x)^3(2\tau_s+l\beta)+3(2x)^3(2\tau_s+l\beta)^3}{(2x)^{\frac{5}{2}}[4x^2+(2\tau_s+l\beta)^2]^2} \right\}. \quad (3.62)$$

So that

$$\lim_{\tau\to\infty} \langle(\Delta v_\perp)^2\rangle^{(2)}_{3,\mathrm{mixed}} \overset{m\to 0}{=} -\frac{g^2}{4\pi^2x^2} \sum_{l=1}^{\infty} \left[\frac{1+2\alpha_l^2}{1+\alpha_l^2} - 2\alpha_l \arctan\left(\frac{1}{\alpha_l}\right) \right]. \quad (3.63)$$

Analogously for the vacuum contribution we find

$$\lim_{\tau\to\infty} \langle(\Delta v_\parallel)^2\rangle^{(2)}_{3,\mathrm{vacuum}} \overset{m\to 0}{=} -\frac{g^2}{8\pi^2x^2} \left[1 - \frac{\tau_s}{x} \arctan\left(\frac{x}{\tau_s}\right) \right], \quad (3.64)$$

$$\lim_{\tau\to\infty} \langle(\Delta v_\perp)^2\rangle^{(2)}_{3,\mathrm{vacuum}} \overset{m\to 0}{=} -\frac{g^2}{8\pi^2x^2} \left[\frac{1+2(\tau_s/x)^2}{1+(\tau_s/x)^2} - 2\frac{\tau_s}{x} \arctan\left(\frac{x}{\tau_s}\right) \right], \quad (3.65)$$

which is the result found for the late-time regime in Ref. [18].

3.5 Distance behavior of the velocity fluctuations

The introduction of a perfectly reflective boundary changes the topology of the space in which the field is defined, as stated before, and when we renormalize the expectation values a divergence appears at the boundary position, in addition to the divergence for $\tau = 2x$. Both divergences are regularized by the sample function, as it suppresses the high-energy modes. In the preceding sections we were able to see how the divergence in $\tau = 2x$ is regularized, and now study the behavior of the field near the wall.

Hence, to investigate how the dispersion behaves with the distance to the plate, note that, when $x/\beta \ll 1$, we have

$$\sqrt{1-\gamma_l^2} = \sqrt{1 + \frac{\beta^2}{4x^2}\left(l + i\frac{\tau}{2\beta}(\psi_{n,p} - \psi^*_{n,q})\right)} = \frac{\beta}{2x}\sqrt{\frac{4x^2}{\beta^2} + \left(l + i\frac{\tau}{2\beta}(\psi_{n,p} - \psi^*_{n,q})\right)}$$
$$\simeq \frac{\beta}{2x}\sqrt{l + i\frac{\tau}{2\beta}(\psi_{n,p} - \psi^*_{n,q})} = \sqrt{-\gamma_l^2}.$$

So that

$$\langle(\Delta v_\parallel)^2\rangle^{(1)}_{D,\mathrm{mixed}} \simeq -\langle(\Delta v_i)^2\rangle^{(1)}_{D,\mathrm{thermal}},$$

and, consequently,

$$\langle(\Delta v_\perp)^2\rangle^{(1)}_{D,\mathrm{mixed}} \simeq \langle(\Delta v_i)^2\rangle^{(1)}_{D,\mathrm{thermal}} - 8\pi x^2 \langle(\Delta v_i)^2\rangle^{(1)}_{D+2,\mathrm{thermal}}.$$

Thus, for the dispersion in the parallel direction the mixed and thermal part cancel near the wall, and we have only the modified vacuum term which does not depend on temperature, as it is shown by the convergence of the curves in Fig. 15. As for the perpendicular

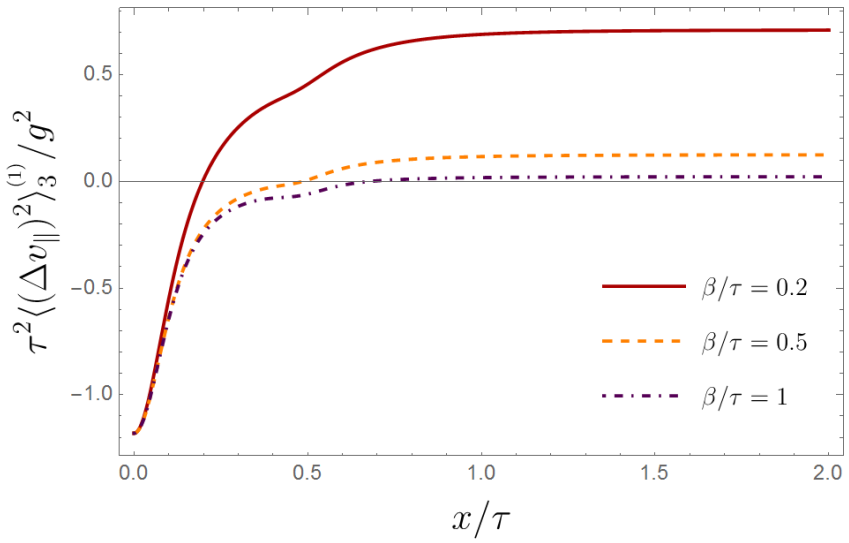

Fig. 15 – Distance behavior of the parallel dispersions, here $n = 5$, $D = 3$, and $m\tau = 1$. On the wall the curves converge, there the dispersions in the parallel directions does not depend on the temperature.

direction, Fig. 16, the mixed part equals the pure thermal as $x \to 0$, and the dispersion grows with temperature near the wall. Note that the same behavior is found for the massless vector field [20].

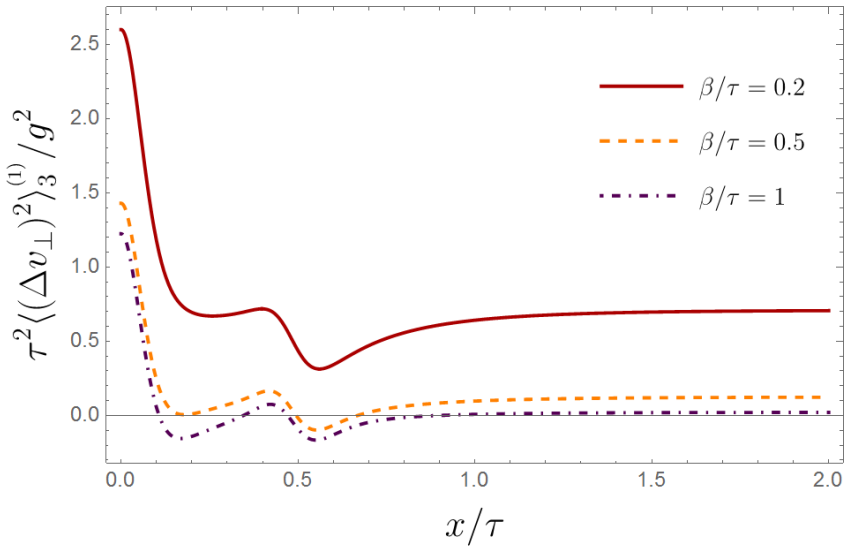

Fig. 16 – Distance behavior of the perpendicular dispersion, here $n = 5$, $D = 3$, and $m\tau = 1$. for low temperatures the dispersion oscillates between positive and negative values, and the dispersion grows with the temperature, at any position.

Now, as was done in Ref. [20] for the electromagnetic field, we investigate the mean squared velocity near the wall:

$$\langle v^2\rangle_{D,\beta} = \sum_i \langle v_i^2\rangle_{D,\beta} = (D-1)\langle(\Delta v)_\parallel^2\rangle_{D,\beta} + \langle(\Delta v)_\perp^2\rangle_{D,\beta}. \tag{3.66}$$

We define the quantity

$$\eta_{_D} = \left| \frac{\langle v^2 \rangle_{D,\beta} - \langle v^2 \rangle_D}{\langle v^2 \rangle_D} \right| \tag{3.67}$$

where $\langle v^2 \rangle_D$ is the the mean squared velocity at $T = 0$. Then, when $\eta_{_D} > 1$ thermal effects dominates, and if $\eta_{_D} < 1$, vacuum effects dominates.

Rewriting Eq. (3.67) we have

$$\eta_{_D} = \left| \frac{D\langle (\Delta v_i)^2 \rangle_{\mathrm{D,thermal}} + (D-2)\langle (\Delta v_\parallel)^2 \rangle_{D,\mathrm{mixed}} + 8\pi x^2 \langle (\Delta v_\parallel)^2 \rangle_{D+2,\mathrm{mixed}}}{(D-2)\langle (\Delta v_\parallel)^2 \rangle_{D,\mathrm{vacuum}} + 8\pi x^2 \langle (\Delta v_\parallel)^2 \rangle_{D+2,\mathrm{vacuum}}} \right| \tag{3.68}$$

we will study the late time regime, for which, when $x \to 0$ we find

$$\lim_{\tau\to\infty} \lim_{x\to 0} \eta_{_D}^{(2)} = \left| \frac{2 \lim_{\tau\to\infty} \langle (\Delta v_i)^2 \rangle^{(2)}_{D,\mathrm{thermal}}}{(D-2) \lim_{\tau\to\infty} \lim_{x\to 0} \langle (\Delta v_\parallel)^2 \rangle^{(2)}_{D,\mathrm{vacuum}}} \right| \tag{3.69}$$

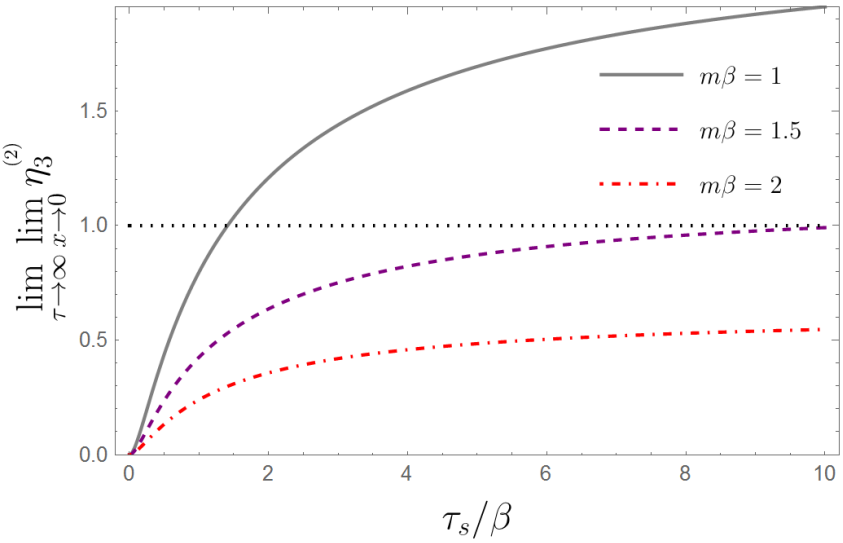

Fig. 17 – Vacuum versus thermal dominance in the wall for different values of τ_s/β and $m\beta$, here $D = 3$. For high values of the mass the vacuum always dominate, independently of the switching time.

Note that, for $D = 2$, η diverges. However, that just means that $\lim_{\tau\to\infty} \langle (\Delta v_\parallel)^2 \rangle^{D}_{\mathrm{vacuum}}$ vanishes when $x = 0$. Hence, as the thermal part is not zero, it dominates near the wall

for $D = 2$. When $D \neq 2$ we have

$$\lim_{\tau\to\infty}\lim_{x\to 0}\eta_D^{(2)} = \left|\frac{4}{D-2}\sum_{l=1}^{\infty}\left\{\left[\frac{m\beta}{2\pi(2\tau_s/\beta+l)}\right]^{\frac{D-1}{2}} K_{\frac{D-1}{2}}(m\beta(2\tau_s/\beta+l)) - \frac{(2\tau_s/\beta+l)(m\beta)^D}{2^D\pi^{D/2-1}\Gamma(\frac{D}{2}+1)} I\left(D, m\beta(2\tau_s/\beta+l)\right)\right\}\right.$$
$$\left.\times\left\{\left[\frac{m\beta}{4\pi(\tau_s/\beta)}\right]^{\frac{D-1}{2}} K_{\frac{D-1}{2}}(2m\beta(\tau_s/\beta)) - \frac{2(\tau_s/\beta)(m\beta)^D}{2^D\pi^{D/2-1}\Gamma(\frac{D}{2}+1)} I\left(D, 2m\beta(\tau_s/\beta)\right)\right\}^{-1}\right|, \tag{3.70}$$

which reduces to the expression found for the electromagnetic case in Ref. [20] when $m \to 0$.

One can see, from the expression above, that it becomes zero for the sudden transition, $\tau_s/\beta \to 0$, as there we have the divergence near the boundary from the vacuum contribution. As τ_s/β increases the divergence is regularized and the value of the vacuum contribution to the fluctuations is weakened, thence $\lim_{\tau\to\infty}\lim_{x\to 0}\eta_3$ grows as well, before it stabilizes for greater values of τ_s. Notwithstanding, the mass plays an important role, as depicted in Fig. 17, it lowers the curve and for masses higher than around $m\beta \simeq 1.5$ the vacuum term dominates for any switching time. Such behavior comes from the suppression of the thermal contribution due to the mass of the field. For $D = 1$ the graph is similar, but the curve is more inclined.

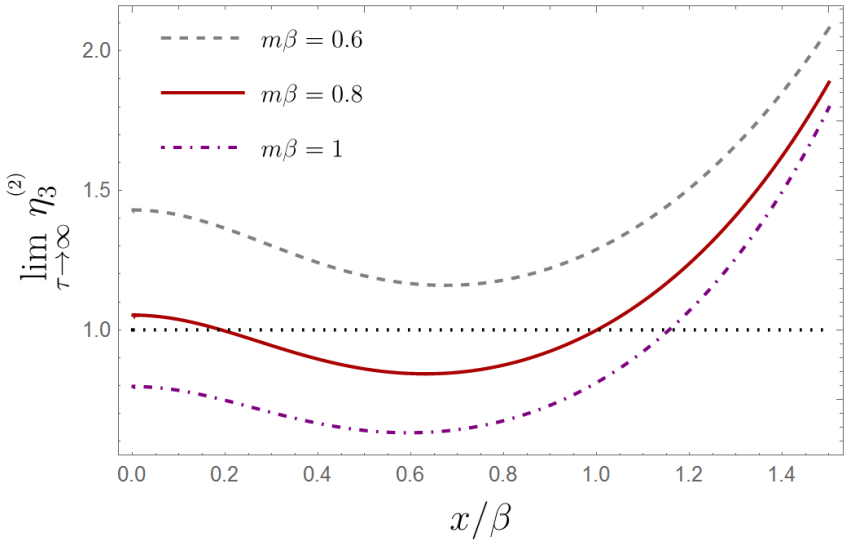

Fig. 18 – Distance behavior of the vacuum versus thermal dominance for different values of $m\beta$, here $D = 3$ and $\tau_s/\beta = 1$. When $m\beta = 0.8$ thermal effects always dominate, then, when the mass is increased, vacuum effects begin to dominate in some regions.

Further, we investigate the distance behavior of η as $\tau \to \infty$. As expected, deep in the bulk $x/\beta \to \infty$, $\eta \to \infty$, i.e., the boundary effects no more contribute to the

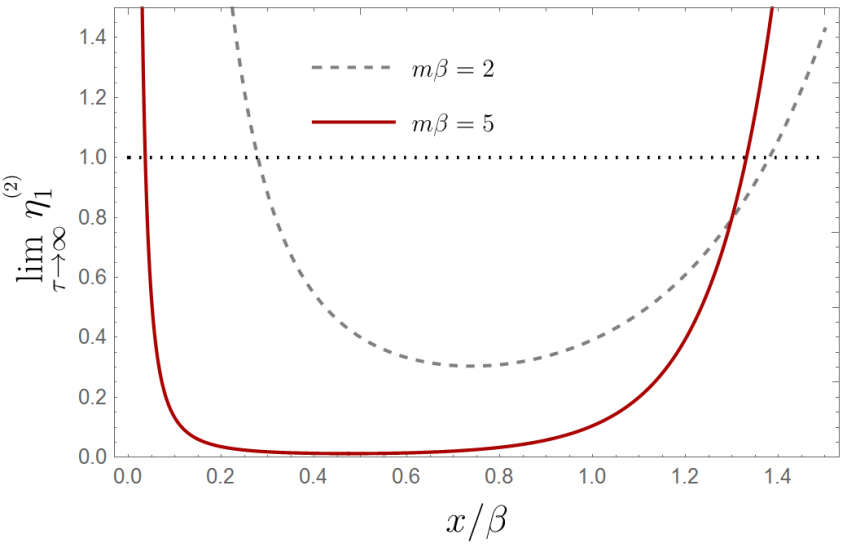

Fig. 19 – Distance behavior of the vacuum versus thermal dominance for different values of $m\beta$, here $D = 2$ and $\tau_s/\beta = 1$.

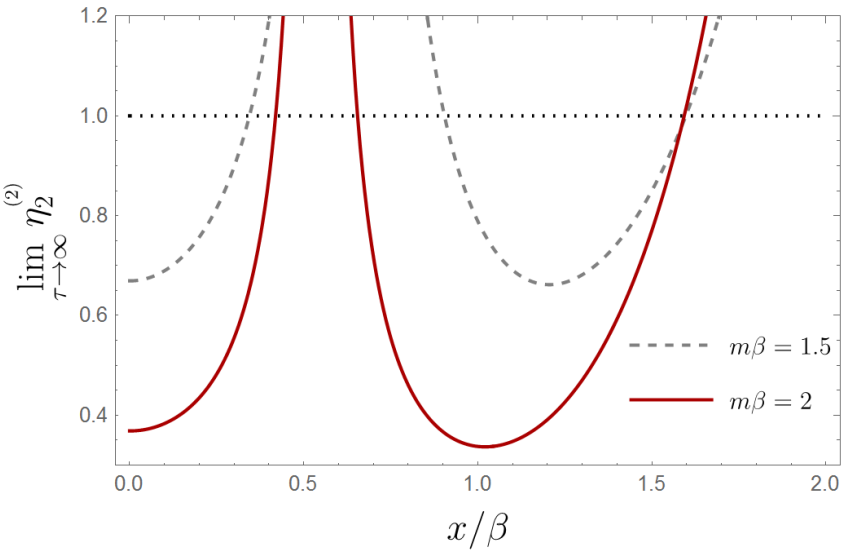

Fig. 20 – Distance behavior of the vacuum versus thermal dominance for different values of $m\beta$, here $D = 1$ and $\tau_s/\beta = 1$.

dispersions. When $D = 3$, see Fig. 18, we see that the dominance is highly dependent of the mass, for $m\beta = 0.6$ only thermal effects dominate, then, for $m\beta = 1$ the vacuum dominates near the wall. However, for intermediary values of the mass, as $m\beta = 0.8$, the behavior oscillates: first the thermal part, then the vacuum, and finally the thermal contribution dominates.

For $D = 2$, Figure 19 thermal effects dominates near the wall for any value of the mass, as we have seen. When the distance grows, for high values of the mass the vacuum dominates, after which thermal effects dominate in the bulk.

Finally, for $D = 1$ the mass plays the same role as before, for low masses only thermal effects dominates. However, here, the vacuum part contains only one component, the perpendicular direction, when it is zero a divergence appears, meaning that thermal effects dominate. Thence, for values of the mass for which vacuum dominates in the wall, there will always be an interchange in the dominance, as the divergence makes the thermal part dominates, after which vacuum dominates again and, in the bulk, only thermal contribution is left, as one can see in Fig. 20.

Final Remarks

Here we gave a step further on a series of works on stochastic motion induced by quantum fluctuations by unveiling the effects due to fluctuations of a massive scalar field at finite temperature. As said, in Ref. [1], it was shown how the non-Huygesian character of massive fields creates an oscillatory pattern in the dispersions. In the presence of thermal bath, we were able to see how mass effects opposes ones due to temperature, as for higher temperatures the oscillatory pattern is weakened, and, in opposition, the mass weakens the fluctuations. Such interplay between mass and temperature becomes more relevant in the presence of a reflective boundary. The modified vacuum contribution is just the zeroth order term in the convergent summation, as the mass grows, the thermal contribution is suppressed earlier, and the modified vacuum becomes prominent. Further, it has also interesting consequences concerning the thermal versus vacuum dominance near the boundary. For fields with higher masses, the distance to the plate for which the pure vacuum term dominates over thermal ones increases, and for some cases we can even see an interchange in this dominance as the wall is approached. Also, we demonstrated that, in a thermal bath near a boundary, subvacuum effects are presented at finite temperatures, as negative values of the dispersions. The case of a boundary at finite temperature, where pure thermal effects are considered as a residual dispersion, reveals a remarkable feature: temperature increases subvacuum effects.

Moreover, the model here investigated accounts for a more realistic situation with a transition time between different physical states of the system. Whereby the divergences of previous models [10, 19] are regularized, and the treatment of the quantum field presented here becomes consistent with the axiomatic construction presented in [30]–as there observables can only be defined smeared over continuous functions with compact support.

Henceforth, the boundary for the electromagnetic case is just a representation of a perfectly conductive plate, and for the scalar field it represents an infinite potential barrier the field is subjected to. Both types of boundaries being overidealizations: neither perfectly conductive plates nor discontinuous physical potentials exists in nature. Thence, a different test function, but with the same mathematical features described here, would arose for realistic boundary conditions. Nonetheless, if the transition time between the states is such that it discards propagating modes of frequencies lowers than the cut-off of the boundary, the realistic boundary will not alter the contributing modes, and the result present here will hold. Also, we have calculated the dispersions in the presence of a Dirichlet's wall. However, the result can be drastically changed if Neumann boundary conditions were used. It was shown in [23] that in such case the mixed and vacuum terms change by an overall sign. Thence, we could not have subvacuum effects for the parallel

directions, only in the perpendicular one, as there is not only a valley, but also a peak in the boundary contributions.

Further, the assumption that the particle position does not significantly change, i.e, $\langle(\Delta x_i)^2\rangle = \int_0^\tau d\,t \int_0^\tau d\,t' \langle v_i(t) v_i(t')\rangle \ll x_i^2$, is discussed in Ref. [17] for a massless scalar field at (1+1) dimensions and in Refs. [10, 19] for the electromagnetic case, in both cases it was shown that this assumption restrict the validity of the formulas obtained for the dispersions. Thence, it is an important next step to carefully investigate the position dispersion due to a massive scalar field. Nonetheless, the velocity dispersions for the massless case acts as an envelope for the massive field. Henceforth, as the position fluctuations is an integration of velocity correlations, it is expected that it has a greater value for the massless field. In such case, the regime of validity for massless fields would includes the massive case. Another remark is that, as the position assumption puts some constrains on the interaction time, one can think that the late-time result are compromised. Yet, note that, in the results presented here, after the peak the dispersions oscillate around their late-time value, rapidly approaching it. So, there can be values of the time which satisfy the assumptions and in which the system is in its late-time regime.

Regarding backreaction effects due to particle's emitted radiation, it was shown in Ref. [10, 15] that, for the electromagnetic case in the presence of a boundary, these can be negligible compared to the dispersions due to the change of the vacuum state. Furthermore, the angular spectral density of the radiation emitted as a switching effect from the introduction of the plate has a well understood behavior [39]. Notwithstanding, scalar fields radiates in the monopole, whether electromagnetic fields does not. Thus, they radiate more easily, and this effect should be investigated in an upcoming work. Together with that, the radiation emitted as a switching effect due to the transition from the vacuum to a thermal bath must be addressed. In the thermal bath the retarded propagator is the same as for free vacuum, so we expect no radiation. However, as for the boundary case, radiation will probably be emitted as a transition effect. Finally, the radiation of a massive field is known to exponentially decay with distance and mass, hence we consider the massless case as an upper limiting value.

Thence, we saw that even in the absence of a dissipative force the dispersions of the velocity components are not only bounded at late-times but depend only on the transition time, a feature that distinguishes the stochastic motion here discussed from an usual Brownian motion. For the boundary contributions this behavior is expected [13], however, we saw that it occurs even for the pure thermal contributions. The fluctuations are calculated through an integration of a correlation function, i.e,

$$\langle(\Delta v_i)^2\rangle = g^2 \int_0^\tau dt \int_0^\tau dt' C(\Delta t),$$

so that, for thermal-like dispersions (the usual Brownian motion in the absence of the dissipative force) the correlation function $C(\Delta t)$ is non negative and decays monotonically

with Δt with the relaxation time of the fluid, giving $\langle(\Delta v_i)^2\rangle \propto \tau$, the usual random walk motion, and a dissipative force is needed [13, 40]. In the present case, back in Eq. (3.6) with the renormalized thermal Hadamard function (2.57), the correlation function is

$$C_{_D}(\Delta t) = \frac{1}{\pi}\mathrm{Re}\sum_{l=1}^{\infty}\lim_{\vec{x}\to\vec{x}'}\frac{\partial}{\partial x_i}\frac{\partial}{\partial x_i'}\left[\left(\frac{m}{2\pi i\sigma_l}\right)^{\frac{D-1}{2}}K_{\frac{D-1}{2}}(im\sigma_l)\right]$$
$$= \frac{2}{\beta^{D+1}}\mathrm{Re}\sum_{l=1}^{\infty}\left(\frac{m\beta}{2\pi\sqrt{-(\Delta t/\beta+il)^2}}\right)^{\frac{D+1}{2}}K_{\frac{D+1}{2}}\left[m\beta\sqrt{-(\Delta t/\beta+il)^2}\right],$$

which, as is depicted in Fig. 21, take on negative values, so that the dispersions are bounded for $\tau \to \infty$, just as for the boundary contribution. Not only are they bounded but also, for late-time regime, the contributions from the interaction time vanish, as we saw, and we have left just the switching contribution. Thus, the mean quadratic velocity does not approaches its equipartion value $D/\beta M$, as it is inversely proportional to the quadratic mass of the particle, and, for a fixed temperature T, the late-time value depends on the transition time.

That is due to the fact that, in our model, we have neglected the radiation emitted by the particle. Because of that, the energy flux goes only in one way, from the field to the particle, and a thermal equilibrium can never be reached. Therefore, we envisage that, in a situation in which the particle radiation is taken into account, and the change in position is not neglected, thermal equilibrium could be reached.

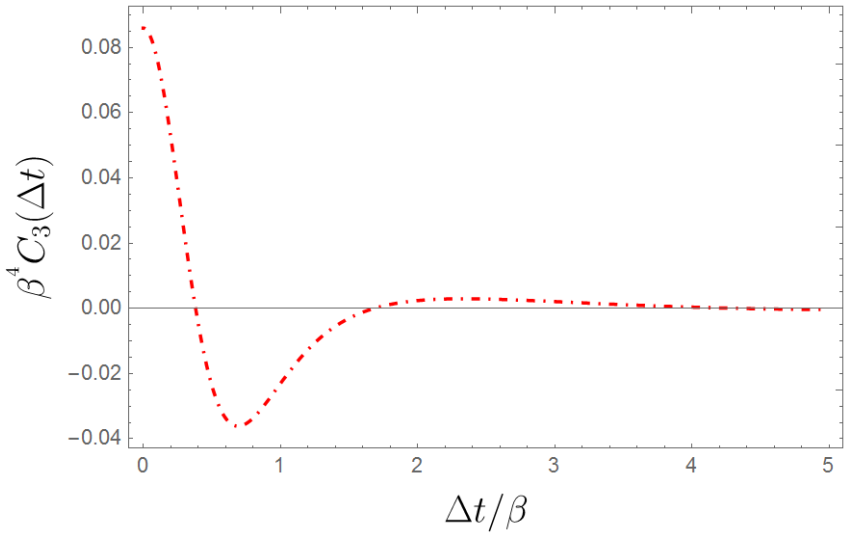

Fig. 21 – Correlation function for the thermal contribution to the velocities dispersions, here we have $m\beta = 1$ and $D = 3$. One can see that the correlation takes on negative values, so that the dispersions become bounded for large values of the interaction time.

Closing, some remarks are in order concerning the interpretation of the negative values of the dispersions. The dispersion of a quantity measures how much it deviates

from its mean value, hence, a negative value is counter intuitive. What happens is that the dispersions of the particle velocity are lessen when compared to their value when the interaction began, opposing the usual behavior of a free particle, in which the wave packet is spread [10]. Moreover, classical contributions from the interaction of the particle with the boundary must be taken in account, with that positive definite quantities, such as the kinetic energy, do not become negative, but the dispersions here calculated just diminishes this classical value [20].

References

[1] Camargo, G. H. S., Lorenci, V. A. D., Ribeiro, C. C. H. & Rodrigues, F. F. Vacuum induced dispersions on the motion of test particles in $d+1$ dimensions. *Phys. Rev. D* **100**, 065014 (2019). 5, 11, 24, 33, 34, 37, 43, 46, 49, 50, 51, 64

[2] Jousten, K. *The History of Vacuum Science and Vacuum Technology*, chap. 1, 1–18 (John Wiley Sons, Ltd, 2016). 9

[3] Parker, L. E. & Toms, D. *Quantum Field Theory in Curved Spacetime: Quantized Field and Gravity* (Cambridge University Press, 2009). 10, 35

[4] Birrel, N. D. & Davies, P. C. W. *Quantum Fields in Curved Space* (Cambridge University Press, Cambridge, UK, 1982). 10, 21, 23, 28, 29

[5] Wald, R. M. *Quantum Field Theory in Curved Spacetime and Black Hole Thermodynamics* (University of Chicago Press, Chicago, USA, 1994). 10, 20

[6] Rickles, D., French, S., & Saatsi, J. *The Structural Foundations of Quantum Gravity* (Oxford University Press, Oxford, UK, 2006). 10

[7] Gour, G. & Sriramkumar, L. Will small particles exhibit brownian motion in the quantum vacuum? *Found. Phys.* **29**, 1917–1939 (1999). 10

[8] Johnson, P. & Hu, B. Stochastic theory of relativistic particles moving in a quantum field: scalar abraham-lorentz-dirac-langevin equation, radiation reaction, and vacuum fluctuations. *Phys. Rev. D* **65**, 065015 (2002). 10

[9] Parkinson, V. & Ford, L. H. A model for non-cancellation of quantum electric field fluctuations. *Phys. Rev. A* **84**, 062102 (2011). 10

[10] Yu, H. & Ford, L. H. Vacuum fluctuations and brownian motion of a charged test particle near a reflecting boundary. *Phys. Rev. D* **70**, 065009 (2004). 10, 33, 34, 64, 65, 67

[11] Bessa, C., Bezerra, V. & Ford, L. Brownian motion in robertson-walker spacetimes from electromagnetic vacuum fluctuations. *J. Math. Phys.* **50**, 062501 (2009). 10

[12] Bessa, C. H. G., Lorenci, V. A. D. & Ford, L. H. Analog model for light propagation in semiclassical gravity. *Phys. Rev. D* **90**, 024036 (2014). 10

[13] Ford, L. H. Stochastic spacetime and brownian motion of test particles. *Int. J. Theor. Phys.* **44**, 1753 (2005). 10, 65, 66

[14] Seriu, M. & Wu, C. Switching effect on the quantum brownian motion near a reflecting boundary. *Phys. Rev. A* **77**, 022107 (2008). 10

[15] Lorenci, V. A. D., Ribeiro, C. C. H. & Silva, M. M. Probing quantum vacuum fluctuations over a charged particle near a reflecting wall. *Phys. Rev. D* **94**, 105017 (2016). 10, 11, 34, 36, 37, 50, 65

[16] Seriu, M. & Wu, C. Smearing effect due to the spread of a probe particle on the brownian motion near a perfectly reflecting boundary. *Phys. Rev. A* **80**, 052101 (2009). 10

[17] Lorenci, V. D., Jr., E. M. & Silva, M. Quantum brownian motion near a point-like reflecting boundary. *Phys. Rev. D* **90**, 027702 (2014). 10, 34, 65

[18] Camargo, G., Lorenci, V. D., Ribeiro, C., Rodrigues, F. & Silva, M. Vacuum fluctuations of a scalar field near a reflecting boundary and their effects on the motion of a test particle. *J. of High Energy Phys.* **173** (2018). 11, 34, 37, 58

[19] H. Yu, J. C. & Wu, P. Brownian motion of a charged test particle near a reflecting boundary at finite temperature. *J. of High Energy Phys.* **58** (2018). 11, 64, 65

[20] Lorenci, V. A. D. & Ribeiro, C. C. H. Remarks on the influence of quantum vacuum fluctuations over a charged test particle near a conducting wall. *J. of High Energy Phys.* **72** (2019). 11, 37, 45, 59, 61, 67

[21] Bezrukov, F. & Shaposhnikov, M. The standard model higgs boson as the inflaton. *Phys. lett. B* **659** (2008). 11

[22] na, J. M. & Matos, T. A brief review of the scalar field dark matter model. *Journal of Phys.: Conference Series* **378** (2011). 11

[23] Lorenci, V. A. D., Gomes, L. G. & Jr, E. S. M. Local thermal behaviour of a massive scalar field near a reflecting wall. *J. of High Energy Phys.* **096** (2015). 11, 32, 64

[24] Brown, L. S. & Maclay, G. J. Vacuum stress between conducting plates: An image solution. *Phys. Rev.* **184**, 1272 (1969). 11, 28

[25] Neumann, J. V. *Mathematical Foundations of Quantum Mechanics* (Princeton University Press, Princeton, UK, 1955). 13, 15

[26] Weinberg, S. *The Quantum Theory of Fields: Vol 1* (Cambridge University Press, Cambridge, UK, 1995). 14

[27] Huang, K. *Statistical Mechanics* (Wiley, New Jersey, USA, 2000). 15

[28] Cohen-Tannoudji, C., Bernard, D. & Laloe, F. *Quantum mechanics* (Wiley, New York, NY, 1991). 17

[29] Sakurai, J. *Modern quantum mechanics; rev. ed.* (Addison-Wesley, Reading, MA, USA, 1994). 17

[30] Streater, R. F. & Wightman, A. S. *PCT, Spin and Statistics, and All That* (Princeton University Press, Princeton, UK, 2000). 18, 20, 23, 25, 35, 64

[31] Haag, R. *Local Quantum Fields: Fields, Particles and Algebras* (Springer-Verlag Berlin Heidelberg, Berlin, Germany, 1996). 20

[32] Arfken, G. *Mathematical Methods for Physicists* (Academic Press, New York, USA, 1985). 21, 26, 41, 42

[33] Fulling, S. A. & Ruijsenaars, S. N. M. Temperature, periodicity and horizons. *Phys. Rept.* **152**, 135 (1987). 25, 27, 32

[34] Blumenson, L. E. A derivation of n-dimensional spherical coordinates. *The American Mathematical Monthly* **67** (1960). 26

[35] Gradshteyn, I. S. & Ryzhik, I. M. *Table of Integrals, Series, and Products* (Academic Press, New York, USA, 2007). 27, 42, 44

[36] Anderson, J. L. *Principles of Relativity Physics* (Academic Press, New York, USA, 1967). 33

[37] Barton, G. On the fluctuations of casimir force. *J. Phys. A: Math. Gen.* **24**, 991 (1991). 36

[38] Barton, G. On the fluctuations of casimir force: Ii the stress-correlation function. *J. Phys. A: Math. Gen.* **24**, 5533 (1991). 36

[39] Karlovets, D. V. & Potylitsyn, A. P. On the theory of diffraction radiation. *J. Exp. Theor. Phys.* **107**, 775–768 (2008). 65

[40] Pathria, R. K. *Statistical Mechanics* (Butterworth Heinemann, Oxford, UK, 1996). 66